**TECHNISCHE
UNIVERSITÄT
WIEN**

**VIENNA
UNIVERSITY OF
TECHNOLOGY**

DIPLOMARBEIT

Atomic Force Microscopy of the alga
Euglena gracilis

Ausgeführt am Institut für
Allgemeine Physik

der Technischen Universität Wien

unter der Anleitung von
Ao.Univ.Prof. Dipl.-Ing. Mag.rer.nat. Friedrich Aumayr
und Univ.Ass. Dipl.-Ing. Dr.techn. Ille C. Gebeshuber
als verantwortlich mitwirkender Universitätsassistentin

durch

Clemens Gruenberger

Draschestraße 86,
1230 Wien, Österreich

Wien, am 16.10.2007

Clemens Gruenberger

Atomic Force Microscopy of the alga
Euglena gracilis

(diploma thesis)

»Later I have been asked many times if I feel bad for missing the effect? The answer is clearly no, because to make an experimental discovery it is not enough to observe something, one must also realize the significance of the observation, and in this instance I was not even close.«

Ivar Giaever, about the Josephson effect[1] he had missed during his experiments of electron tunneling in superconductors. All the samples showing the Josephson effect were simply discarded as having shorts. (from his Nobel Prize speech, 1973)[2]

---

[1] Brian Josephson predicted that it should be possible to pass a supercurrent with zero voltage drop through the oxide barrier when the metals on both sides were superconducting. This is now called the dc Josephson effect.

[2] In 1973, Leo Esaki (USA), Ivar Giaever (USA) and Brian D Josephson (UK) were awarded the Nobel Prize in Physics by the Royal Swedish Academy of Sciences. The official press release reads: "The award is for their discoveries regarding tunneling phenomena in solids. Half of the prize is divided equally between Esaki and Giaever for their experimental discoveries regarding tunneling phenomena in semiconductors and superconductors respectively. The other half is awarded to Josephson for his theoretical predictions of properties in a supercurrent flowing through a tunnel barrier, in particular the phenomena generally known as the Josephson effects. [...]"

Abstract

Nanotechnology as of today is still in its infancy. Although we learnt about twenty five years ago how to actually "see" individual atoms, the assembly and creation of nanoscale structures is still a difficult undertake. It is either slow if atoms must be manipulated one by one or the process can only be controlled to a limited degree (e.g. when bulk matter is treated in such a way that structures with features at the nanoscale are produced).

One way to extend our nanotechnological knowledge is drawing inspirations from naturally occurring systems and processes.[3] Within the tiniest realms of nature we can already find robust concepts for marvelous miniaturization, the accommodation of a maximum of functional units within only small volume. Incessant evolutionary optimization provides the driving force behind efficiency, versatility, and often simple and elegant solutions - knowledge that can often be applied to the study, design and engineering of nanotechnological systems.

Matter produced and assembled by even simple life forms is remarkable. *Euglena gracilis*, a single-celled algal species, performs tasks as diverse as sensing the environment and reacting to it, converting and storing energy and metabolizing nutrients, living as a plant or an animal depending on the environmental constraints. Cell functions are often based on materials produced with molecular precision.

In this thesis, a method for Atomic Force Microscope investigation of the alga *Euglena gracilis* was developed and measurements under different scanning conditions were carried out. Data was obtained on whole cells as well as cell organelles. Some of the obtained morphological algal features were compared to existing literature data (mostly Transmission Electron Microscope and Scanning Electron Microscope images). The possibility of AFM force spectroscopy and viscoelastic analysis on the nanoscale concerning this biological system has been demonstrated. The outlook points at possible directions of future research, that extend the approach here presented.

---

[3]A good example that those concepts can work in the engineering context, is the already highly successful field of bionics, where design principles from Nature are applied to artificial systems. Some found solutions have also had great commercial success (e.g. Velcro, airplane winglets or hydrophobic paint).

Contents

Chapter 1

Introduction

1.1 Exciting Possibilities

We live in exciting scientific times. Much physical groundwork has been done, especially during the last century, when the theory of relativity and quantum mechanics were formulated. All of the basic forces[1] governing our universe have been discovered - so it seems - and our theories predict experimental outcome very accurately[2].

The framework of theories describing these forces has been refined over time. The description of the electromagnetic force and the weak force for example has been unified into the theory of the electroweak force. The ingenious physicist Albert Einstein (1879-1955) already suggested that a unified theory describing all of the forces of nature should exist, and he was struggling for much of his later life to find such a theory - though without success. In this spirit many possibilities have been tried out and today there exist some candidates for being what is called the "Theory of Everything" (TOE)[3], one of the most promising ones being String

---

[1]These are the strong force, tying together the quarks in the atomic nuclei. The electromagnetic force (or so called Coulomb force), responsible for the interaction between charged particles such as electrons and protons. The affiliated force-carrying particles are the photons, in their different appearances such as light rays, radio waves or gamma rays. Then there is the weak force, governing the radioactive decay of some elementary particles. And finally the weakest force of all, but very familiar to us, the gravitational force. It is very weak, about 10^{-40} times weaker than the strong force, but is infinite in range and responsible for the attraction between celestial bodies. Only the electromagnetic and gravitational forces can be directly experienced in our mesocosm as only these possess infinite range and thus extend beyond the scale of atoms.

[2]As example, one of the most precisely tested theories is the theory of Quantum Electro Dynamics (QED), with which it is possible to compute the dimensionless magnetic moment of the electron with a precision better than 1 part in a trillion (and it is equally astonishing to reach similar accuracy in experiments in order to test these predictions).

[3]Usually the term "Theory of Everything" refers to a collection of equations, a single theoretical model, from which all fundamental interactions and possibly the fundamental physical properties can be derived.

theory (see e.g. [1]).

Now I call our times exciting, because we can build upon this hard work that has already been done, providing the foundations for understanding how particles interact and what effects have to be taken into account for a particular problem. As soon as such a collection of physical laws is in place, statements of the kind "It should be possible to do this and that" can be made. Ideas of what is possible can be derived from what we know. A theoretical prediction in this sense is nothing else than a statement that it should be possible to do this and that (the experiment) and obtain a certain result. The reasoning has been done a priori, before we carry out the actual experiment, the real thing.

This is not something new and I will cite here a statement that has been made quite some time ago (in 1959) by a well know physicist - Richard Feynman (1918-1988). He stated "..there exists no reason why we shouldn't be able to write the entire Encyclopedia Britannica on the head of a pin.." ([2]), while he discussed the idea that the laws of physics do not oppose the intentional manipulation of single atoms, assembling them as one wishes. Back then however, there was no imaging method having atomic resolution, and even less a way to manipulate single atoms in a controlled way.

Then, in 1981, with the invention of the Scanning Tunneling Microscope (STM) (see Chapter 3) it was for the first time possible to directly acquire images of solid surfaces with atomic resolution. Along with the STM came the possibility to move atoms across a surface one by one. Since then the science of the small has seen explosive growth - Nanotechnology. For phenomena at the nanoscale, the tiniest realm of nature, we can today rephrase those statements (with good chances to find answers) of what should be possible into "How can we build, what we think is possible?".

This is an extraordinary position to be in - We now can try out what could only be hypothesized before. The past two and a half decades have extended the knowledge and techniques greatly and the range of what seems possible to do is almost frightening. A new scientific continent is waiting to be discovered, rich in concepts, applications and deep consequences that reach too far than can be predicted beyond the near future.

1.2 Complexity

As soon as real systems have to be investigated, understood and built, a new challenge arises. In order to apply ideas from physics to progressively larger and more complicated structures, the interactions between many elementary constituents

have to be taken into account. Complexity[4] is a property of a system in its own right. It is even an essential ingredient of real systems, containing more than just a hand full of atoms.

The philosopher Aristotle (384-322 b.C.) already knew that "The whole is more than the sum of its parts", intuitively pointing at the possible emergence of new phenomena when systems increase in size and in number of parts.

It is for example well understood what happens when two atoms collide, but a very different matter trying to understand what happens when an atom collides with a whole cluster of atoms or even a surface of a solid. There can e.g. be atoms of different kinds, having different energy states, chemical bonds and the like. As one can imagine, the complications steeply rise in number and difficulty. The laws of particle interaction can only provide a first basis of an explanation how these things behave.

How electrically charged atoms (ions) impact surfaces is for instance a very interesting but difficult question. There exists a variety of models trying to explain the mechanisms of energy transfer between ion and surface or the formation of ion-induced defects at the surface, but none can be easily applied to a specific problem. Possible applications include nanopatterning, surface alteration or doping, surface analytics, surface cleaning, surface sputtering and more ([3], [4]).

In the world of nanoscale objects, new systems with only nuclei, electrons and photons can be devised endlessly. The newly acquired freedom and ability to manipulate the small also comes at a price - the need to understand at least in part the complexity that these real systems exhibit. Additionally, other effects such as quantum mechanical ones become important at this small scale, or the high surface to volume ratio of small objects assigning new importance to many of the common physical effects[5] otherwise too tiny to make a difference.

As bottomline, citing Peter Wolynes, a biophysicist at the University of Illinois, "The new frontier about which we know nothing is how to describe complex systems far from equilibrium in a unified way. [...] Such systems range from sand piles to biological cells to computers, but it is not clear whether or how the principles of statistical mechanics apply to them.". The more sophisticated our nanotechnological creations become, the more thorough understanding of complex systems is needed. Every bit of acquired knowledge potentially unlocks new ways to look at things, new possibilities to interact and experiment, new challenges to

---

[4]There is some difficulty (and complexity) in the definition of the term "Complexity" itself. An attempt to classify and define its different facets can e.g. be found in [5].

[5]For example combustion engines do not work anymore at this scale, chemical energy must be turned directly into mechanical energy without using intermediary heat. Gold turns red when present in form of very small particles. Particles under a certain size are able to pass unhindered through cell membranes, e.g. to target disease sites. Defectless nanostructured materials can be built orders of magnitude stronger than what is available today (e.g. carbon-nanotube enforced matrix materials)

understand phenomena at a larger scale. A living cell, a nanotechnological system of unchallenged precision and beauty, can teach us a lot of how energy is effectively conversed, how molecular sensing can be accomplished, how self-healing or even self-replicating systems might work - but we need to discover and understand first.

1.3   About this Work

Nanotechnology is changing our view of what is thinkable and maybe possible. We are at the advent of a major change of how we build things[6], changing everything around us - we will be able to make materials in an extremely precise fashion, defining exactly the three-dimensional positioning of atoms and molecules. The wealth of possibilities to refine these, exchange or invent new ones altogether is immense.
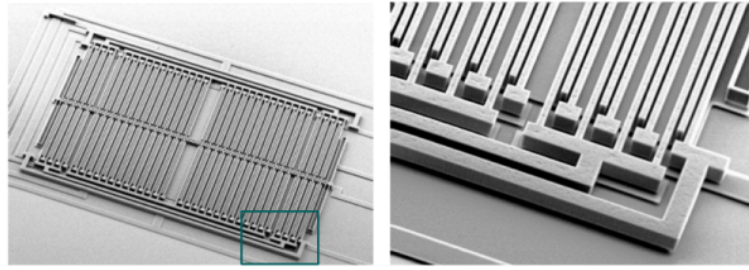
Figure 1.1: A silicon based MEMS accelerometer as seen with a scanning electron microscope (SEM). An accelerative force changes its capacitance which in turn can be used for very precise measurements of the magnitude of this force. The right image is a magnification of the rectangle area in the left image. Typically these devices have dimensions in the micrometer range. Images adapted from [6].

Observing what already exists in nature can help finding new principles of design. Mimicking nature and abstracting from its successful designs (sometimes referred to as biomimetics and bioinspiration, see [7]) has for long been a source of inspiration for inventions and innovations.

The myth of Icarus and Daedalus draws inspiration from the flight of birds, telling the story of how the greatest inventor of antique Greece attached artificial wings to his and his son's arm in order to flee from Crete where king Minos held

---

[6]An example, that already grew out of the conceptual stage, with very successfully applications are Micro-Electromechanical Systems (MEMS) - Also its cousins NEMS (Nano-Electromechanical Systems) and BioMEMS/BioNEMS are beginning to have their first successes. Of accelerometer MEMS in car airbags for instance, were 90 million pieces sold in the year 2004. MEMS have become an integral part of many products, reducing size and weight, while being precise and cheap in production costs ([8]).

them captive. Later Leonardo da Vinci fills whole notebooks with his sketches of bird flight maneuvers, making detailed observations of how birds execute turns, noting their wing and tail postures. He used these then to devise novel concepts for man-carrying machines (see Fig. 1.2) and devices for the testing of wings. Then
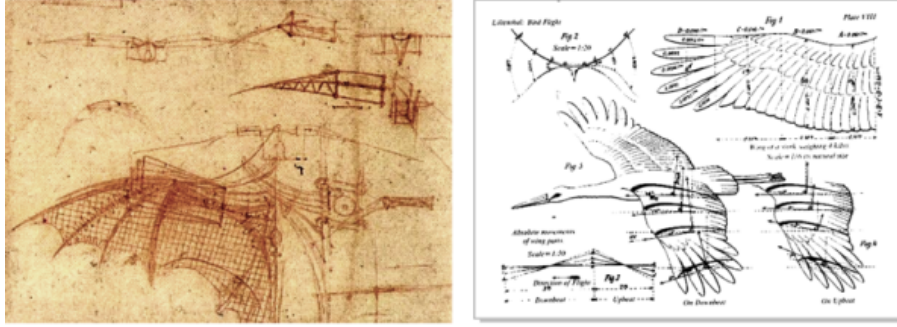
Figure 1.2: To the left a part of a flight machine sketch of Leonardo da Vinci. To the right a bird wing study of Otto Lilienthal. Images adapted from [9]

other inventors like Sir George Cayley (1773-1857), Otto Lilienthal (1848-96) and the Wright brothers Orville and Wilbur (1871–1948, 1867–1912), also deduced key principles of flight from their studies of birds ([10]). The winglet, an inspiration drawn from bird flight, was already invented in 1897. It can be described as small fin sticking straight up on the wingtip of many modern airplanes and considerably helps reducing fuel consumption ([11]).

This work investigates such a promising system - the alga *Euglena gracilis*, exhibiting many properties with high potential interest for nanotechnological applications.

How nanotechnology can be characterized and some of its main aspects are discussed in the second chapter (3).

The third chapter (3) deals with Atomic Force Microscopy (AFM). Techniques are explained and classified, with a focus on the application to biological systems.

The biological system *Euglena gracilis* is investigated in chapter 4. The description focuses on its morphology in respect to structure, organization and function. Subsystems of the alga are evaluated regarding their potential as templates and idea supply for man-made nanotechnological applications.

The experimental part of this work is divided into two chapters. The setup of the experiments as well as the methods of investigation used is presented in chapter 5. This includes how the algal cultures had to be kept under laboratory conditions, how they were collected, treated and prepared and how the AFM investigations were carried out. A preparation method for atomic force microscopy investigation

of whole dried *Euglena* cells in air was developed and provided data on whole cells as well as cell organelles.

In the results chapter 6, obtained image data is presented and compared to already available Transmission and Scanning Electron Microscopy data. Compared to traditional imaging approaches of biological samples, AFM can be used as a non-destructive imaging method. New features on the pellicle not seen by former TEM and SEM studies were found and questioned.

Finally, the outlook chapter sketches out possible directions of future research. The need for an interdisciplinary approach when investigating or conceiving nanosystems is apparent.

The consequences of nanotechnology and bionanotechnology will reach everywhere in our daily lives - ethical, social and political consequences. But Science by itself never can solve the question, how we can responsibly use our knowledge and abilities to the benefit of mankind. Such questions must be posed as early as possible, in order to be openly addressed and discussed.

Chapter 2

Nanotechnology

2.1   Introduction to Nanotechnology

Nanotechnology can be defined as the research and technology development at the atomic, molecular and macromolecular levels, in the length scale of approximately $1-100\,nm$ (a nanometer is a billionth of a meter, the diameter of a human hair is about 100,000 nanometers) (according to [12]).

When objects sufficiently decrease in size otherwise negligible phenomena and properties (physical, chemical, biological, mechanical, electrical...) become important. Just as computers have gone from bulky, room-filling monstrosities to handheld computing devices, our ability to understand and manipulate matter at smaller and smaller levels increases. The scientific and technical revolution based upon the ability to systematically organize and manipulate matter at the nanoscale has just begun and its consequences reach too far than can be predicted beyond the near future.

On December 29, in 1959, the physicist Richard P. Feynman (1918-1988) presented a talk to the American Physical Society entitled "There's Plenty of Room at the Bottom: An Invitation to enter a new Field of Physics". He reasoned that "..there exists no reason why we shouldn't be able to write the entire Encyclopedia Britannica on the head of a pin" and by that introduced the concept of nanotechnology. Simply put, he reasoned that if information were to be encoded in binary form - strings of zeros and ones, as in computers - and if each bit of information were to be composed in heaps of 100 atoms, then all the books in the world could be written in a cube measuring just $1/200\,th$ of an inch wide ($\cong$0.127 mm).

Another staggering claim of this talk was that one day it would be possible to simply synthesize every molecule we need by building tiny machines[1] that perform

---

[1]Some researchers conclude that Feynman was not interested in building miniaturized versions of existing macroscopic machines, but rather wished to construct microbiological machines and tools that would enable scientists to mimic microbiological materials. ([13])

these assembly functions for us.[2]

These claims touched the heart of the subject, the structuring and the functionalization of matter at the nanoscale. But only more than twenty years later, in 1981, with the invention of the Scanning Tunneling Microscope (STM) (see chapter 3) it became possible to directly acquire images of solid surfaces with atomic resolution. Along with the STM came the possibility to move and manipulate atoms one by one.

Since then the science of the small has seen explosive growth. Nanotechnology today is a huge field in which various sub-fields begin to shape, some having counterparts in macroscale physics ([14]):

Nanomaterials/**Nanochemistry** - These fields are dealing with the creation and manipulation of chemical and supramolecular functional systems and materials. These new structures possess a wide range of novel properties, e.g. systems that can be switched or controlled, systems with adjustable characteristics or functional coatings (e.g. with nanoparticles).

Nanoelectronics - Although the transition from microelectronics to nanoelectronics is not clearly defined, integrated circuits with feature sizes of 90 nm and below are generally called nanoelectronics. It is reckoned that a further miniaturization of electric circuit feature sizes down to 20 nm and below is going to take place within the next decade. In order to achieve this, optical lithography for circuitry layout will have to be replaced by new technologies, as it is limited by the minimum wavelength that can be used.

Nanooptics - Includes the research, development and production of optical components, structures and systems at the nanoscale. That includes ultraprecision photonics, nanometer precise lens systems or laser technology for optoelectronical components. It deals with technologies for photon generation, detection and control at the nanoscale.

Bionanotechnology - Technological processes are combined with the knowledge of biosystems at the nanoscale. The connection is made coming from two di-

---

[2]One of these functions even could be the replication of the machine itself. This replicator could then make copies of itself, and those copies make copies again and so on. After a little while there were just enough of these robots for whatever purpose they where designed primarily for, given enough resources to work with. ([15])

That these thoughts are not so exotic as they might seem is backed up by a NASA study document ([16]) of 400 pages reviewing the possibility of putting such replicating machinery to use in space (as early as 1980 and with conventional technology). A lunar factory, as self replicating system (SRS) that could expand itself to the required extent, reproducing parts of itself as needed and assemble them accordingly. One can conceive the idea of autonomously exploring space and in this way prepare the arrival of human astronauts. The analogy from such a self replicating lunar facility to systems on the nanoscale is reviewed in detail by Merkle ([17]). E. Drexler called the ability of self replication the 'holy grail' of mechanosynthetic nanoassembly ([18]).
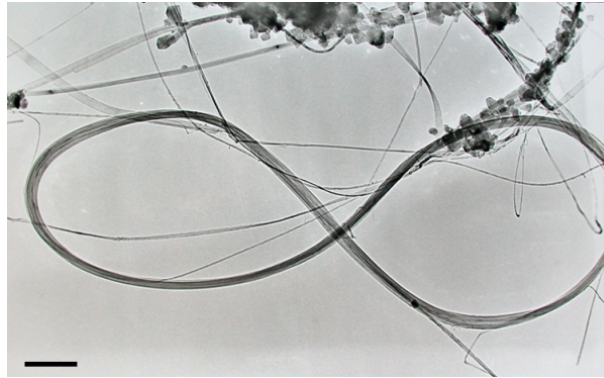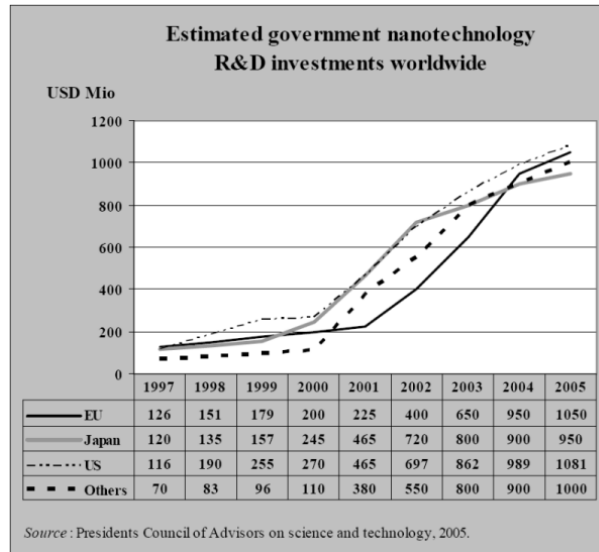
Figure 2.1: Transmission electron microscopy image of boron-nitride nanotubes grown through laser melting of a boron-nitride target. Nanotubes seem to be ideally suited for many nanotechnological applications because of their exceptional mechanical and electrical properties. Scale bar is $200 nm$.

rections. Either by making use of scientific findings about biological systems as patterns for developing technological applications (bio → nano) or applying nanotechnological processes to the interaction with biosystems (nano → bio).

Nanoanalysis - Refers to all techniques available for the determination of nanoscale structures of materials. Used in all of the other sub-fields it supplies analytic methods and means for recording basic phenomena and gathering information at the nanometer scale. As such it is concerned with measurements of structures and processes required by extreme miniaturization as well as with suitable measuring devices.

Nanotechnology will possibly play a technological key role in the 21st century. This interdisciplinary technology is already today increasingly relevant to economic areas such as chemistry, medical technology, automobile and the food industry. Current prognoses assume a dramatic increase in the economic significance of nanotechnology, associated research and production. This is also reflected in a sharp increase in national spending for research in this area during the last years (see Fig. 2.2).

Nanotechnology is not a mere reduction in size of existing technologies. It is based on different working principles and theoretical models that take these principles into account. Effects that are negligible at the macroscale can become major contributions at the nanoscale, such as quantum mechanical phenomena or consequences of high surface to volume ratio. Engineering structures in an extremely precise fashion and tailoring them to our specific needs by defining exactly the three-dimensional positions of the atoms and molecules they are built of is one of the goals of nanotechnology.

16

Estimated government nanotechnology R&D investments worldwide

USD Mio

	1997	1998	1999	2000	2001	2002	2003	2004	2005
EU	126	151	179	200	225	400	650	950	1050
Japan	120	135	157	245	465	720	800	900	950
US	116	190	255	270	465	697	862	989	1081
Others	70	83	96	110	380	550	800	900	1000

Source: Presidents Council of Advisors on science and technology, 2005.

Figure 2.2: Rise in public spending for nanotechnology research from 1997 to 2005. Graph taken from [14].

2.2   A Proposed Classification of Nanotechnology

From a technical point of view nanotechnology can be divided into three different sections (classification adapted from [19] according to Nobel Laureate R. Smalley[3]).

2.2.1   Dry Nanotechnology

The term derives from surface science and physical chemistry with focus on fabrication of structures in carbon, silicon, and other inorganic materials. Dry techniques use metals and semiconductors, with the slight disadvantage that conduction electrons make them reactive when operated in a "wet" environment. A great advantage is the possibility to fabricate nanostructures with promising electronic, magnetic, and optical properties.

2.2.2   Wet Nanotechnology

Wet nanotechnology on the one hand relates to the study of biological systems existing primarily in aqueous environment. On the other hand it also includes engineering proteins, genetic engineering and the like (this part of wet nanotechnology is sometimes referred to as "soft" nanotechnology in contrast to the naturally occurring biological nanotechnology).

---

[3]Richard E. Smalley (1943-2005), University Professor, Gene and Norman Hackerman Professor of Chemistry and Professor of Physics & Astronomy. In 1996, he was awarded the Nobel Prize together with R. Curl Jr. and H. Kroto for the discovery of fullerenes.

Investigated structures are e.g. genetic material, membranes or enzymes. The power behind wet nanotechnology derives from the actual existence of functioning nanomachines - living systems. No proof of concept is needed, these structures interact already successfully on the nanometer-scale.

2.2.3 Computational Nanotechnology

Computational Nanotechnology is a prerequisite for designing and testing complex nanostructures. The predictive and analytical power of simulations is an important ingredient to success in nanotechnology. For example, in order to know what an enzyme will be able to do, its 3D-structure must be determined. How its shape emerges from a sequence of amino acids is one goal of protein folding simulations. To predict this is highly desirable as it helps to understand how enzymes work, what defects are caused by misfolding or even for designing functional enzymes[4]. At the same time such efforts are very resource intensive.[5]

Computational nanotechnology may help to combine wet and dry nanotechnology, selecting from their strengths while avoiding their weaknesses. It can also help to reduce the development times of such systems.

It is thinkable that advances made in nanotechnology do not only lay the basis for new discoveries but will also contribute to the pace of advancement in nanotechnology itself. E.g. the development of nanoelectronics yielding higher computing power should have considerable effect on the ability to better describe and develop the next generation of nanoelectronics.[6]

---

[4]Such protein molecular machines are quite contrary to the ideas of diamond/carbon/metallic molecular manufacturing, which is predicated on rigidity/stability and absence of corrosive solvents. A cooled down protein machine becomes at a certain point too rigid to work. Such a machine works because because its non-bonding interactions are weak and a warm, wet environment where Brownian motion is omnipresent and aids the internal logic of conformational change of the molecule.

[5]The computational power required is sometimes so high that with today's supercomputers these are hardly treatable problems. For the protein folding problem there exist initiatives to involve the public. One example is the Folding@Home project, where a Stanford research group works on the theory and simulations of how proteins, RNA, and nanoscale synthetic polymers fold. The Folding@Home project uses distributed computing, i.e. private personal computers that are given instructions over the Internet work on pieces of a simulation in parallel. Everyone with an internet connection can take part by downloading a client program that will collect simulation assignments and run them whenever the computer processor would otherwise be in an idle state. Special algorithms are used in order to break up calculations, distribute the workload and then combine them again in order to act like a single, very fast computer. The project is currently using about 2 million processors with a total computational power of 920 Teraflops (1 Teraflop designates a trillion floating point operations per second). In comparison, the most performant supercomputer as of today, the "BlueGene/L", only reaches about 300 teraflops. ([20], [21], [22])

[6]A bold idea advocated by some researchers (e.g. R. Kurzweil, see [23]) is that our ability to build tools that enhance our ability to build tools follows the trend of a generalized Moore's law.

The presented three types of nanotechnologies are interdependent. Every type profits from advances of the two other, and innovative solutions are often a mixture of all three fields.

2.3   Nanotechnological Products

Despite its short history, nanotechnological devices are already used in a considerable number of applications. There exists a number of developed techniques to reproducibly investigate, create and change structures at the nanoscale.

2.3.1   Single Structure Nanotechnology

Single structure nanotechnology aims at the manufacturing of complete, distinct functional units, that are well defined it their purpose. This approach is generally tedious because of the great number of precise manipulations of single atoms or groups of atoms involved. The advantage of the method is that the resulting structure can act in a very specialized way and is targeted at a well defined purpose.

- MEMS and NEMS (see 1.3). Each device can act independently of the other devices.

- Lab-on-a-chip (also chemistry-on-a-chip). Many substances and reagents can be analyzed on a single chip providing much of the functionality of a macroscopic laboratory. Reactions can take place in tiny reaction chambers that are filled through microchannels.

- Elements in nanoelectronics, e.g. single molecule transistors (one example in [24]) or molecular switches (such as presented in [25]).

2.3.2   Bulk Material Nanotechnology

Bulk Material Nanotechnology on the contrary arranges large portion of matter in one step. These manipulations of large quantities of atoms and molecules however strictly limit the complexity of treatment and attention each atom receives. Manipulations on bulk material are done in parallel with the obvious advantage to produce large amounts of matter in short time. Although there is only a limited

---

This should also apply to intelligent software and thus computational nanotechnology. Once the point is reached where an artificial general intelligence will be available, the development cycles of producing even higher intelligences becomes extremely short. The point of this culmination is called the Singularity. Scientific activity would reduce itself to pose the right questions to these evolved super intelligences.

degree of control over individual atoms and molecules, it is still possible to obtain structures with nanoscaled feature sizes.

In comparison to the single structure nanotechnology, nanoscale bulk materials usually have smaller unit cell dimensions and these unit cells exhibit their desired properties only as members in the molecular collective. As the name "materials" suggest, further processing is needed to obtain a final functional result. Thus their function is not as specifically targeted as is the case for single nanostructures.

There are many types of nanomaterials and nanotechnological products available today. ([26])

- Nanotubes, fullerenes or buckyballs as basis for nanocomposite materials

- Nanocrystals, nanopowders and nanoparticulates (e.g. quantum dots). Applications include optical displays, computer memory, cryptography, photovoltaics, storage media, flexible electronics, telecommunications components, and quantum computing

- Nanogels, aerogels, hydrogels and other nanoporous materials. Used for thermal insulation, as scaffolds for nanocomposite manufacturing, and to capture fragrances, chemical catalysts and biochemicals.

- Nanofibers and nanowires

Most nanocomposites consist of a matrix and a dispersed second phase in particulate, fibrous, or continuous form. This second phase may alter the nanomaterial's electrical, thermal or magnetic properties, enhance its wear or erosion resistance or serve as a strengthening or stiffening agent.

Single structure nanotechnology and bulk material nanotechnology tend to drift together as it is desirable to manufacture highly specialized nanostructures with less effort, more reproducibility and on a larger scale. For bulk material nanostructures a higher degree of control is desirable as well as the ability to add specialized functionality to specific subdomains.

2.4   Selected Issues in Nanotechnology

As stated earlier in the introductory section, nanotechnology is a huge interdisciplinary field, spanning a large diversity of phenomena and approaches. Yet there exist a number of recurrent principles, ideas and problems accompanying the science of the small, some of which are mentioned here.

2.4.1 Self-Assembly and Emergent Structures

Many of the nanoscale systems are produced in large quantities. The processing steps required (e.g. chemical additives, light, heat, altered solvent conditions) are often completed by and interact with behavior intrinsic to the building blocks themselves. This behavior emerges out of the interaction within the collection of atoms and molecules. Every day life examples are the alignment of the polar molecules to form the skin of soap bubbles or the growing of ice crystals when water is sufficiently cooled down. Similar processes happen at the nanoscale, when e.g. nanotubes start to grow at crystalline nucleation sites, when nanopores distribute themselves evenly in a material ([27]) or when proteins fold and self-assemble to attain their conformational structure required to perform their function.

2.4.2 Reliability

Functional nanostructures should work reliably. That implies a reliable manufacturing method and means to test a finished device or material. Problems are adhesion, friction, wear, fracture, fatigue and contamination. Due to the high surface/volume ratio, devices with moving parts are particularly prone to stiction (high static friction). Furthermore not all material properties, e.g. for thin films, may be well known, making it difficult to predict their behavior and are possibly error prone.

The tools from macroscopic domains may not longer work, classical mechanics (Young's modulus of elasticity, hardness, bending strength, fracture toughness and fatigue life) must be partly replaced by molecular mechanics and finite element modeling to simulate the behavior nanosystems.

As of today, there exist no fabrication standards for nanoscale devices and materials, making comparison difficult. Main techniques are rather experimental than state of the art.

Storage issues, especially of MEMS and NEMS, as e.g. dust or debris can provoke failure. E.g. mechanical parts can be blocked or damaged or short-circuits provoked. ([8])

2.4.3 Environmental Implications

Because of their small size, nanoparticles can in certain cases penetrate cell membranes and integrate themselves into larger molecules. They can resist cellular defense systems but are large enough to interfere with cell processes. For example, in an inhalation experiments with rats, using ^{13}C-labeled particles, it was found that nanosized particles ($\sim 25\,nm$) were taken up by the nerve cells and deposited in the central nervous system (CNS). Investigation also showed that these particles

were transported via (in this experiment olfactory) nerves at a speed of 2.5 mm per hour ([28]).

Despite widespread use e.g. in public consumables such as makeup and creams, the very traits that make nanoparticles useful might also generate toxic effects. There is a lack of knowledge about possible risks arising from exposure to nanoparticles. ([29], [30])

The release of nanoparticles in the environment and thus possible exposure to humans and animal species remains thus to be investigated. As with any new technology the benefits may be accompanied by possible risks and its abuse. The health and safety implications should be openly addressed and not be taken lightly.

2.4.4 Information Challenge

One of the big challenges of today's nanotechnology will be the management of the fast growing knowledge associated with it, where much specific and detailed interdisciplinary information necessarily must be connected to advance further. One idea is that progress will stand in a direct relationship to the intelligent disposal of knowledge.

For instance, in 2004 the European network Nanoforum[7] conducted an online survey to assess responses to the European Commission's proposed document "Towards a European Strategy for Nanotechnology". Altogether 749 persons were interviewed across Europe. In this context it is especially noticeable, that an urgent need to develop nanotechnology education and training was expressed, with 90 % of participants indicating that interdisciplinarity is a crucial ingredient. ([14])

2.5 Natural Nanotechnology

Nanotechnology is accessible since only a couple of decades, nature builds and controls nanoscale machinery since the first forms of life have been populating earth. This makes for a lead of around 4 billion years of nanotechnological engineering. Every cell's daily business includes the synthesis of protein from the corresponding DNA encoded information, the build up of large structures molecule by molecule like tough cell walls, the signaling and repair of damaged structures or the provisioning for energy for its functional cell organelles.

---

[7]Nanoforum was originally funded by the European Commission as a project in the Fifth European Community Framework Programme covering Research, Technological Development and Demonstration activities. Since July 2007 Nanoforum has been operating as an independent European Economic Interest Grouping.

After diligent investigation such systems can provide a wealth of robust recipes and approaches, inspire man-made structures or be possibly applied to them in analogous form.[8]

Nanotechnology in nature features various advantages from an scientific and engineering perspective. Natural systems offer diversity and availability and the freedom to study them for innovative applications. No legal issues exist that would restrict their investigation or translation into technological applications.

Desirable principles incorporated by natural systems include amongst others the ability to self-replicate, self-heal, awareness, motility and intelligence. Organisms are highly autonomous, their inner workings are reversible or cyclic and most of the functions performed within are very efficient.

---

[8] As Nobel Prize–winning chemist Richard Smalley observed in 1999, "Every living thing is made of cells that are chock full of nanomachines. . . . Each one is perfect right down to the last atom."

Chapter 3

Atomic Force Microscopy (AFM)

3.1 Introduction to Scanning Probe Microscopy

Nanoscale science and technology strongly depend on the ability to investigate and manipulate structures down to the atomic scale. When the Scanning Tunneling Microscope (STM) was invented in 1981 by G. Binning, H. Rohrer, Ch. Gerber and E. Weibel ([31]) it was for the first time possible to directly acquire three-dimensional (3D) images of solid surfaces with atomic resolution.

In STM an electric potential difference is applied between the STM scanning tip and the sample surface. Although the vacuum between these two represents an ideal potential barrier, electrons can "tunnel through"[1] with a probability that depends exponentially on the distance between tip and surface. The lateral resolution is typically less than $1\,nm$ and vertically less than $0.1\,nm$ - sufficiently precise to define the position of single atoms.

In 1986, only five years after the invention of STM which generally is applicable only to conducting samples the Atomic Force Microscope (AFM) was invented by G. Binnig, C. F. Quate and Ch. Gerber ([32]). Originally this kind of Scanning Probe Microscope (SPM) was developed for measuring ultrasmall forces (less than

---

[1]This so-called "tunnel-effect" is made possible because of quantum physical properties of electrons. They can behave both like particles and like waves and can be described by solutions to the so-called Schroedinger equation. These waves can penetrate a potential barrier that would be otherwise a forbidden area if the particle was described in the classical way. The particle can therefore "tunnel through" the forbidden area. One of the earliest cases of tunneling was explained for the alpha decay of heavy atomic nuclei in 1928. Many interesting tunneling phenomena in solids were anticipated but it had been difficult until 1960 to reconcile theory and experiment.

The principle of electron tunneling in normal and superconducting state had been effectively demonstrated in 1960 by I. Giaever when he observed current between two metallic parts separated by a thin layer of oxide ([33]). The ability to measure a tunneling current in these experiments gave very direct evidence that electrons could indeed penetrate a potential barrier and behave like a wave according to quantum mechanics.

$1\ \mu N$) between a probe and the sample surface. Soon it became evident that it was also a convenient tool for obtaining topological information of a surface by rastering across it. In the recent years probe–sample interactions were also increasingly used for quantitative analysis of mechanical, electronic, magnetic, biological, and chemical sample properties. The AFM can map this information with atomic resolution to the sample surface and in contrast to STM is not limited to conductive samples. ([34], [8])

3.2   Principles of AFM

The Atomic Force Microscope (AFM) measures the forces between a probe, the AFM cantilever tip, and the surface. In order to obtain a 3D image [z(x, y)] of the surface, multiple scans [z(x)] displaced laterally from each other in the y direction are acquired. The cantilever is rastered across the surface by means of piezoelectric drives. This can be done either by dragging the tip over the surface or by oscillating it just above the surface.
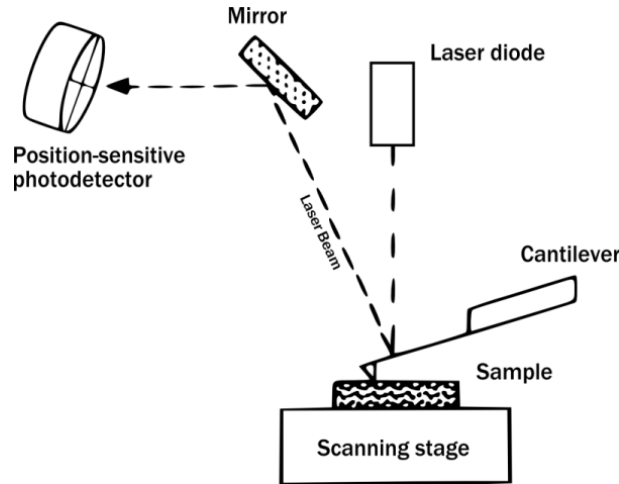

Figure 3.1: Generalized scheme of an Atomic Force Microscope (AFM) with optical beam sensing. Image adapted from [35].

The movement of the cantilever probe can be sensed by either tunneling, capacitive, or optical detectors. Optical beam deflection methods are often preferred because of their sensitivity, reliability and ease of implementation ([36], [37]). Advantages are a large working distance, insensitivity to distance changes and capability to measure angular changes (i.e. related to friction forces) when using a four-quadrant optical detector. A laser beam is deflected from the top side of the cantilever onto a position-sensitive photodetector (see Fig. 3.1). Because of the relatively large laser travel distance (in the *cm* range or more) the slightest skewness or bending of the cantilever or change of resonance frequency while

25

it scans across the surface can be recorded and used for deriving information on surface topography and other surface properties. The forces exerted on the sample during the scanning process can be limited in the feedback circuit that regulates the z-height of the cantilever tip.

There are basically two modes of operation in AFM, the static mode and the dynamic mode. (This classification follows [38].)
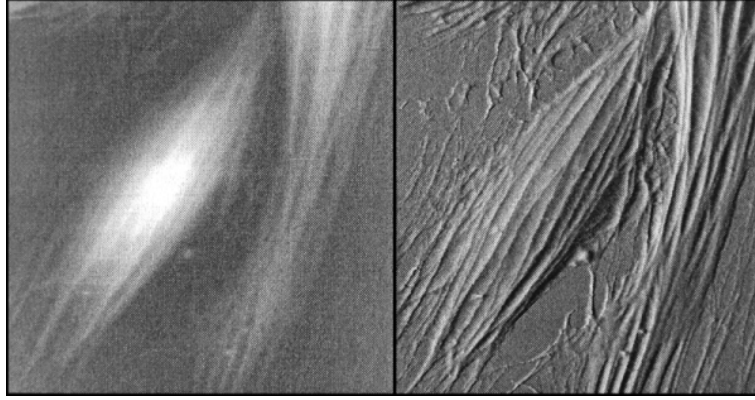
Figure 3.2: AFM Contact Mode images of endothelial cells. $65 \times 65\,\mu m^2$, left: height trace, right: first derivative of height trace. A thin layer of endothelial cells builds the interior surface of blood vessels. They are present in the entire circulatory system, from the heart to the smallest capillary and reduce friction between the circulating blood and the vessel walls. The height of endothelial cells typically measures up to $4\,\mu m$. Image adapted from [39].
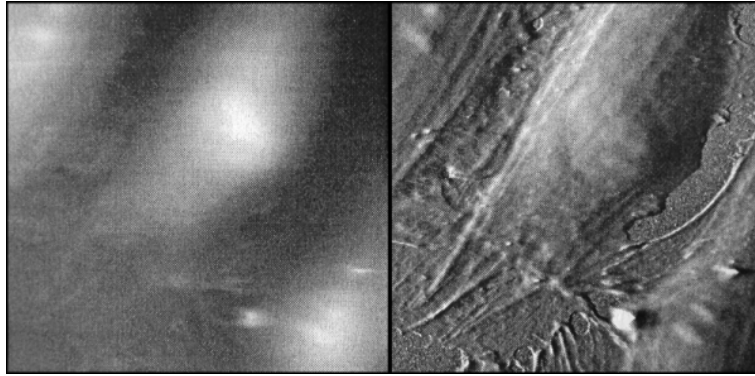
Figure 3.3: AFM Intermittent Contact Mode images of endothelial cells. $65 \times 65\,\mu m^2$, left: height trace, right: first derivative of height trace. Because of the reduced contact forces, the imaged cell membranes are pressed less against the cytoskeleton than in Contact Mode. ([39])

3.2.1 Static Mode

In Static Mode (also referred to as **Contact Mode** or Repulsive Mode) the AFM cantilever tip contacts the sample surface during moving over it or while the sample is moved below and the tip rests immobile. The tip-atoms feel a force caused by the electronic orbital overlap with the surface atoms. This repulsive force in the range of 10^{-9} N causes the cantilever deflection (example in Fig. 3.2).

The cantilever is moved relative to the sample surface with a piezoelectric positioning element. During the scanning process, the deflection of the cantilever is permanently sensed and compared in a direct current (DC) feedback amplifier to a preset value of deflection (setpoint). Through variation of this setpoint, the contacting force between probe and sample surface can be influenced. If the feedback loop measures a deflection different from the preset value, the applied voltage to the piezo is raised or lowered according to whether the cantilever must go up or down to keep a constant force on the sample.

The measured cantilever extension, the height position along the z-axis, on every point of the sample is function of the surface feature height of the sample in that point. This is true for hard samples but must be verified for scanning soft samples. Excessive applied imaging force could induce sample deformation and thus distorted topography data. Such forces applied by the probe to the sample can cause various problems in contact mode AFM. While such effects can be reduced by minimizing imaging forces, there are practical limits. Low forces usually have the benefit of interfering little with the sample surface, higher forces give a better signal during scanning.

Under ambient conditions, sample surfaces are covered by a thin water layer. When the probe makes contact with this layer, a so-called meniscus forms and the cantilever is pulled by surface tension toward the sample surface. This meniscus force and other attractive forces may be minimized or even neutralized if the probe-sample interaction takes place in liquid (such an AFM setup is shown in Fig. 5.9, p. 76). Elimination of capillary forces, the reduction of van der Waals' forces and the ability to study technical or biological processes at the liquid-solid-interface are important benefits of this variation.

3.2.2 Dynamic Mode

Non-Contact Mode

For investigation of more sensitive samples the operating mode of choice could be the so-called Non-Contact Mode (developed in 1987, [40]). Main characteristic is that the cantilever tip interferes very little with the sample surface, only hovering above it.

The tip hovers $5-15$ nanometers above the sample surface and only van der Waals forces between the tip and the sample, mostly attractive, are present. Since these forces are substantially weaker than the forces used in contact mode, the tip is deliberately vibrated near its resonance frequency - by measuring the change in amplitude, phase, or frequency of the oscillating cantilever when it approaches the surface the small forces present between the tip and the sample can be detected.

The fluid layer is usually thicker than the range of the van der Waals force gradient and therefore, attempts to image the surface with non-contact AFM under ambient conditions fail (or result in imaging the fluid layer respectively), as the oscillating probe may be trapped in the fluid layer or hovers beyond the effective range of the forces it attempts to measure. However non-contact mode AFM is a very successful and useful method in Ultra High Vacuum (UHV).

Intermittent Contact Mode

The Intermittent Contact Mode (sometimes referred to as "Tapping Mode"[2]) is a technique ideal for imaging sample surfaces that are easily damaged, loosely attached to their substrate or difficult to image by other AFM techniques. Lateral forces on the sample are smaller than in contact mode and therefore this imaging mode is especially suited for soft samples such as biological samples. This method can be used in air and liquid and the resolution is similar to contact mode (See Fig. 3.3).

The tip is only brought in short contact with the surface and then moved away from the surface to avoid scratching it. In tapping mode the cantilever is oscillated at or near its resonant frequency, usually in the range of $10-500\,kHz$ using a piezoelectric crystal. At first, when the tip is not yet in contact with the surface, the cantilever oscillates with a high amplitude ,typically greater than $20\,nm$. The tip is then approached to the surface until it begins to gently touch or tap the surface. The amplitude of the cantilever oscillation is reduced due to energy loss caused by the tip contacting the surface. This reduction can be used to identify and measure surface features. In contact mode, the preset scanning parameter is the deflection, while in tapping mode the cantilever oscillation amplitude is kept constant by a feedback loop (again called setpoint). The amplitude is reduced when the tip passes over a bump in the surface, since it has less room to move. Passing over a depression, the cantilever has more room to oscillate and the amplitude increases and approaches the maximum free amplitude. The oscillation amplitude is permanently measured and the digital feedback loop adjusts the tip-sample separation to reattain the given amplitude setpoint.

From the phase differences between the oscillations of the driving piezoelectric

---

[2]Operating an AFM in "Tapping Mode" was patented by Veeco Instruments Inc. In the beginning of 2006 their related European patent No. 839,312 was confirmed by the European Patent Office in Munich, Germany when the patent office dismissed the opposition filed by Asylum Research Inc.

crystal and the cantilever tip (phase imaging) additional information about the viscoelastic properties of the sample can be gained (see Figs. 3.4, 3.5) .

Figure 3.4: The phase shift is calculated from the horizontal displacement of the cantilever oszillation (solid line) relative to the oszillation of the driving piezo crystal (dashed line) in time. The shift depends on different surface properties (e.g. elasticity, stickiness) and parameters of the AFM operation.

The phase offset is caused by interaction with the surface and changes for different materials as it depends on various parameters such as adhesion, friction or viscoelasticity. Therefore phase imaging can help distinguish different areas of interest on the sample not distinguishable by their topologies.

Choosing a cantilever with a high frequency lets the surfaces seem stiff, and the tip-sample adhesion forces are greatly reduced. Unlike contact and non-contact modes, when the tip contacts the surface, it has sufficient oscillation amplitude to overcome the tip-sample adhesion forces. ([41], [38])

Resolution Limits

In order to obtain atomic resolution with the AFM, the spring constant of the cantilever should be weaker than the equivalent spring constant between atoms. For example, the vibration frequencies of atoms bound in a molecule or in a crystalline solid are typically on the order of $10^{13} \, Hz$ or higher. Combining this with the mass of the atoms m, on the order of $10^{-25} \, kg$, gives an interatomic spring constant $k(\omega^2 m)$, on the order of $10 \, N/m$. Therefore, a cantilever beam should have a spring constant of around $1 \, N/m$ or lower. To compare with a macroscopic object, the spring constant of a piece of household aluminum foil that is $4 \, mm$ long and $1 \, mm$ wide is also about $1 \, N/m$.

Second, tips as sharp as possible are desirable when imaging solids. The tip diameter naturally sets a resolution limit as features smaller than this diameter
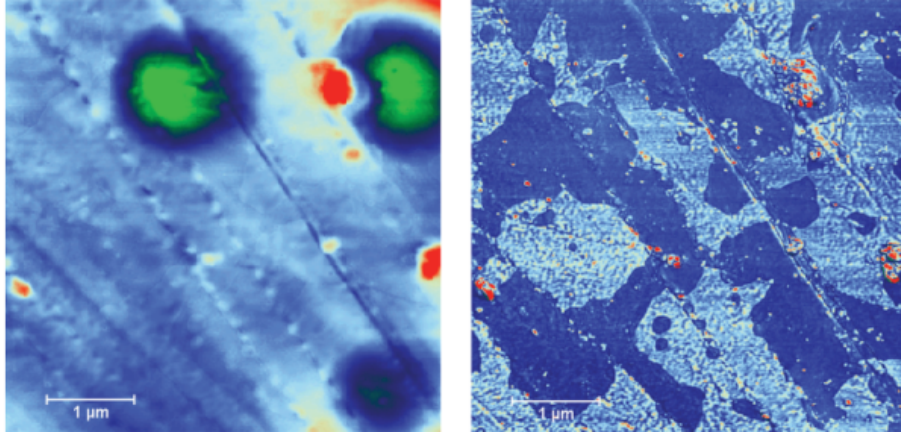
Figure 3.5: The left image is a topographic image of a polyurethane tube coated with a lubricious hydrogel. Colors indicate surface height (dark blue being low, red being high). Height range is $100\,nm$. The right image is a phase image of the same area, acquired simultaneously with height information. It displays the phase lag of the oscillating cantilever relative to the driving force as a function of lateral position. The coating has areas with different physical characteristics that cannot be seen in its topology. Image adapted from [42].

cannot be fully resolved. In comparison, for biological samples often larger tip diameters are used, because of easily perforated membranes. Tips with radii ranging from 5 to $50\,nm$ are commonly available.

Ambient atomic force microscopes can be enhanced for better resolution in a variety of ways. The most common ways are the addition of a fluid cell (no water meniscus between cantilever tip and surface), operation in UHV (no water meniscus and clean sample surfaces) and operation at low temperatures, when thermal motion of atoms must be reduced for very high resolution imaging. An example for a sub-nanometer resolution as can be achieved by AFM is given in Fig. 3.6. ([8], [43], [44], [45], [46])

3.3   Analytical Microscopy Probing

While investigation of topology was the predominant use in the early stages of SPMs, it soon became evident that there was a much richer set of information and possibilities to be gained from these techniques.

These new methods can roughly be divided into methods that characterize the sample on the single atomic or molecular level, e.g. unit cell structure, atomic species or identification of protein binding sites, and methods that characterize the sample as a system of atoms, e.g. bulk properties or emergent properties
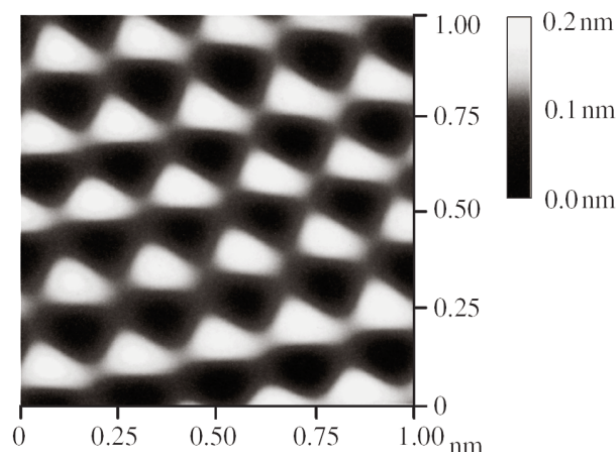
Figure 3.6: Highly ordered and freshly cleaved pyrolytic graphite at atomic resolution imaged with an AFM in UHV. Image adapted from [8].

characteristic for a collection of atoms like electrostatic, magnetic, tribological, and viscoelastic properties.

A selection of the most widely used techniques is given beneath.

3.3.1 Single Atom and Molecule Information

- Position of single atoms and single molecules (e.g. pyrolytic graphite in Fig. 3.6)

- Chemical identification of individual surface atoms. The onset of chemical bonding between the approaching tip and surface atoms gives rise to short-range forces that depend sensitively on the chemical identity of the atoms involved. These can be measured by sensitive AFM. (Tin (Sn), Silicon (Si), Lead (Pb) as detected by AFM can be seen in Fig. 3.7, [47])

- **Molecular recognition** studies using AFM open the possibility to detect specific ligand–receptor interaction forces and to observe molecular recognition of a single ligand–receptor pair. The approach is to bind either ligand or receptor to the AFM tip when its counterpart should be found on the investigated surface. In a force–distance cycle (as graphed by a force curve, see below), the tip is approached towards the surface and, if the counterpart is present, a receptor–ligand complex is formed because of the specific ligand receptor recognition. Upon retraction an increased force (unbinding force) must be exerted in order to break the ligand–receptor connection (e.g. antibody binding and recognition in [48]). Such experiments allow for estimation of affinity, rate constants, energies ([49]) and structural data of the binding pocket ([48], [50], [51], [52], [53], [54]). There have also been attempts to

31

apply recognition force microscopy to living cells (e.g. [55]). The ligand-receptor binding is generally a reversible reaction. An advancement of above technique led to the possibility of simultaneous identification of two types of proteins in compositionally complex samples. ([56])

- **Recognition imaging** combines molecular recognition with surface imaging. It means the mapping of ligand-receptor interaction sites on surfaces with nanometer positional accuracy. E.g. identification and localization of receptor binding sites distributed on biological membranes.

- **Real Time Protein-Protein Interactions** ([57])
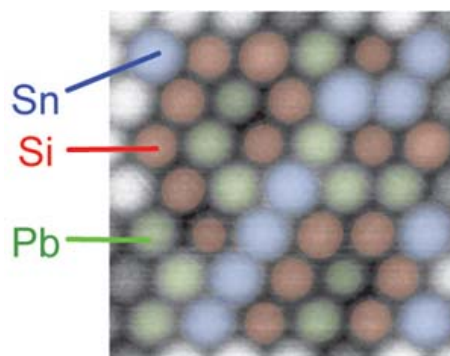
Figure 3.7: The differentiation of atomic species by AFM as achieved through measurement of short-range forces. Atoms of the same type are colored the same. ([47])

### 3.3.2   Atomic Collection Information

- **Surface topography**

- **Surface profiling**

- Measurement of **adhesion and friction** of solid and liquid surfaces. This can be achieved through measurement of lateral forces on the cantilever tip. Any AFM that can measure the tilt (see Fig. 3.9) of its scanning cantilever, e.g. with a four-quadrant photodiode, can perform lateral force measurements. Lateral force microscopy (LFM) measures lateral deflections (tilt) of the cantilever arising from forces on its tip parallel to the plane of the sample surface. (ref. [58], [59], [60], [61], [62])

- **Magnetic Force Microscopy (MFM)**. With an AFM cantilever, that is coated with a ferromagnetic thin film, the spatial variation of magnetic forces on a sample surface can be imaged. The tip is hovered over the surface in
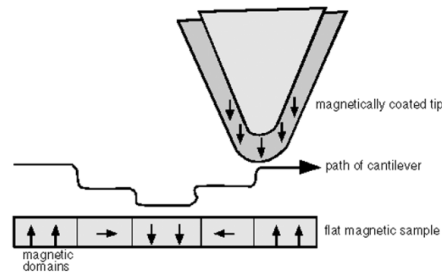
Figure 3.8: Schematic drawing of the principle of Magnetic Force Microscopy. The resonant frequency of the cantilever is influenced while the cantilever hovers in the magnetic field of the sample. Image adapted from [63].

non-contact mode and changes its resonant frequency upon variation in the present magnetic field (see Fig. 3.8).

- Cell membrane and lysis kinetics ([64])

- Measurement of **scratch resistance**, **wear**, and **elastic and plastic mechanical properties** such as indentation hardness and the modulus of elasticity. ([65], [66], [67])
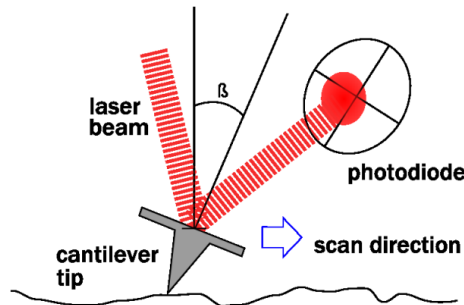

Figure 3.9: The amount of tilt (angle β) a cantilever has while scanning the surface in contact mode can be used to derive friction coefficients of that surface. If probe sensing is performed with an optical detector, a four-quadrant photodiode can be used to measure bending and twisting of the cantilever.

- **Surface potential** determination. After a first contact scan a second scan is performed hovering a certain distance above the surface. This time a dc-voltage is applied to the tip that equilibrates the local electrostatic potential on the sample so as to eliminate forces on the AFM tip caused by electric repulsion or attraction between tip and sample. This technique is called scanning surface potential microscopy (SSPM). A real example is e.g. the investigation of the electric surface potential of carbon nanotubes ([68]).

- **Force curves** provide detailed information on viscoelastic properties of the material. They record the response of the material to forces applied by the cantilever tip.

Force curves

Force curves are an excellent tool to investigate the viscoelastic properties of a material at the nanoscale. The main elements of a force curve are shown in Fig. 3.10. A force curve is made by pressing and releasing the cantilever against and from the surface. The material responds through small deformations to the exerted forces. For a hard material the deformation stays small, the lowering of the cantilever base corresponds to the bending of the cantilever tip in the opposite direction (as in Figs. 3.11, 3.13). Soft materials show higher compliance and materials with adhesive properties bend the cantilever towards the surface upon retraction (Figs. 3.14, 3.15).
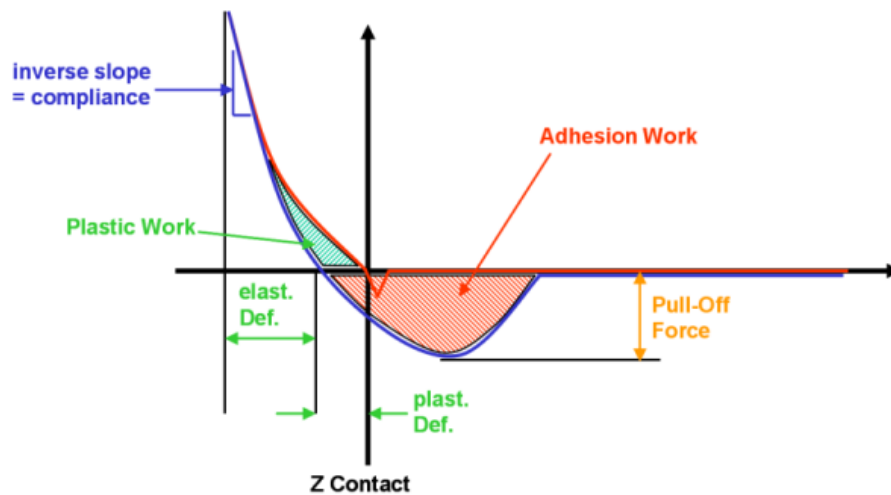

Figure 3.10: A selection of information that can be gained from a force curve graph. The red curve corresponds to the lowering of the cantilever, the blue to its retraction. Values on the abscissa correspond to the height of the cantilever base, ordinate values correspond to the measured displacement of the cantilever tip. Image adapted from [69].

The information of a force curve can also be represented in a force-distance graph, showing the deformation of the contacted surface area as a function of the applied cantilever force. The forces also can be pulling forces, if the cantilever is held back during retraction e.g. on adhesive surfaces and while performing molecular recognition. For a single protein that unfolds while one end is attached to the surface and the other is being pulled by the cantilever, this graph is called a force extension profile. The steplike character of such a curve is characteristic of how the protein unfolds under a pulling load. A force extension profile of a single

34
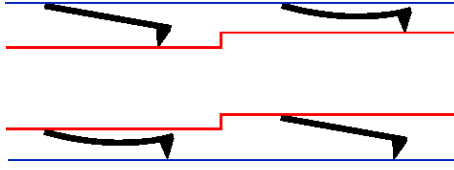
Figure 3.11: The cantilever deflection (bending). For a hard surface it amounts to the same effect if either the cantilever is pushed against the surface or a surface feature pushes against the cantilever. This fact can be used in order to calibrate the reading from the photodiode measuring cantilever bending.
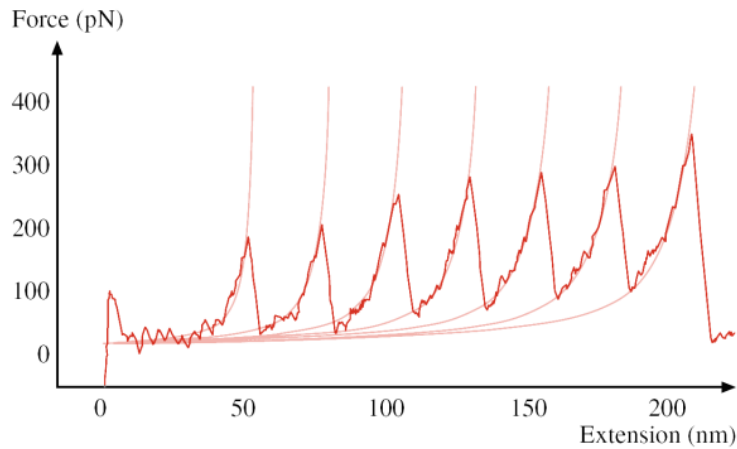

Figure 3.12: Force extension profile of a single titin molecule. The titin protein is folded in several subunits that unfold in sequential order when the protein is stretched. Each unfolding event is recorded as a sharp drop of the pulling force that acts on the cantilever. Image adapted from [8].

titin molecule is show in Fig. 3.12. The periodic sawtooth-like pattern reflects domain unfolding in the peptide chain consistent with its modular construction and can be explained as a stepwise increase of the molecule's length upon each unfolding event. ([70])

3.4   AFM Manipulation Techniques

Besides information collection the AFM can be used to manipulate matter on the small scale. Although this can be a time consuming process, only having one cantilever to do the work, the sample can be altered in a very precise way. The techniques can be classified into three categories, adding matter to, rearranging or removing matter from the substrate. Some of the methods, of course, may overlap in those categories as more effects apply at the same time.
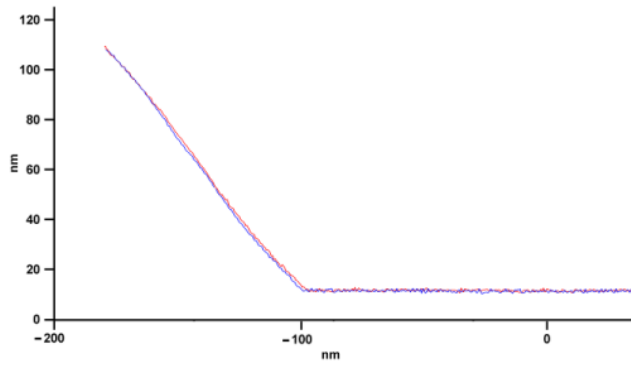
Figure 3.13: The above force curve is a typical calibration force curve on glass. Once the cantilever tip has contact with the hard glass surface lowering the cantilever base further results in displacement of the tip relative to its normal position by the same amount (see also above Fig. 3.11). The red curve corresponds to the lowering of the cantilever, the blue to its retraction. Values on the abscissa correspond to the height of the cantilever base, ordinate values correspond to the calculated displacement of the cantilever tip (zero points are arbitrarily chosen).

The combination of the information gathering methods from the previous section and the methods to manipulate things at the nanoscale represents a strong toolset for investigating and building small structures. Eventually, scientists will have a great collection of these tools to their disposal arranged in a large database combined with smart software, managing all this knowledge. One could imagine a Lego^{TM}-like building kit for thorough investigation, simulation and creation of robust and versatile nano- and microstructures.

A selection of important manipulation techniques follows.

3.4.1 Rearrangement of Matter

- AFMs have been used for **manipulation of individual atoms** of Xenon(STM) , molecules ([71]), silicon surfaces ([72]), and polymer surfaces.

- STMs have been used for formation of **nanofeatures** by localized heating or by inducing chemical reactions under the STM tip ([73], [74], [75]) and **nanomachining**. ([76])

- AFM **Nanopatterning** processes.

36
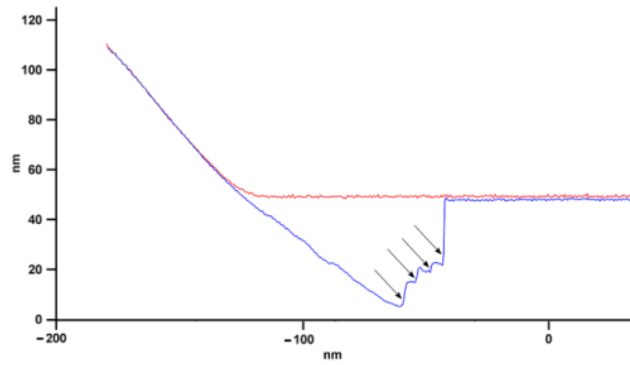
Figure 3.14: This force curve shows the effect of tip interaction with a sticky surface. Upon retraction (blue curve) the cantilever tip is hold back until the pull off force is great enough to break the remaining bonds between tip and surface. Steps in the curve (arrows) indicate individual unbinding events happening until full detachment.
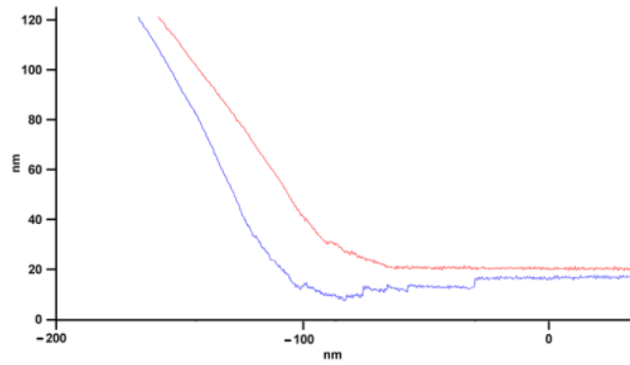
Figure 3.15: This force curve Biological soft material, force curve

3.4.2 Addition of Matter

- Dip-Pen lithography. The cantilever tip is used to take up material (by contacting it or dipping into it) and deposit it at a given position.

- Aggregation of surface particles into the area of interest. E.g. the pushing of nanoparticles of $La_{0.7}Sr_{0.3}MnO_3$ ([77]).

3.4.3 Removal of Matter

- AFM has been used for nanofabrication ([78], [79], [80]) and nanomachining ([81]).

Chapter 4

Euglena gracilis

4.1 Overview

4.1.1 Introduction

The algal flagellate *Euglena* has for long been an outstanding subject of study for biologists. It has been maintained in culture in many laboratories as an experimental organism and almost every biology student has observed it during microscopy courses. As of today this species is one of the most completely studied. ([82])

These small yet complex organisms dispose over a plethora of bionanotechnological machinery in order to live, survive and procreate. Their long feature list includes amongst others a flexible outer shell (the pellicle) that protects them, a mobile thread (the emergent flagellum) that propels them with high speed through the liquid, a protein crystal that enables them to sense light and chloroplasts that convert sunlight photons into storable energy. This energy is in turn stored through means of lipid vesicles and semicrystalline starch deposits (paramylum[1] grains). If the cell cannot use its flagellum for locomotion it can move by metabolic movements (this so-called "euglenoid movement" is similar to that of a worm contracting the back and extending the front part) - sliding along solid material and being lubricated by its own muciferous lubricant excreted from pellicle pores.

The ability to feed on sunlight only (although it must take up the vitamin B-12, which it cannot synthesize itself, from the surrounding) and to survive even with no light present at all by forcing itself to heterotrophic[2] metabolism has raised some discussion whether this organism is more 'plant-like' or 'animal-like'. Photosynthesis (and its prerequisites, the chloroplast plastids within the cell) is a strong argument to classify it amongst plants, yet an *Euglena* cell has no cellulose cell wall

---

[1]"paramylum" is equivalent to "paramylon"

[2]Heterotrophic means that the cell requires organic substrates as source for carbon in order to grow and develop.
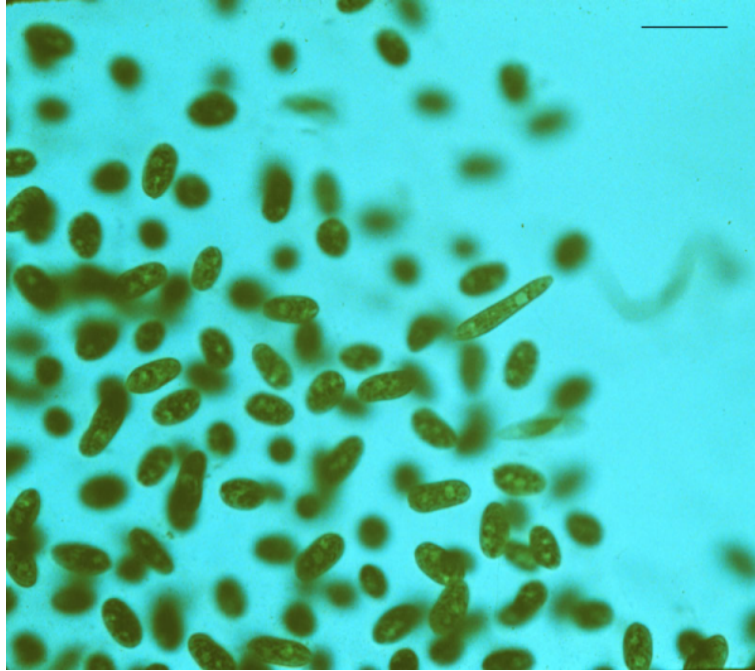
Figure 4.1: A group of *Euglena* organisms. The naked human eye can see them only as tiny green dots or as a greenish coloring of the water. Scale bar is 50 μm. Image adapted from [83].

(its protective hull, the pellicle, is inside the plasmalemma) and is a very active swimmer using its whip-like flagellum, an ability rather associated with animals. This lets guess the unusual cross-functionality regarding metabolism, organelles and lifecycle exhibited by *Euglena*. All these things are marvels in their own right, often based on functional materials produced with molecular precision and evolutionary optimized throughout millions of years. That said, it seems like an open invitation for nanotechnologists to explore and learn from this organisms versatile materials and structures. Long before the term "nanotechnology" was born, this intuitive understanding of how delicately crafted nature's creatures are was expressed by german philosopher Schopenhauer (1788-1860) with the following:

> Every short-witted boy can tread down a beetle, but all professors in the world cannot build one.[3]

Maybe we can build beetles one day, but we should start out a little bit smaller, by studying the components that make these beautiful creatures possible.

---

[3]The german original citation reads: "Jeder dumme Junge kann einen Käfer zertreten. Aber alle Professoren der Welt können keinen herstellen."

4.1.2 Origin of the name "*Euglena*"

Euglena was named by the german naturalist Christian G. Ehrenberg (1795–1876) and diagnostically defined by him already in 1838. The word "Euglena" is formed from the two greek words "eu" and "glene" which mean "good" and "eyeball" respectively, because of the clearly visible (with optical microscopes) stigma, also called the eyespot ([84]). It was thought that this "eyespot" was light-sensitive and used by the alga to direct itself towards the light[4]. But we know today that its role is only to intermittently shade the photoreceptor (attached to a flagellum inside the vacuole of the cell) as the cell revolves around its long axis. In this sense it is only a sub-part of the algal optical system.

Experimental work on *Euglena gracilis* effectively began in 1900, when Zumstein ([85]) succeeded in axenically[5] cultivating this flagellate, which then became a major subject of physiological reports. Most of the present studies still use this species and very often even Zumstein's original strain "Z". ([86])

4.2 General characteristics

4.2.1 *Euglenophyta* (*Euglenida*)

Euglenophyta are single celled organisms living in clean to nutrient-rich standing water bodies depending on genera. Some marine forms, living in salty water, are also known. They propel through water using actively rotating flagella. As they are commonly green, mass occurrences are responsible for greenish water coloring. The green color stems from chlorophyll used by these organisms for performing photosythesis. Under certain circumstances some of these genera pass over to heterotrophic food. They then loose their chlorophyll and feed on organic material that can be taken up through osmosis.

A subgroup of flagellates even exempts all chlorophyll feeding on detritus and bacteria. These algae have lost the ability to reassemble their chlorophyll when brought back to ambient light conditions. (e.g. *Khawkinea quartana* is a natural occurring euglenoid that lost its chlorophyll plastids permanently. There is evidence that the ancestor of the colorless *K. quartana* was a pigmented *Euglena*. ([87], [88]))

Amongst the genus *Euglena* over 1000 species of *Euglena* have been described. Marin et al. ([89]) revised the genus so that it forms a monophyletic[6] group, moving

---

[4]Thus the german name "Augentierchen".

[5]Growing a culture of cells "axenically" means that this culture is not contaminated by or associated with any other living organisms.

[6]In the study of evolutionary relatedness among various groups of organisms (phylogenetics), a group is monophyletic if it consists of a common ancestor and all its descendants. ([90])

several species with rigid pellicles to the genus *Lepocinclis* and including several species without chloroplasts, formerly classified as *Astasia* and *Khawkinea*. Size varieties range from 25 μm to 500 μm in length and cells can be of various body shapes.

4.2.2 Diagnostic Features

The euglenoid flagellates are a well-defined group of closely related organisms. Interestingly, hardly any forms are known which appear to be intermediate between the *Euglenophyta* (*Euglenida*) and other algal phyta or protozoan orders[7].

The main characteristics of this group include:

- **Two flagella**, one of which emerges from the canal as the **locomotory flagellum**, whereas the other is so short as to be **non-emergent** from the reservoir.

- Usually colored green (rarely colorless)

- **Phototrophic and heterotrophic**

- Chloroplasts discoid, shield-shaped or ribbon-shaped, entire or dissected, with or without pyrenoids, pyrenoids naked, double-sheathed or inner. Each **chloroplast type is characteristic of a species**.

- A stigma (eyespot) and a flagellar swelling (with the photoreceptor inside) are present.

- The cell is non-rigid or semi-rigid, but **never completely rigid**. The body of the cell is enclosed by the pellicle, a very tough but flexible structure built out of ridged, articulating strips. The alga can actively change its shape to move forward (**metaboly or so-called euglenoid movement**). ([91])

- Cell flattening apparent in some species

- **The cells are free-swimming and solitary** but cysts and palmelloid stages are known (see 4.2.5). A contractile vacuole (see 4.3.6) is present, even in marine forms [8].

---

[7]A phylum (pl. phyta), also called division, is a rank in the classification of organisms, below kingdom and above class. An order is a rank between class and family. ([90])

[8]Why is it noteworthy that a contractile vacuole (see 4.3.6) is present in marine forms? Usually the concentration of solubilized molecules or certain ions within the cell is higher than in the outer medium (for example sucherose, sodium ions and chloride ions). This corresponds to the fact, that the cell actively accumulates and stores carbohydrates for later use. And it indicates that life took its origin in the sea where those concentrations are much higher. The chemism of the inner cell represents a "memory" of these past habitats from even millions of years ago

- Many species are known, mostly fresh-water. A few marine species have also been recorded.

A good characteristic for differentiation between *Euglena* genera is the shape of their chloroplasts. For example *E. pisciformis* possesses sideways bands of chloroplasts, *E. terricola* has a scattered distribution of band chloroplasts and *E. viridis* exhibits center orientated band chloroplasts. There are also disc-shaped chloroplasts like these of *E. variabilis, E. intermedia, E. ehrenbergi, E. acus, E. acutissima, E. oxyuris, E. tripteris, E. deses, E. sanguinea,* last of which has red colored ones. And then *Euglena gracilis* has cornered chloroplasts. ([92], [93])

4.2.3 Characteristics of *Euglena gracilis*

4.2.4 Natural Habitat

Euglena gracilis is a relatively rare species amongst other *Euglena* types found in nature, characteristically encountered in ponds and ditches containing rotting leaves or in other nutrient-rich waters.
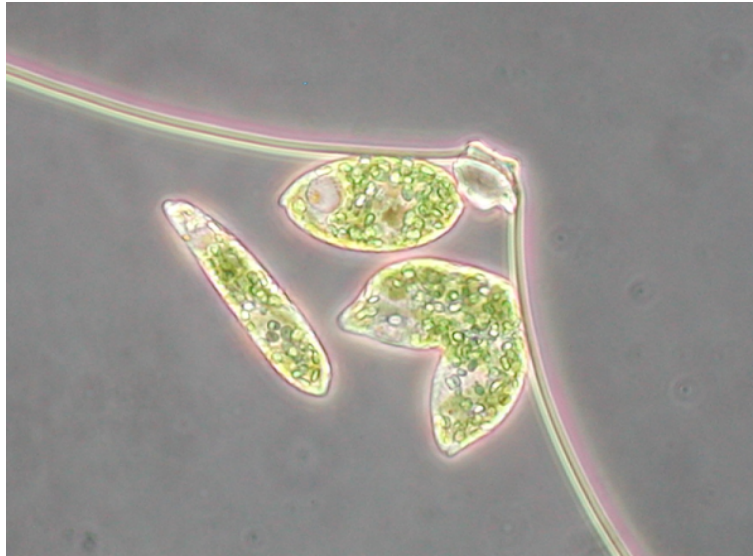
4.2.5 Lifecycle

A *Euglena* cell is not born, nor does it hatch. A parent cell divides into two daughter cells, not to be told apart, which then again enter a new lifecycle. The cell division primarily takes place in darkness, and thus mostly during nighttime and along the cells' long axis. This can happen either in the normal state or in the palmella state (see below). A division takes usually between two and four hours. One could argue, (astonishingly enough!) that *Euglena* cells do not die but literally live on in their offspring. For cultured cells on the contrary, it has been observed that, if they live in old cultures, they become packed with phospholipid vesicles and the culture starts looking brownish.

When turning into the so-called palmella state, *Euglena* discards its flagellum, then forms itself into a spherical shape and excretes a muciferous layer covering all of the body. The colony then flocks together in a jelly like matrix where they cannot move. When the habitat living conditions improve *Euglena* can transform back again into the motile state.

([93]). That means marine forms of *Euglena* are put under much less stress to preserve the right concentrations especially of ions. Liquid leaking into the cell through osmotic pressure is already close in composition to what the cell needs, so ejecting H_2O periodically through the contractile vacuole is much less imperative.

Figure 4.2: The rightmost cell can be seen in the process of cell division. After 2-4 hours, two equal daughter cells will begin their new lifecycles.

4.3 *Euglena* Subsystems and Technical Application

Interesting subsystems of *Euglena gracilis* can be found on every scale, from its entire body pellicle down to the light capturing and transduction mechanism where single protons play a major role.

Accordingly many aspects of theoretical nature are involved such as the mechanics of proteinaceous strips composing the pellicle, the biochemistry of rebuilding lost chloroplasts, the electrochemistry of aforementioned signal transduction from the stimulated light receptor, the biophysics of concerted microtubuli contraction and detraction for euglenoid movement and many other processes sometimes also to be found in other living systems. Thorough investigation demands an interdisciplinary approach, especially since at small scales, as acknowledged by the nanosciences, a wealth of effects begin to have considerable influence that would be negligible in the macro-cosmos.

I will focus here on some of the cells essential functional units, and the tasks they perform. As every other organism *Euglena* senses the environment (Photoreceptor 4.3.3), converts and processes this information (Photoreceptor Signal Transduction 4.3.3) and as a result acts within and on the environment (e.g. Motory System, Phototaxis 4.3.2, Euglenoid movement 4.3.4). In order to perform all these tasks *Euglena* has to assure it stays in operational conditions, where main requirements are mechanical and chemical protection (Pellicle 4.3.4, Vacuole 4.3.6) from the environment and by taking up Energy and storing it (Metabolism 4.3.5).

Possible technical applications inspired by subsystems of *Euglena* are given in 4.4.

4.3.1 Structural Overview

A schematic drawing of *Euglena gracilis* can be seen in Fig. 4.3. The motory system of *Euglena* possesses two flagella, one of which emerges from the reservoir (the emergent flagellum). The second is termed non-emergent flagellum. Attached to the emergent flagellum, still within the reservoir is the photoreceptor, a proteic crystal, located. Besides the reservoir the stigma can be found, (also called "eyespot"), that consists of pigment granules (containing carotenoids), and is part of the visual system.
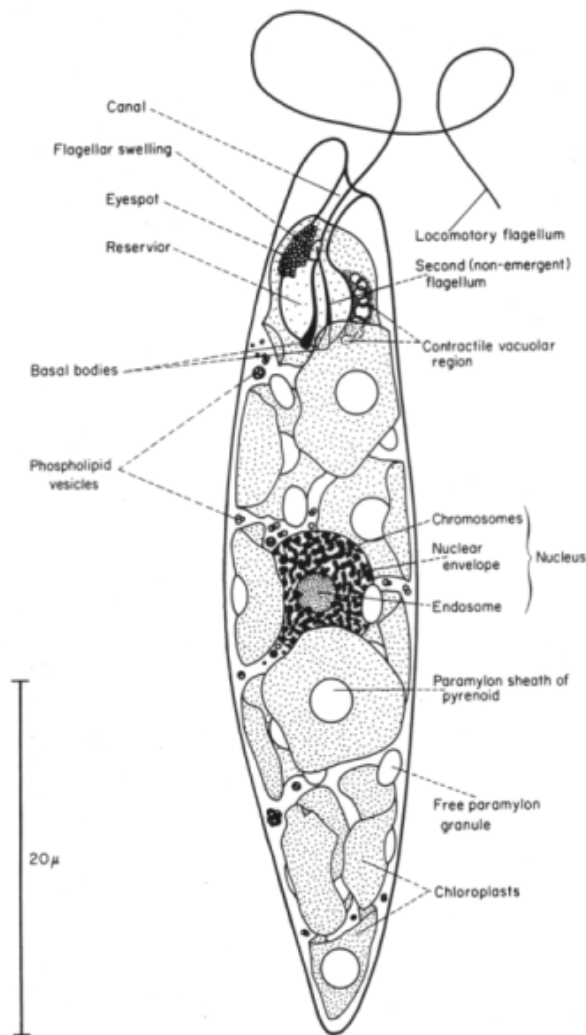
Figure 4.3: Schematic drawing of an *Euglena gracilis* cell. Image adapted from [84].

Next to the stigma sits the contractile vacuole, that empties into the reservoir

cavity and is used for regulatory functions concerning the cell fluid (cytosol[9]). The vacuole surrounds the bases of the flagella. It is limited by a unit membrane and discharges rhythmically every $20 - 30$ seconds.

The boundaries of the elongated *Euglena* body are formed by the outer tri-partite (three-layered) plasmalemma membrane surrounding the pellicle composed of interlocking and articulating flexible strips. These ribbon-like strips are spirally arranged and underlain by microtubuli.

Inside the cell fluid, near the center of the cell the nucleus containing all the cell DNA can be found. The chloroplasts of *Euglena* account for a great percentage of cell organelles - its main energy providing facility. The cornered shape of these is characteristic for *Euglena gracilis*. A lot of other entities such as paramylum granules, lipid bodies, crystalloid bodies and phospholipid vesicles can be found spread throughout the cell.

4.3.2 Motory System and Phototaxis

The elongated cell swims edgewise while it rotates around its long axis. It pulls itself through the water by means of the flagellum - thus moving in the direction of the apical part, where the locomotory (emergent) flagellum protrudes.
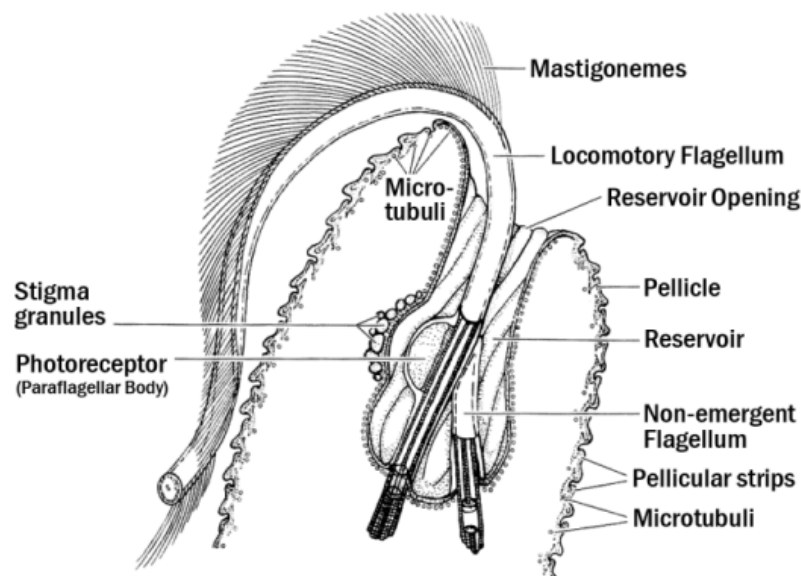

Figure 4.4: Apical part of *Euglena viridis*. Image adapted from [94].

The apical part of the cell bears the reservoir, an inversion of the pellicle, with two thin rods emerging out of its base part, the two flagella. One of these

---

[9]The cytoplasm in comparison is defined as the sum of the cytosol and the embedded organelles and inclusions.

45

is protruding to the outside and thus called the emerging flagellum, the other one ends inside. Both take their origin in the basal bodies embedded in the base of the reservoir (see Fig. 4.4). The emergent flagellum contains a paraxial rod, bears mastigonemes (hairlike structures covering the flagellum) and is characterized by a swelling that contains the photoreceptor. The other flagellum is reduced to a short stub and its distal end approaches the emergent flagellum in the region of the swelling.

The photoreceptor, also called paraflagellar body (PFB), is connected to the flagellar rod and protected by a surrounding membrane. It is a highly efficient light detector (see 4.3.3) and forms together with the stigma the visual system of *Euglena*. The stigma (indicated by an arrow in the leftmost image in Fig. 4.8) consists of tiny carotenoid droplets just adverse to the photoreceptor. The droplets shield the photoreceptor from incident light once every revolution during swimming. This simple but complete visual system allows *Euglena* to orientate itself towards a light source. [82]
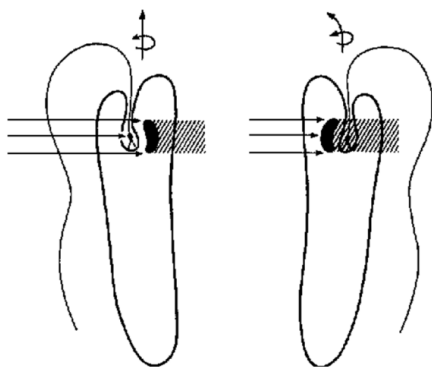
Figure 4.5: *Euglena* in different positions relative to the light source (the incident light comes from the left, the shaded area is drawn hatched). Swimming direction is upwards. Image adapted from [95].

The light-orientated movement of the cell, the phototaxis, is caused by the teamwork of the stigma and the photoreceptor. During its movement, the cell permanently rotates and the stigma comes between the light source and the photoreceptor (see Fig. 4.5). *Euglena* experiences a periodical decrease in light intensity and changes its direction of movement until the detected light is no longer modulated by the stigma. Then the cell is moving towards the light source.

If the light intensity is very strong, the cell flees from the light, also referred to as negative phototaxis. Interestingly enough this process seems not to involve the stigma - it also occurs after removal of this cell organelle. This enables *E. gracilis* to either swim towards the light (if the organism receives less light than the optimum) or away from it when too much light (especially UV-light) could damage the cell. The changes of direction for positive phototaxis can be seen

as phobic reactions, because the cell is not directly swimming towards the light. Only after a series of seemingly chaotic changes a topic approach of the light source appears.

During nighttime the motility of *Euglena* cells is low, they founder to the ground. During daytime they rise again. But even when the organisms are brought into the dark for a longer period, their activity shows a circadiane rhythm.

Euglena possesses a second important mode of locomotion. When swimming ceases, so-called "euglenoid movement" which alternates phases of contraction and elongation appears. When only little space is given to the alga to move, e.g. between two flat glass slides, this kind of movement can be forced. In order to support such a vicious change in shape during euglenoid movement, the pellicle of *Euglena* has evolved into a very elastic and refined structure (see 4.3.4).

4.3.3 Photoreceptive Apparatus

The ability to perceive light and adapt to changing light conditions is crucial to photosyntactic organisms, therefore detecting low light intensities becomes an adaptive advantage. A photosynthetic organism in dim light can obtain more metabolic energy if it is able to discriminate and move toward better illuminated areas.

Euglena's emergent flagellum consists of an axoneme, a paraxial rod running parallel to it, and a swelling (containing the photoreceptor, or so-called paraflagellar body) near its base. The paraflagellar body is the exceptional light-sensing unit of the alga. It is a small proteic crystal and enables the alga to detect even very low light intensities (i.e. single photons). Although only $1\,\mu m$ in diameter, it reaches an absorption rate close to $100\,\%$ of the incident light within its absorption band spectrum (see Fig. 4.6).

Rhodopsin

Embedded within the layered structure of the photoreceptors is its main ingredient, a rhodopsin-like protein. Rhodopsins are special proteins for intercepting light, universally used from archebacteria to humans, consisting of a proteic part, the opsin, organized in seven transmembrane helices, and a light-absorbing group, the retinal (i.e. the chromophore). The retinal is located inside a pocket of the opsin, approximately in its center.

Several properties make the retinal-opsin complex an excellent light detection unit. It has an intense absorption band whose maximum can be shifted into the visible region of the spectrum, over the entire range from $380\,nm$ to $640\,nm$. Second, light isomerizes the retinal inside the protein very efficiently and rapidly. The isomerization, i.e. the event initiating the vision reaction cascade, can be
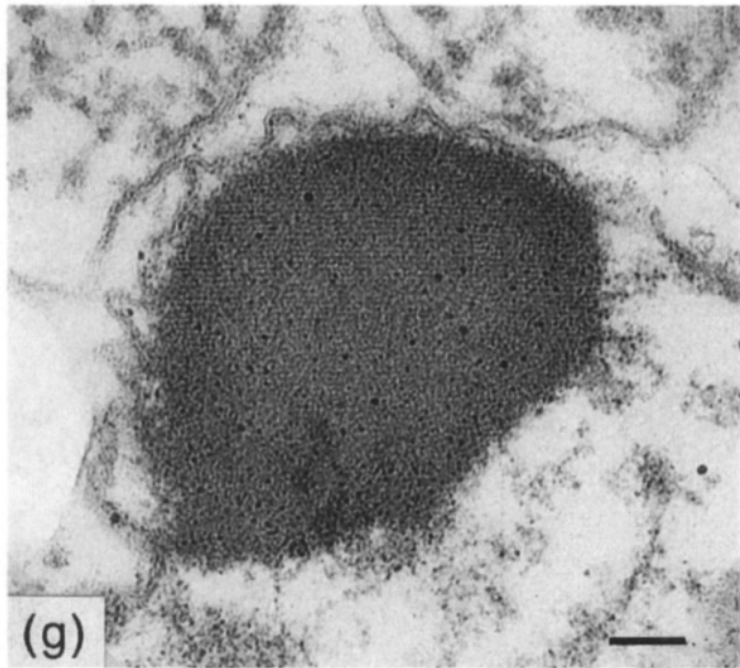
Figure 4.6: A photoreceptor cross section as imaged by TEM. Note the horizontal striations attributed to the regular layered structure of the photoreceptor - it consists of about one hundred layers stacked on top of each other. Image adapted from [87]. Scale bar is 0.1 μm.

triggered almost exclusively by light. In the dark it occurs only about once in a thousand years.

The isomerization and possible conformational changes of the protein follow a photocycle and are therefore repeatable. The photocycle leads through a series of conformational changes from the initial state to an excited state and back again. Usually also a number of intermediates can be identified. The photocycle of the chromophore in the photoreceptor of *Euglena* shows such a cycle including a ground and an excited state, (the so-called optical bistability is visualized in Fig. 4.7). As different conformational states possess different fluorescence characteristics, a photoreceptor whose chromophore proteins are mostly excited differs in emission from a photoreceptor containing chromophore protein mostly in the ground state (see Fig. 4.8).

When the excited state is reached, the signal transmission is triggered and the cellular signal transduction pathway is responsible for amplification of the signal, signal processing and delivery.

The time it takes for the whole photocycle to complete is only in the order of microseconds or less. The isomerization alone is one of the fastest processes ocurring in nature, completing in only about 200 femtoseconds. ([96])
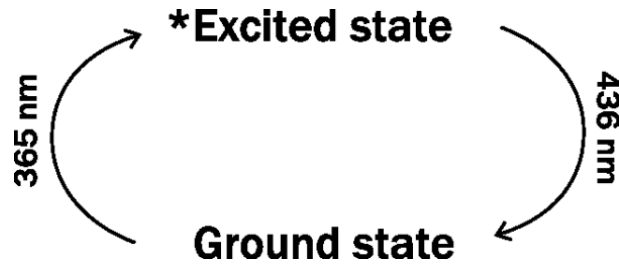
Figure 4.7: Scheme of the photoreceptor photocycle (intermediate states omitted). Upon absorption of light with a wavelength of around $365\,nm$ the rhodopsin-like protein changes into the excited state, then upon a second absorption at a wavelength of around $436\,nm$ it falls back again into the ground state. This last step from the excited state to the ground state is almost exclusively triggered by light. It occurs only once in a thousand years through thermal deactivation at ambient temperature.

Sensitivity

For detecting the direction of the light of a specific range a photoreceptor demands a high packing density of chromophore molecules organized in a lattice structure, with high absorption cross section (high absorption probability) of the chromophore and very low dark noise[10]. For transmitting the detected signal a photoreceptor must generate an electrical potential difference, or an electrical current. This is exactly what *Euglena*'s photoreceptor is designed for.

One of the most investigated photoreception systems is that of *Chlamydomonas*. It consist of a patch of rhodopsin-like proteins in the plasma membrane. The packing density of these molecules appears to be about $20 - 30,000/\mu^2 m$ of membrane, with a molar absorption coefficient of $40 - 60,000\ M^{-1} * cm^{-1}$ and a dark noise of almost zero. The number of embedded molecules per $\mu^2 m$ of membrane, the absorption, the absorption cross section, and the dark noise are at the best of theoretical limits. Nevertheless, the fraction of photons absorbed from a single layer of these molecules is less than 0.05%.

An estimate of how many photons this simplest but real photoreceptive system can absorb is effectuated here. On a sunny day about 10^{18} photons $*m^{-2} * s^{-1}$ per nanometer wavelength are incident. On a cloudy day this lowers to 10^{17} photons $*m^{-2} * s^{-1}$ per nanometer wavelength. Through absorption of the water column this number is lowered to 10^{17} and 10^{16} respectively. Thus a photoreceptor of a cross section of about $1\mu m^2$ can catch at most 10^5 photons, 10^7 in its $100\ nm$ absorption band. Since only about 0.05% of these are effectively caught by the protein monolayer, the maximum number lowers to $5 * 10^3$. Now during revolving motion of the algae it is illuminated for about $400\ ms$ and shaded by the stigma

---

[10]Dark noise is inherent to such a receptor and independent of light level. It arises from the random thermal motion of the molecules.
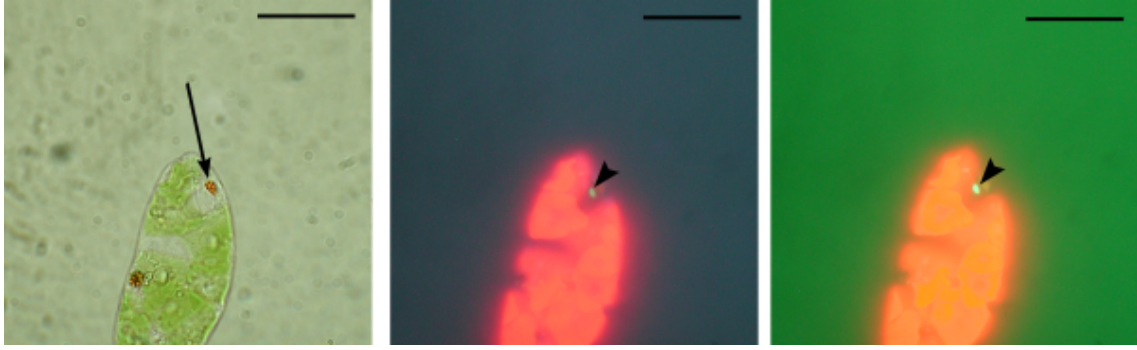
Figure 4.8: Three images of the apical part of the same cell. The leftmost image shows the cell as seen in phase contrast, with no UV-light illumination. The image in the middle shows the cell during illumination with $365\,nm$ light - upon absorption of photons of this wavelength the rhodopsin-like proteins present in the *Euglena* photoreceptor change into the excited state. The green emission of the photoreceptor is only faint. In the rightmost image, the cell is irradiated with photons of $436\,nm$ wavelength. At this wavelength the light sensitive proteins fall back into the ground state, emitting bright green light and completing the photocycle. Arrowheads indicate the photoreceptor crystal in the images, the arrow indicates the stigma responsible for intermittently shading the alga when rotating during swimming. The scale bar in each of the images is $20\,\mu m$

for $600\,ms$. If the shading lowers the detected signal by 50%, the signal difference during revolutions is about 2500 photons per second or $250*sec^{-1}$ on a cloudy day. Detection rates under real conditions might be considerably lower. Thus a photoreceptor must possess a very low threshold and a very low or negligible dark noise. In the experiment it has been demonstrated that single photons not only induce transient direction changes but also that fluence rates as low as $1\,photon*cell^{-1}*s^{-1}$ can actually lead to a persistent orientation in *Chlamydomonas* (*Chlorophyceae*). ([97])

Euglena for its part has evolved a simple strategy in order to increase the sensitivity of its photoreceptor. The photoreceptor is made of a stack of many pigment containing membranes (around 100 layers, see Fig. 4.6) increasing absorption rates near to $100\,\%$ of the incident light in the direction of the light path. The three-dimensional proteic crystal is about $1\,\mu m^3$ in volume and of rounded shape. Its stack of 2-dimensional layers is held together by in-plane hydrophobic interactions and by inter-plane hydrophilic interactions. Its crystalline monoclinic unit cell dimensions have been measured to be $a = 8.9\,nm$, $b = 7.7\,nm$, $c = 8.3\,nm$, $\beta = 110°$ ([98]). That amounts to a unit cell volume of $534.5\,nm^3$ as shown in Fig. 4.9.

Although these outstanding properties of *Euglena*'s photoreceptor have incited a lot of interest in the last years, it was not yet possible to resolve the three-
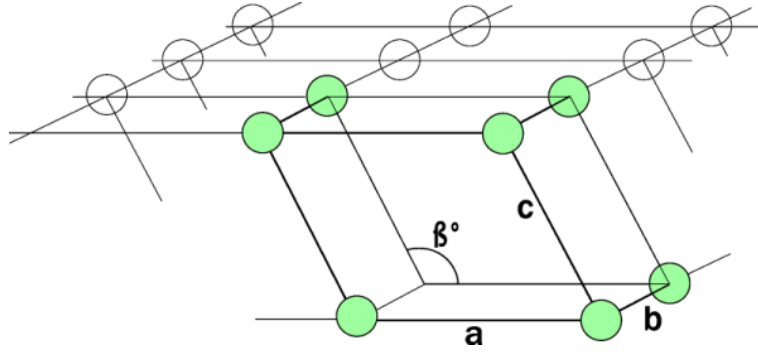
Figure 4.9: Measured monoclinic unit cell of the photoreceptor crystal. $a = 8.9\,nm$, $b = 7.7\,nm$, $c = 8.3\,nm$, $\beta = 110°$.

dimensional structure, especially how the chromophore pockets are distributed within the stacked layers (the scheme in Fig. 4.10 shows a possible arrangement). The TEM image in Fig. 4.6 gives an indication of the spacing and the number of these layers and counts to the best data available to date.

Signal transduction

Although the interplay of the photoreceptor and the stigma constitutes the most vital part of the visual system of *Euglena*, the detection part, the system would be useless without a corresponding signal transmission mechanism.

The flagellum allegedly plays the key role in signal transduction and finally receives locomotory commands depending on light stimulus. When a light stimulus promotes chromophore proteins of the photoreceptor from the ground state to the excited state, a chain of events is triggered.

The piezoelectric theory is one of the theories how the information of a photon detection is passed on. The core of this theory is the assumption that the photoreceptor due to its crystalline nature acts as a capacitor, relaying electrons to the paraxial[11] rod (PAR) to which it is attached. The photon flux acting on the pigment mass would induce a flux of electrically charged particles that in turn generate a signal in the form of an electrical potential. As the PAR contains fibers that potentially can contract and act upon a flagellar response to the stimulus. The present microtubuli and ATPase activity could provide further response to this initial stimulus and it was suggested that they even do a rudimentary form of information processing (see below). ([82], [99])

---

[11]The PAR is a thin rod between the main core of the flagellum and the photoreceptor swelling.
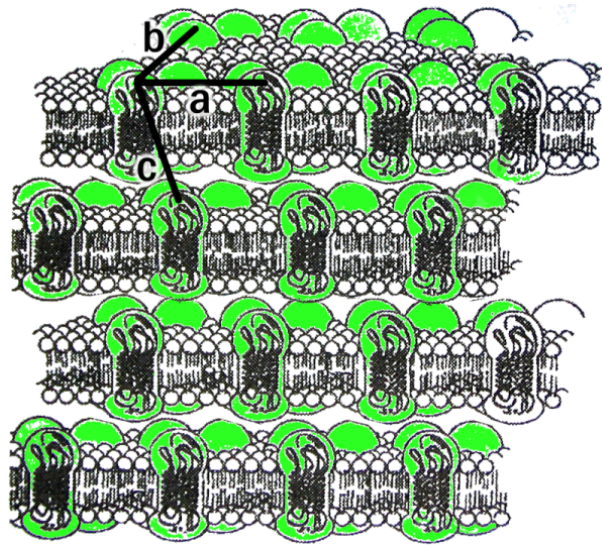
Figure 4.10: Preliminary model of the arrangement of rhodopsin-like proteins (colored green) in the photoreceptor. It is hypothesized that these are arranged in groups of three in a regular pattern across the layers. Each group would sit on a corner of the measured monoclinic unit cell shown in Fig. 4.9. a,b,c are the correspond edge lengths of the unit cell. That would lead to twelve molecules of rhodopsin per unit cell, about $2*10^6$ unit cells per crystal and therefore around $2.4*10^7$ molecules of rhodopsin in the photoreceptor. Diagram adapted from [100].

4.3.4 Pellicle

The pellicle defines the basic shape of the cell. Its role is vital to the organism as it must function as protection from the environment, yet cannot be fully impermeable as it must permit e.g. exchange of information or matter with the exterior as in sensory pathways or uptake of the vitamin B12. Additionally, euglenoid movement requires the strips of the pellicle to be highly flexible and articulate against each other. During my laboratory experience the cells have also shown excellent pressure resistance up to 100 *bar* and beyond.

This sounds exciting enough for organic material, but still isn't the whole story. There is strong evidence that the microtubuli within the strips (aligned in parallel) are responsible for the sliding of the strips against each other, meaning the pellicle changes its shape actively at the command of the cell! The fact that this protective shielding is self-assembling through means of special binding sites inside the plasmalemma membrane and binding proteins adds to this exceptional part of *Euglena*. ([101])

If the cell is disrupted the pellicle can be seen dissociated along the striations into flat strips of material which have a thickened edge and a thinner flange. Electron microscopy sections clearly show how these strips interlock and how they
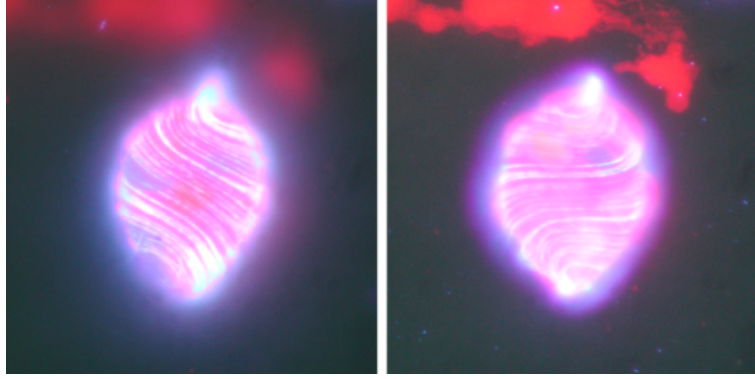
Figure 4.11: Twice the same *Euglena* cell as seen with an optical microscope, using UV-light illumination. The focal plane in the left image is adjusted such that the part of the pellicle closer to the observer is rendered. The image one on the right shows the far side of the pellicle. The light-dark pattern follows the alignment of pellicle strips fusing partly at top and bottom.

pass helically along the cell (see Fig. 4.11). These strips are intracellular structures lying immediately beneath the plasmalemma, a continuous tripartite membrane $0.8 - 1\mu m$ thick. The pellicle is thus not equivalent to a cell wall, since the latter is always laid down outside the plasmalemma (like a cellulose wall of plant cells).

The throughs between adjacent strips start as a whorl at the posterior end of the cell, bifurcate a few times before passing helically along the length of the cells and then meet again as they reach the canal opening. The strips of the pellicle curve over and continue into the canal, where the also fuse. Although variation occurs concerning thickness and shape the form of construction is the same in all euglenoids. The cross section of a pellicle surface can be seen in Fig. 4.12 (TEM image) and a schematic drawing in Fig. 4.13.
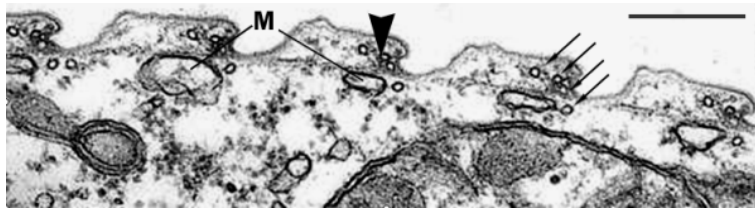
Figure 4.12: A cross section of an *Euglena* pellicle. M designates muciferous bodies, the arrows indicate microtubuli locations. Around the area where the arrowhead points to, the ridge of the right pellicle strip articulates inside the groove of the left strip. The muciferous bodies additionally possess canals leading to this grove and on to the exterior. Scale bar is $0.5\,\mu m$. Image adapted from [84].
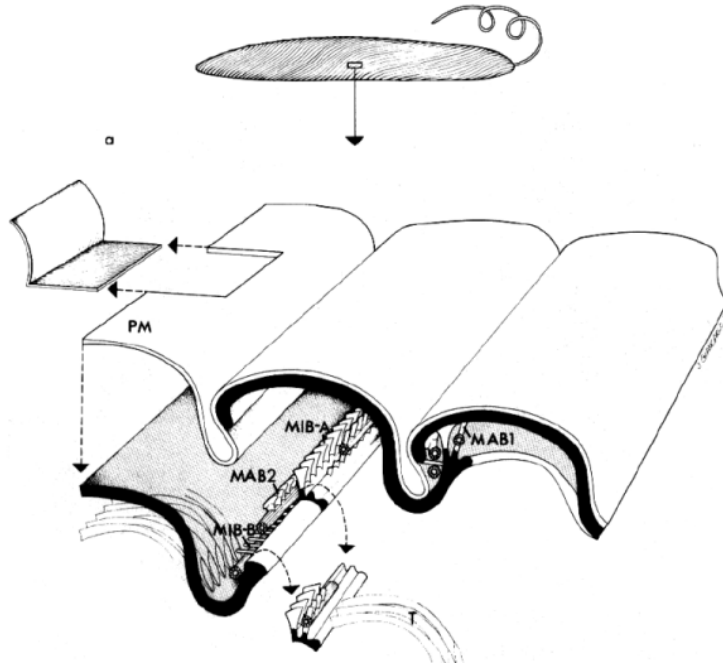
Figure 4.13: On top a swimming *Euglena*. The schematic drawing depicts a transverse section of its cell surface. Details of the articulating S-shaped strips of the membrane skeleton and the infrastructure associated with strip overlap. The position of the skeleton and the bridges are well suited to mediate the sliding of adjacent strips occurring during shape changes. The portion of the plasma membrane not subtended by the cytoskeleton may provide the fluid region, which accommodates sliding as well as a region for the insertion of new strips during surface replication. The traversing fiber is positioned to maintain the S-shaped configuration and it may contribute an elastic component to the sliding skeleton. MAB1 and MAB2, microtubule associated bridges; MIB-A and MIB-B, microtubule independent bridges; PM, plasma membrane; T, traversing fiber. ([91])
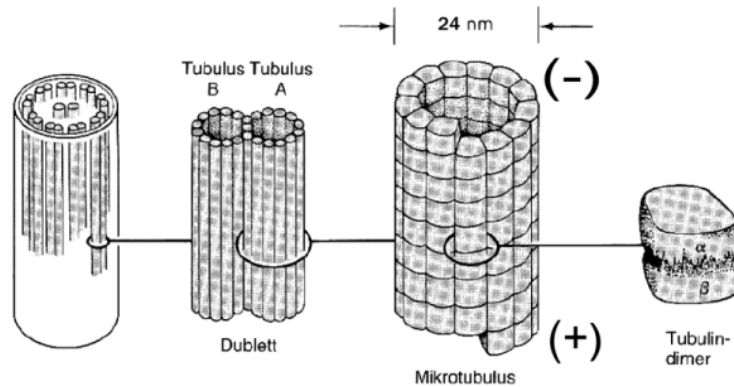
Microtubuli

In cell biology microtubuli (MT) are almost omnipresent, e.g. playing a major role during cell division, are part of most cell architecture and can be found in cilia and flagella. Microtubuli are hollow tubes with an outer diameter of $24\,nm$ and within their structure the position of every atom is precisely defined. A joy for every nanotechnologist! They are also an important ingredient to the structure and function of the pellicular strips. The tubes are built from smaller subunits, heterodimers, each of which are composed by two proteins, the so-called $\alpha-$ and β-tubulin. A schematic drawing how a flagellum is constructed from microtubuli is given in Fig. 4.14.

What makes microtubuli so special apart from having favorable mechanical properties is the following: The tubes have an associated direction (see Figs. 4.14,

4.15), their ends are termed the (-) and the (+) end, and there exist protein families that can move along the tubes in either of these directions. The two fascinating protein antagonists are kinesins and dyneins (see Fig. 4.15). These proteins are capable of moving along a microtubule and, since the tubule has a defined direction, kinesins always move in the (+) direction and dyneins usually move in the (-) direction. Even more remarkable is that they are able to move attached masses. Alone they can move single vesicles, but when acting in unison it is possible to move direct whole structures!

Together with their motor proteins MTs are essential in molecular cell architecture for providing transport highways and a mechanism generating relative motion. Mechanical properties of MT have been described by measuring bending stiffness with Laser Tweezers, AFM, hydrodynamic flow and buckling in vesicles. Measured values correspond to Young's moduli between $1\,MPa$ (rubber) and $7\,MPa$ (plexiglass). ([102])

Figure 4.14: Schematic drawing of microtubule architecture and how it is assembled into a flagellar structure (9 doublets of microtubuli forming the outer wall, a pair is inside). This kind of structure is not only found in alga but also e.g. as motory flagellum of human sperm. The single microtubule would have its (-) end on top, its (+) end at the bottom, depending on the orientation of the heterodimers building the tubule. α−tubulins always face the (-) end, β−tubulins the (+) end. Image adapted from [102].

Conventional kinesin (or simply 'kinesin') is the best known member of the KinNs (one of the three known families of kinesins)

- Kinesin walks on MT to the (+) end in steps of $8.3\,nm$ per hydrolyzed ATP (see below). Each second such a motor can complete 100 ATP turnovers and walk $800\,nm$. A single powerstroke of the motor can generate a force of $6\,pN$. ([103])

- Kinesin is a processive motor, i.e. it does not dissociate from MTs during walking.

- It possesses a hand-over-hand (h-o-h) moving mechanism: its two heads pass over one another when the protein moves along the tube. In this way it is similar to the human walking style. (see Fig. 4.15, [104])

- The theoretical prediction of this model predicted a 16.6 nm step size per head.

- By labeling one head with a fluorescent dye, the average step size of one single head was shown to be 17.3nm as predicted by the h-o-h model (another model, the inchworm model in contrast predicted only 8 nm). ([104])

The movement mechanism of dyneins is less well understood.

ATP

In order to move along a MT a motor protein has to dispose of enough energy. The cell provides this energy to many of its subsystems through the protein adenosine triphosphate (ATP). ATP is regarded as the main energy currency of biological systems. The ATP molecule owes much of its energy to the terminal three phosphate ions attached to an adenosine base. When the third phosphate group of ATP is split off by hydrolysis, free energy of a value of about 7.3 kcal (the exact amount depending on various other conditions) per mole is released.

$ATP + H_2O \Rightarrow ADP + P_i$
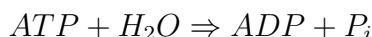
Adenosine diphosphate (ADP) and inorganic phosphate (P_i) are left as the products. The released energy can be used to drive biological processes.

- ATP is the main energy currency of the cell, providing the energy for most of the energy-consuming activities of the cell.

- It is used as monomer in the synthesis of RNA and, after conversion to deoxyATP (dATP), DNA.

- Necessary for the regulation of many biochemical pathways.

ADP and the phosphate group on the other hand are recombined to form ATP again by a very efficient enzyme motor assembly called the F_0F_1-ATP synthase protein (F_0F_1-ATPase). This energy cycle, the splitting of the phosphate group and the reattachment by ATPase, is reversible and highly efficient. ATP synthase can be found inside the mitochondria of animal cells, in plant chloroplasts, in bacteria, and some other organisms.

Thus the energy for dynein and kinesin movement comes from the splitting of ATP molecules. Through regulation of ATP accessibility their activity can be
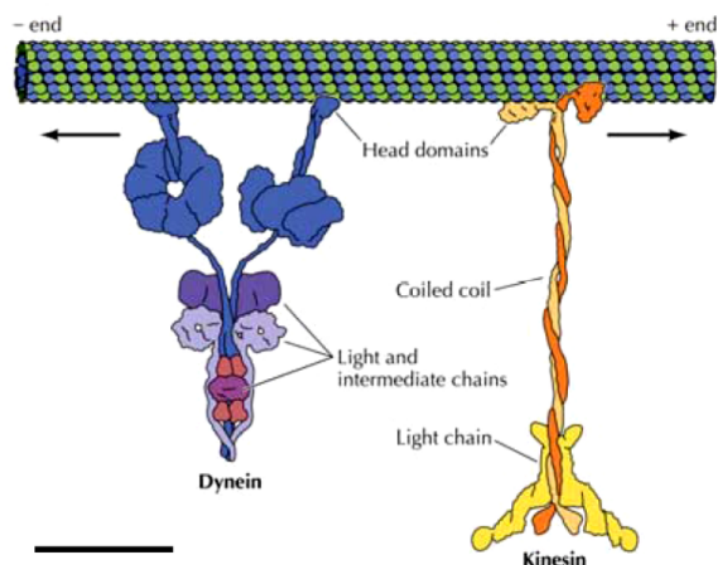
Figure 4.15: Kinesin and dynein and their direction of propagation along a microtubule. Kinesin has a remarkable way of moving by using the hands-over-hands method. Its two heads pass over another when the protein moves along the tube. In this way it is similar to the human walking style, putting one foot in front of the other. Scale bar is $50\,nm$. Image adapted from [102].

precisely regulated, such that a complex concerted action like euglenoid movement is made possible.

Besides providing the pellicle with dynamic properties one major area of microtubule usage can be found in the flagellum. The core structure of *Euglena*'s flagellum consists of nine outer doublets of microtubli and one inner doublet. The cross section of such an arrangement shows that each outer doublet has a dynein protein attached to it, enabling the flagellum to actively slide within its shaft. This basic mechanism is responsible for the typical flagellar ondulatory movement.

A very interesting fact about the *Euglena* pellicular strip is their assembly process. Instead of being transferred and attached in part to the plasma membrane, they are assembled molecule by molecule. The location where the individual proteins bind is directed by special binding sites spread on the inner side of the plasma membrane. The membrane skeleton (pellicle) of *Euglena* is primarily assembled from a $80\,kDa$[12] membrane skeletal protein binding to the plasma membrane through noncovalent interactions with a small cytoplasmic domain of the plasma-membrane protein IP39. ([101])

The pellicle, or membrane skeleton, underlying the plasma membrane plays a

---

[12]A dalton (Da or D) is a unit of mass, equivalent to the unified atomic mass unit (u). It is defined to be one twelfth of the mass of an unbound atom of the carbon-12 nuclide, at rest and in its ground state. $1kDa = 1000\,Da$. E.g. a caffeine molecule has a mass of $194\,Da$.

Figure 4.16: An image of *Euglena spirogyra*, demonstrating some of its pellicle flexibility. Image adapted from [105].

key role in maintaining cell form and elasticity in at least two widely divergent cell types: mammalian erythrocytes and unicellular *Euglenas*. In *Euglena* two smaller proteins (80 and 86 kDa) associate stoichiometrically to generate filaments that are arranged perpendicularly to the cell surface. In erythrocytes and probably *Euglena* the peripheral membrane skeleton is attached to the plasma membranes through one or more integral membrane proteins. These membrane anchors are of considerable interest because they seem to select the specific membrane skeletal proteins that bind to the plasma membrane and they could then determine in what regions of the cell the membrane skeleton assembles. In [101] it was shown, that incubation of stripped membranes with solubilized membrane skeletal proteins results in the reformation of a membrane skeletal layer, indicating that the plasma membrane retained appropriate membrane skeletal protein binding sites in vitro.

Lubrification

Certain structures, mucilage producing bodies (designated M in Fig. 4.12), occur in regular association with the pellicle. Parallel to each pellicular strip a row of these structures can be found from which narrow canals pass to the groove and then to the exterior. One possible function of the muciferous bodies is to supply a lubricant - mucilage (mucus) - to the pellicle strip articulations. This is an intracellular release of mucilage, since the whole of the pellicular system lies within the plasma membrane.

Mucus is typically a dilute network of proteins and polysaccharides. These molecules take on an extended configuration that causes them to become entangled,
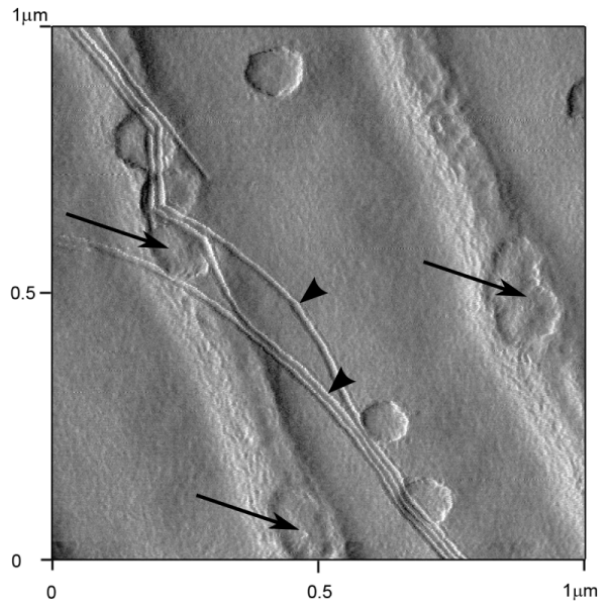
Figure 4.17: (Image reproduced from chapter 6, Results) Pellicular strips of an *E. gracilis* cell showing ridges, mucilage (arrows) excreted at canal openings between the strips and a bundle of three microtubuli (arrowheads) presumably stemming from a disrupted cell. Image size $1\,\mu m^2$, Intermittent contact mode AFM image, Amplitude trace.

thus forming a weak gel.[13]. Some organisms such as limpets are also known to further crosslink and modify this network of proteins, raising its viscosity or giving it adhesive properties. ([106], [107])

In conclusion, a number of essential parts make up the pellicle and provide it with the ability to actively alter its shape. The pellicle strips are allowed a certain amount of relative sideways movement, accomplished by the ridge sliding in the groove together with compression and stretching of the pellicular material. Microtubuli, arranged parallel to each pellicular strip and varying in numbers and distributions in different species, motor these movements. Additionally, mucilage producing bodies reduce friction and protect the articulations of the pellicle from wear.

---

[13]In mammals, lubricating mucous gels line and protect the digestive, reproductive, and respiratory tracts. In marine invertebrates, mucus typically forms a slippery coating that prevents bacteria and debris from accumulating on the body surface and keeps other organisms from adhering to it.

4.3.5 Energy Storage and Metabolism

As energy resource *Euglena* builds carbohydrates, fats and oils, that are produced exterior to the chloroplasts and are then stored in so-called paramylum[14] grains, and in lipid, crystalloid and pyrenoid bodies.

Paramylon is isomeric with starch, but has additional $\beta - 1, 3$-glucose linkages. Paramylon occurs as membrane bound granule in the cytosol, the surrounding membrane is somewhat distinctive since most storage grains are not directly bound by a membrane. The paramylon granule also is unique among carbohydrate storage products in plant groups because of its high crystallinity. Microfibrils of $4\,nm$ cross-section traverse the paramylon grain, composed of rectangular segments and wedges (see Fig. 4.18), in an overall concentric pattern. ([108])
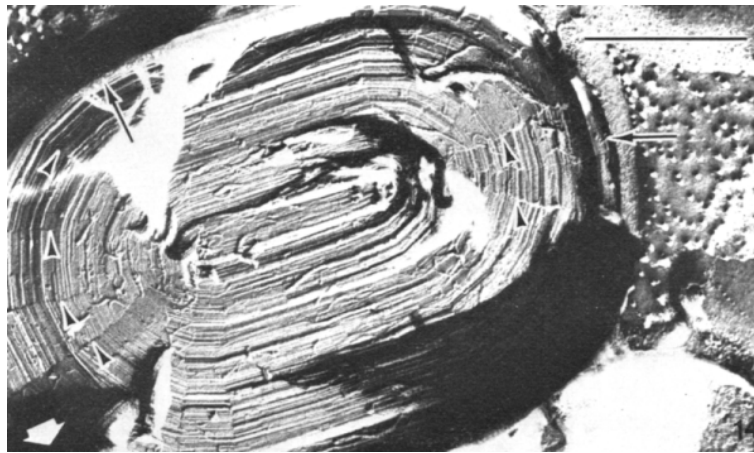
Figure 4.18: Electron micrograph of a freeze-etched paramylum granule. The fracture plane has revealed the concentric layers of the inner material. The arrow heads indicate where possible wedging or segmentation of the inner material has occurred. The outer layer (remains of the unit membrane) is indicated by the arrows. Scale bar is $500\,nm$. Image adapted from [109].

If there is not enough light to feed on, *Euglena* can turn for some time to a heterotroph organism. It then uses energy rich compounds synthesized by other organisms. Chloroplasts dissolve into proplastids and *Euglena* takes up its food in an osmotrophic way through the cell surface. Additional to the uptake of solubilized organic substances *Euglena* can transfect detritus and bacteria at the invagination of the pellicle.

The numerous proplastids (with a size of $1 - 2\,\mu$m in diameter) can regenerate

---

[14]Paramylum is not detectable by the classical iodine-starch test. As iodine is not very soluble in water, it is dissolved in water in the presence of potassium iodide - this makes a linear triiodide ion complex which is soluble. The iodine molecule then slips inside of the amylose coil (if it is not present the color of the solution stays orange or yellow) and the liquid changes to intense blue-black color. ([110])

into fully functional chloroplasts again as soon as enough light becomes available. But even with its chloroplasts *Euglena* is not fully photoautotroph - it cannot synthesize vitamin B12. The alga can therefore be used to prove the occurrence of vitamin B12.

4.3.6 Vacuole

Under the Reservoir, *Euglena* possesses a contractile vacuole, that can excrete water that diffused into the cell interior in the sweet water regime. The concentration of osmotically active elements within the cell is higher than in the sweet water surrounding (a hypertonic regime). The cell wall is a semipermeable membrane, letting pass water molecules but not bigger ones. The concentration gradient between inside and outside is heading towards an equilibrium and must be counteracted by the vacuole that acts as a pump.[15] The vacuole surrounds the bases of the flagella. It is limited by a unit membrane and, when full has a diameter of $5\mu m$. It pulsates rhythmically, every 20-30 seconds it discharges.

This is an example of natural nanotechnology that controls precisely in which environment the processes should run. Encapsulation plays an important role, as certain functions have to be constrained to a subdomain, where environmental conditions are guaranteed to be stable within certain limits.

4.4 Technical Applications

Each of the subsystems exhibits a range of properties desirable in technical applications.

Photoreceptor

As one of the most interesting nanotechnological elements in *Euglena*, the high yield of photons means a good sensing performance, thermal stability and tunable wavelengths. Conversion of electrical into chemical energy.

A natural fit as application could be a data storage system. A disk coated by a layer of photoreceptor protein could be written on by activation and deactivation of individual chromophore proteins (repeatable). Laser light of the right wavelength could be used for the switching and the low thermal deactivation as well as the simple photocycle make it suited for this task.

---

[15]The hypertonic solution has the lower osmotic pressure of two fluids. It also describes a cell environment with a lower concentration of solutes than the cytosol of the cell. In a hypertonic environment, osmosis causes a net flow of water into the cell, that can lead the cell to swell and even burst.

Second the high photon yield of the photoreceptor and its small size make it an outstanding detector. It could be used for detecting very low light levels in environments where space constraints are major issues.

Although the protein sequence has not yet been elucidated and the transduction pathway remains still enigmatic in part, there is energy conversed from photons to electrical and then to chemical energy. Converting light into usable energy is one way for autonomous microdevices to operate. As devices become smaller and mobile it is crucial that energy is provisioned by the environment and not from a depletable built-in source. If the photoreceptor of *Euglena* uses variation of electrical potentials for its signal transduction as the piezoelectric theory suggests, it also would be possible to store this energy for later use.

Pellicle Strips - Microtubuli

Self-assembly is a very powerful concept for creating nanostructures. This is one mechanism the cell uses for the assembly of pellicular strips where individual proteins bind to binding sites spread on the inner side of the membrane. Functionalization and coating of surfaces, where the area of effect must be precisely controlled is also of interest in technical devices. One step further self-assembly of three dimensional structures as done with pellicular strips starts to emerge also for artificial materials (e.g. self-assembled batteries, see below).

Microtubuli provide a cell with efficient transportation, information pathways, gating mechanisms and structural fortification. They exhibit good mechanical properties and can self-assembly if the tubulin proteins are present. They could be used in artificial systems that require mechanical flexibility or even active shape shifting in combination with molecular motors (as pellicular strips being moved relative to each other). A simple rotory motor could be imagined e.g. as an assembly of a microtubular ring and an array of kinesin motor proteins that rotate it (Fig. 4.19).

Vacuole

The vacuole is part of a tuned system to regulate element concentrations in an aqueous environment. As such it acts as a selective micropump (the output fluid contains different element concentrations than the reservoir fluid) and its mechanisms could be useful in a whole range of technical applications. Examples include the "lab on a chip" for the analysis of different substances (e.g. blood) or regulated drug release inside the bloodstream.
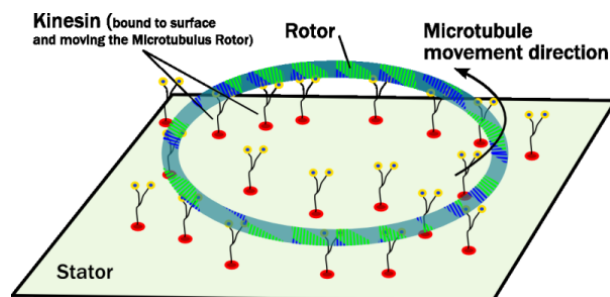
Figure 4.19: How a microtubule-kinesin based motor could be built. Once a circular microtubule has been achieved it can be brought to a surface covered with kinesin protein. Depending on the side this ring comes to lay on these molecules it starts rotating in one or the other direction, if the kinesin is fed the needed energy in the form of ATP molecules.

Energy Storage

Energy storage is important to small devices if either they must depend on it for the rest of their use lifespan or if the energy supply rate does not overlap with the energy expenditure rate over time. For example a watch using the kinetic energy of one's moving arm is required to have a means of energy storage, usually a spring or a battery, so that it can function during times when no energy can be taken up (such a watch might have e.g. a rotating pendulum used to tighten the spring). The more compact and high density this energy storage is, the better. The energy cycle of the *Euglena* cell is very efficient and uses lipid bodies and carbohydrates (paramylum granule) to store its long time energy reserves. The crystallinity of paramylon also suggests an optimum packing density of its isomeric starch microfibrils.

In comparison, the energy density of todays batteries is in the region of $0.2 - 1\ kJ/g$ while carbohydrates possess an energy density of about $17\ kJ/g$ and fat even one of about $37\ kJ/g$, that is $20 - 200$ times more! One first step to enhance efficiency is the nanoscale assembly of battery layers avoiding defects almost entirely and providing large surface areas.

For example, a patent application was recently made for a bionanotechnological battery using self-assembled layers of ferritin proteins, carrying electrical charges. The thin-film electrode was produced employing a spin self-assembly procedure where alternately charged layers of ferritin were formed on the top of each other. Advantages of this thin-film electrode are stability and robustness, enhanced packing density and optimal charge density. ([111], another self-assembled molecular nanocathode is found in [112]).

It could also be possible to use carbohydrates directly as intermediary energy storage. The synthase protein of *Euglena* sythesizing paramylon has been

isolated and characterized ([113]). The complex even remained active throughout the isolation procedures and produced the paramylon starch beta-1,3-glucan in vitro.

Conclusion

A living cell is a very complex object combining a high number of efficient functional modules at the same time. It seems that its design principles as well as many of their realizations can be adapted to fit and inspire technological applications.

Chapter 5

Materials and Methods

The basis of the results presented in this work is data from experiments that were acquired on three different sites.

I was introduced to *Euglena gracilis* at the Institute of Biophysics at the CNR (National Research Center) in Pisa by the research group under the lead of Paolo Gualtieri. The great expertise of the group in studying these organisms, they count amongst the most active research groups in this field, was very helpful to get acquainted with the subject and to learn various preparation techniques. Much of the sample preparation as well as fluorescence microscopy and spectroscopy measurements were done there.

The main part of the work presented in this work, the Atomic Force Microscope (AFM) investigations of whole cells and cell parts, was performed in Vienna at the Institut für Allgemeine Physik within the group of Prof. Aumayr.

For AFM sample preparation investigation I carried out fluorescence microscopy in Vienna at the Institut für Verfahrenstechnik with the kind help of Prof. Stachelberger.

5.1 *Euglena gracilis*

5.1.1 Culturing cells

Cultures of *Euglena gracilis* cells strain Z (supplier: Sammlung Algenkulturen Göttingen, $1224 - 5/25$) were grown in autotrophic Cramers-Myers medium $0.025\,M$ in sodium acetate (pH 6.8)(Cramer-Myers 1952 [114]), under constant temperature ($24°C$) and continuous illumination ($500\,lux$). The average incubation time in fresh nutrient medium was 4 to 5 days.

Any experiments and preparations of cell part solutions that was done in Pisa used algal cells grown under these conditions. The population was kept bacteria

free, manipulations were done under a sterile hud (UV-light sterilized) over an open gas flame.

Experiments with whole cells carried out in Vienna used algal cells from the same strain as in Pisa and were kept at room temperature and under natural lighting. On average every 4 months a new incubation was carried out. Experiments investigating cell parts were using a cell part solution prepared and kindly provided by Laura Barsanti of the Gualtieri group.

Figure 5.1: Receptacles of 4 to 5 days old algal cultures of *Euglena gracilis* under constant illumination.

5.1.2   Cell Parts Solution

The following protocol resumes the steps to be followed to obtain the solution of cell parts that was used for the experiments. This protocol aimed at the extraction and purification of intact photoreceptor proteins in the first place, but was discovered to be also useful as starting point for AFM investigation of crystalline cell parts. The protocol attempts to clean the solution by either removing or dissolving unwanted skeletal features (like pellicle parts) and membrane tissue as far as possible.

Cell Collection

For the cell collection 4-5 days old cultures are used. The cells, contained in their culture medium at a concentration of $7 - 8 * 10^6 \, cells/ml$, are harvested at low centrifugal force. Then the cells are resuspended in $750 \, ml$ of a $25 \, mM$ sodium acetate solution ($ph \, 7.0$) and cooled to $4 \, °C$ in an ice bath.

Cell Treatment - Demembranation

In order to stop enzymatic activity and dissolve the membranes around the internal cell parts the solution is mixed with a demembranation solution prepared as follows (also see [115]):

The detergent Triton X-100 is added to a HEPES[1]-buffered solution (100mM HEPES-KOH, pH 7.00; 20mM piperazine-N, N'-bis(2-ethanesulfonic acid); 10mM EDTA; 50 mM sucrose; 1 mM dithiothreitol; 7,5% v/v glycerol) to give a final detergent concentration of 4% v/v. It is then filtered and added to the cells (4:1), which were previously suspended in 100 mM HEPES buffer (pH 7.00). Cells are then washed repeatedly with the isolation solution to remove extracted chlorophyll. This cycle of washing and reimmersion can be repeated during a couple of days to weeks for better dissolution. Crystalline structures are not be dissolved.

Cell Explosion

Once the cells are washed free of dissolved membrane tissue, the cells must be broken open. This can be achieved using the method of nitrogen pressurization and rapid depressurization. The cells are stored in a sealed Ashcroft Duralife pressure homogenizer (see figure 5.2) and then nitrogen is let flow in. During pressurization nitrogen diffuses into the cell at an external pressure of 200 *bar*. During rapid depressurization the cells burst (literally explode) because of their internal pressure excess.

Figure 5.2: To the right the container for nitrogen pressurization of the algae can be seen (also called a "Nitrogen-bomb"). The top piece as seen in the left part of the image accommodates a pressure gauge and two valves to pressurize the container and to rapidly depressurize it.

---

[1]HEPES is an organic chemical buffering agent that is widely used in cell culture to maintain physiological pH.

Cell parts can then be collected and purified. The disrupted rigid outer cell walls can be eliminated in another cycle of centrifugation and washing processes. After a series of purification steps a solution of crystalline cell parts containing only a minor fraction of dissolved biological material is obtained. Dependent on the various forms of treatment before the explosion, the results obtained can differ to a great extent. Variations of this procedure included tests on cells treated with detergent, non-treated live cells and fixated[2] cells.

5.2 Experimental Setups

5.2.1 Optical Microscopy and Fluorescence Microscopy

In Pisa optical and fluorescence microscopy were carried out with a Zeiss Axioplan fluorescence microscope equipped with an epifluorescence system, various magnifications and a 100W mercury lamp.

The following filter combination could be used: a UV-blue set (an $8\,nm$ bandpass excitation filter, $365\,nm$; chromatic beam splitter, $395\,nm$; barrier filter, $397\,nm$; $800\,\mu W/cm^2$) and a blue-violet set (an $8\,nm$ bandpass excitation filter, $436\,nm$; chromatic beam splitter, $460\,nm$; barrier filter, $470\,nm$; $1100\,\mu W/cm^2$).

The chromatic beam splitters redirect light from the mercury lamp to be used as fluorescence excitation light (wavelengths smaller than $365\,nm$ and $460\,nm$ respectively). The bandpass filters only let bands around $365\,nm$ and $436\,nm$ wavelength pass. The barrier filters block reflected excitation light from the environment and transmit only the fluorescence light from the specimen..

Fluorescence spectra can characterize algal species (through their chloroplast absorption and emission spectra) and provide valuable information on the composition and photocycle of the Euglena gracilis photoreceptor. E.g. the embedded rhodopsin molecules can change their conformational state depending on the wavelength of absorbed light and thus fluoresce differently.

Images during fluorescence microscopy were taken with a Canon digital camera.

5.2.2 Spectroscopy

Some optical spectroscopy was carried out for educational purposes. Analysis of different parts of the cell was done, using a Jasco 7850 spectrometer and fluorescence spectra were recorded using a Perkin Elmer LS 50 B fluorimeter in Pisa.

---

[2]Fixated cells are treated in such a way that enzymatic activity is shut down. This prevents tissue autodigestion (autolysis), i.e. that unregulated enzymes would otherwise start to decompose cell organelles and membranes.
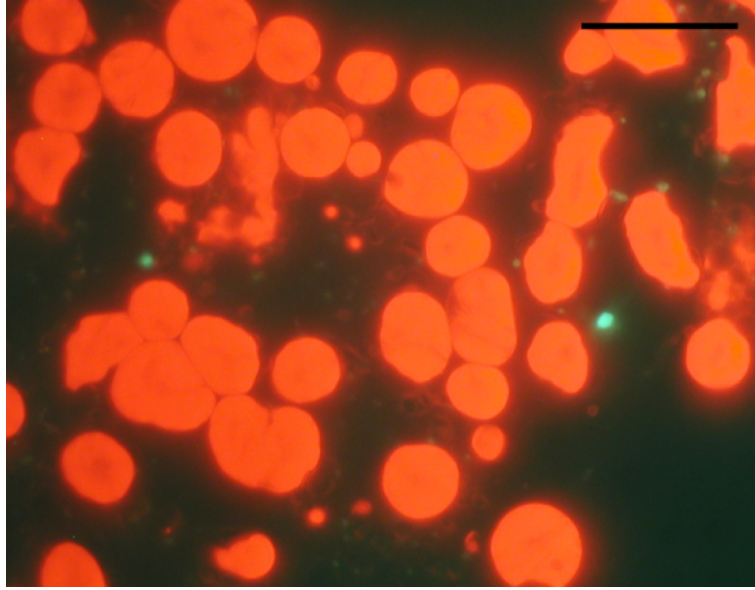
Figure 5.3: This image shows cells that have been previously treated with detergent solution. Most of them are broken open and their chloroplasts float freely (red discs in the picture). The fluorescence seen is the emission during illumination by 436 nm light. The two visible green dots belong to two photoreceptors. Their rhodopsin molecules were previously excited by 365 nm light and change now back into the ground state by emitting characteristic and intense green light. Scale bar is 20 μm.

Those spectra can be used to relate the type of alga to the type of pigments owned (chlorophyll in chloroplasts, carotenoids in eyespot droplets, rhodopsin in photoreceptor) and to position the algae within the phylogenetic tree.

5.2.3 AFM measurements

AFM Setup

Cells and cell organelles were investigated with a prototype MFP-3D atomic force microscope manufactured by Asylum Research (Santa Barbara, CA, USA). The AFM head was mounted on an inverted optical microscope (Axiovert MAT-100, Zeiss, Jena, GER) and equipped with top-view optics. This enabled precise optical positioning and investigation of transparent as well as opaque samples. Optical microscopy images were taken with a Canon digital camera.

A closed-loop XY-stage allowed for AFM scanning across an area of up to $90 \times 90 \, \mu m^2$ as well as fine-grained sample positioning for local experiments. The stage used is compatible with different sample supports, including glass slides, coverslips (very thin glass slide usually placed on top of sample and supporting glass slide), or petri dishes from $35 \, mm$ to $85 \, mm$ in diameter. The setup included

a vibration isolation table, the TableStable TS 150, to actively damp vibration frequencies of $0.7 - 1000 \, Hz$ by up to 40 decibel.

The force signal generated at the photodetector diode was sampled at 5 MHz bandwidth and all further signal conditioning and processing (i.e. filtering) done digitally under software control. For controlling the AFM, the software "Igor Pro" was used (see below).

Measurement method

Olympus AC 240 TS-E cantilevers with a resonance frequency between 61 and 77 kHz in air and a spring constant of 1.2 to 2.5 N/m were used for imaging. The data acquisition for most of the presented images was performed at the slowest possible rate of $0.1 \, Hz$ as it rendered the most details. Various attempts have been made for scanning under liquid, but the results were falling short of those of ambient AFM imaging. A number of problems have been identified, such as the difficulty to firmly attach cells to the surface under liquid, the cell surface motion even when attached to the substrate, and several problems related to the instability of cantilever resonance frequency and deflection drift. For the experiments under liquid another Olympus cantilever (around $13 \, kHz$ resonance frequency) with a low force constant was used.

For the mode of operation mostly used in the experiments, the intermittent contact mode, the driving frequency of the cantilever is an important parameter. For the Olympus AC 240 TS-E a typical setting is resumed here:

Driving Frequency: 58,595 kHz (the frequency at which the cantilever is oscillated. Setting it about 5% lower than the cantilever's resonance frequency achieves good sensitivity for surface measurements),

Piezo Voltage: 1,044 V (a relative measuring unit, related to the voltage needed to oscillate the cantilever),

Amplitude: 1 V (this corresponds to the voltage measured at the photodiode receiving the laser beam reflected from the cantilever. 1 Volt on the photodiode corresponds to the set target amplitude of the cantilever that should be achieved),

Q: 56,8 (the Q-factor, a measure for the quality of the cantilever. It based onto the shape of the resonance curve, and amongst other things takes into account the proportion of peak height and width at half height. Values range from about 10 to 200 where higher is better.)

AFM software

The software used to operate the AFM at the Institut für Allgemeine Physik in Vienna is IgorPro by Wavemetrics. All standard AFM techniques are available through the IgorPro user interface that is open for customized routines and user-defined functions. Direct access of all important controller in- and outputs also

Figure 5.4: The AFM setup at the Institut für Allgemeine Physik at the TU Vienna. A - Scanning Head, B - Scanning Stage, C - Top View Optics, D - Top View Optics Light Source, E - Zeiss Inverted Optical Microscope

open the possibility to implement new measurement techniques. It enables real time control of this type of AFM and possesses data acquisition functions, offline analysis and data manipulation tools. ([69])

In order to ease the analysis of measured data, an Igor script was written, helping to reduce image artifacts resulting from the sometimes slow feedback loop. Only the combination of trace and retrace image data (i.e. scanning along the x-axis in both directions) gives the full information about sample topography (see Fig. 5.5).

This calculation for the combination of trace and retrace images (for height or amplitude information) was included as as Igor script and made accessible through a custom menu (See Fig. 5.6 and Annex 1 on page 105 for the script file).

5.3   Sample preparation

5.3.1   Slide preparation

Well prepared slides are a prerequisite for meaningful optical and fluorescence microscopy. Cell preparation includes the collection by centrifugation, treatment of the cell, immobilizing of cells by applying the proper pressure on the thin glass
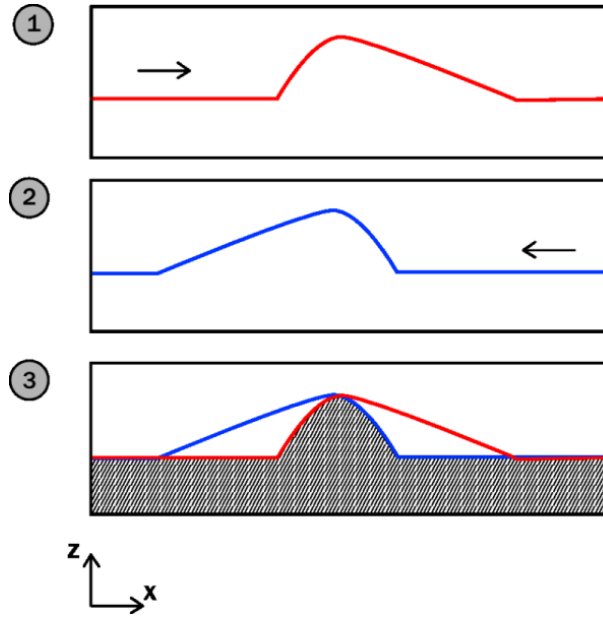
Figure 5.5: The feedback control of the cantilever during a scan is not always fast enough to follow topographic changes of the sample - although retraction (when the cantilever encounters a upwards slope in sample topography) usually closely follows sample topography, lowering of the cantilever to follow a downwards slope is sometimes too slow. In the above figure the cantilever traces a sample hillock moving from left to right (the z-axis corresponds to sample height) (1). In comparison with the retrace image (2), scanning from right to left, it can be seen that in both cases the lowering of the cantilever having passed the peak of the hillock happens too slowly and therefore produces image artifacts. These artifacts can be removed through combination of both traces, where each point is calculated as the minimum height of each trace (3 - the curve limiting the hatched area). The artifact slopes due to the slow feedback loop during the scan can be removed and the obtained image more closely matches the true sample topography.

slide (coverslip) on top of specimen and glass support, sealing the edges to protect against specimen drying and general manipulation.

For observation of the condition of the alga as well as for checking the quality of specimen preparation the optical confocal microscope was additionally used in phase contrast mode and dark field illumination mode. Higher magnification objectives were used with oil.

5.3.2 Preparation for AFM imaging in air

The best results were obtained by imaging of dried dead cells. One of the problems to overcome was the bursting of the cells due to evaporation of the surrounding
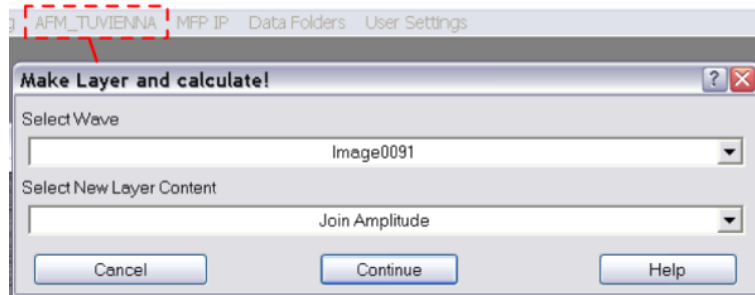
Figure 5.6: If the user menu AFM_TUVIENNA is loaded, the user can chose one of four custom functions to apply to the available scan data

liquid medium. At some point of the drying process the cells outer walls break and the inner cell parts are spilled out. The cells lose shape and material attaches to the outer cell membranes. This hinders imaging of intact cell surfaces. In addition enzymatic activity damages biological membranes that get in contact with it, altering their properties or slowly dissolve them altogether.

Dried whole cells allowing for AFM investigation in air were prepared according to the following protocol (see Fig. 5.7): $100\,\mu l$ of cell suspension were pipetted onto a glass slide and covered with a coverslip. Finger-tight force was applied onto the coverslip, removing excess solution and air bubbles. Slow evaporation of the solvent at room temperature resulted in a concentration gradient of nutrient embedding whole unscathed cells especially at the edges. After 5 minutes the coverslip was carefully removed by dragging it horizontally over the glass slide, and the samples were investigated with AFM. Such preparations were good AFM specimens for several days.

Crystalline cell parts for AFM investigation were prepared according to the preparation method described in 5.1.2. Before AFM imaging, one milliliter of the solution was centrifuged with a home-made centrifuge (see Fig. 5.8) at 800 g for 10 minutes (to remove small suspended particles). Then the fraction of the solid precipitate containing the heaviest particles was resuspended in one milliliter of HEPES solution, spread on a glass slide and dried.

A number of variations of this protocol was tried as well, including the use of specially coated slides (e.g. poly-l-lysine or gelatin coated slides) to improve the adhesion of the algal cells to the slide.

5.3.3 Preparation for AFM imaging under liquid

Plastic petridishes were used for imaging under liquid. The petridish was attached to the scanning stage of the AFM. Then a piece of glass slide was attached at its bottom. A few drops of liquid medium containing the cells or cell parts was spread

on the glass slide. In order to achieve sufficient attachment of the material onto the glass surface the material was given time to adsorb to the surface (incubation time). Depending on preparation type and liquid, this time varied from seconds to over an hour.

Poly-l-lysine coated slides were sometimes used in this setup to improve adhesion of the algae to the slides (see Fig. 5.9).

5.3.4   Experimental Preparations

For experimental purposes other types of preparations were tried out. It turned out that the most effective sample preparation method is the one given in 5.3.2.

Experimental preparations include prior calcium treatment of cells for ejection of the reservoir system and the flagellar apparatus. Through calcium diffusion internal cell pressure was raised until ejection. With the ejection of the flagellar apparatus the paraflagellar body (crystalline photoreceptor) attached to the longer flagellum becomes accessible. This procedure proved viable for good results with the optical microscope. Unfortunately, investigation with fluorescence microscopy showed that the fluorescence characteristics of the photoreceptor had deteriorated. The three-dimensional integrity of the photoreceptor was no longer guaranteed and therefore no additional investigation of these samples under the AFM was carried out.

Another experimental procedure tried was the chitosan matrix procedure. Fixated, demembranated cells were included in a chitosan matrix (its main component is chitin). Subsequent washing with alcohol, and freeze fracturing gave surfaces that were possible to scan with scanning probe techniques. Although this approach yielded some images on cell surface features, it is a time consuming process and the data obtained by ambient AFM investigation of dried specimen was clearly of better quality.
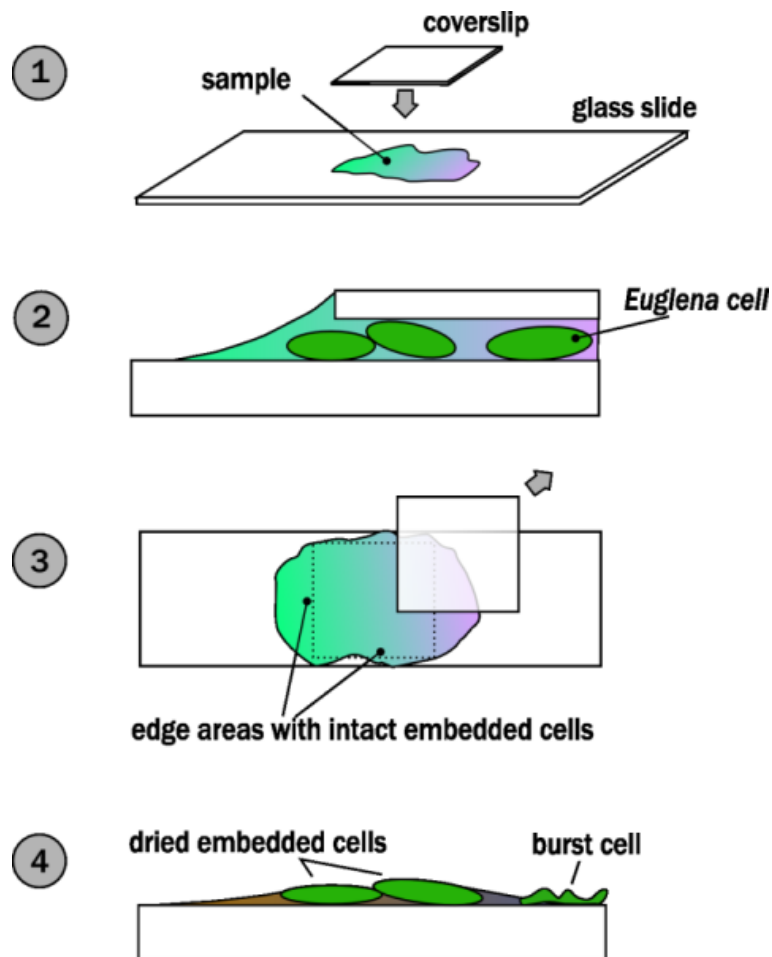
Figure 5.7: Single steps of the sample preparation. A drop of liquid containing cells is applied to the glass slide and covered by a coverslip (1). The evaporation starts at the edges around the coverslip (2 - detail). The coverslip is removed through gentle dragging after about 5 minutes to allow for complete drying (3). Although cells usually burst during the drying process (4 - detail), some areas where the edges of the coverslip have been (designated in 3) still contain embedded intact *Euglena* cells.

Figure 5.8: A small centrifuge was built (with the help of the supportive staff of the mechanical workshop at the TU-Wien) for the condensing of cell parts in the solution for the AFM. Here it is seen equipped with a vial of growth medium containing living algal cells (left) and a counterweight vial filled with water to the right.
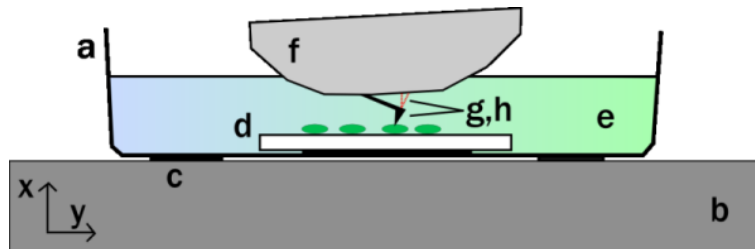
Figure 5.9: A schematic drawing of the imaging setup under liquid. The plastic petridish (a) is attached to the scanning stage (b) via double-sided scotch tape or plasticine (c). At the bottom inside the petridish, a piece of glass slide (d) is attached via double-sided scotch tape. Liquid medium (e) fills the petridish so that the cantilever (h) as well as the laser travel line (g) leaving the AFM head (f - only the lower part of the head is drawn) are fully immersed in liquid when scanning over the surface. A petridish measured about 6 cm in diameter.

Chapter 6

Results

High resolution topographic images of *E. gracilis* acquired with the Atomic Force Microscope are presented in this chapter. Algal features found are related to *Euglenoid* morphology as presented in chapter 4.

Three major goals were reached during the work on *E. gracilis*. First, a preparation method suitable for AFM investigation of *E. gracilis* had to be developed. This was found in a special drying process (see section 5.3) that left whole intact algae to be investigated. Second, AFM data of unprecedented resolution of *E. gracilis* were acquired, on the algal pellicle and even on certain cell parts. A third goal was reached in providing additional AFM data to what is already available from SEM and TEM investigations. Investigated features of the alga included e.g. imaging of the mucilage in between pellicle strips, a feature usually not visible through SEM or TEM due to sample preparation techniques that remove soft biological material. Our AFM investigation of *E. gracilis* also revealed new features that have not been described before.

6.1 Sample Preparation - Challenges and Solutions

The preparation method as presented in 5.3 solved a number of difficulties encountered with earlier attempts to image the alga.

Firstly, the algal cells burst during the drying process if no precautions are taken. Fig. 6.1 shows such a burst *E. gracilis* cell. Obviously, this hinders imaging of intact cell surfaces and in addition enzymatic activity might damage biological membranes, alter their properties or slowly dissolve them altogether (autolysis). Although certain cell features still can be made out this information is unreliable.

A further challenge in the invented drying process had been the amount of residue of the evaporated nutrient solution. As can be seen in Fig. 6.2, the embedding residue does not only prevent cells from bursting but can also prevent
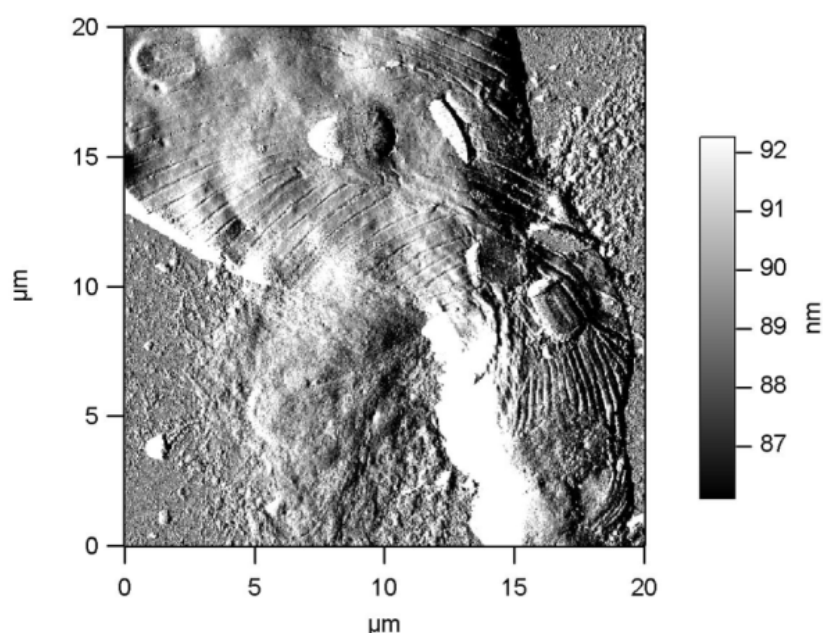
Figure 6.1: A burst *E. gracilis* cell. The pellicle is torn apart and due to the inner pressure of the cell the cytoplasm including cell organelles is ejected. If the cell has not been fixated, enzymatic activity starts to dissolve tissue, making AFM investigation even more difficult. Intermittent contact mode AFM image, Amplitude trace.

successful imaging. The proper balance is required for the residue to support the cell enough against bursting but not to cover it.

Much better results were achieved following the steps from section 5.3.2, Fig. 5.7 (on page 75) to avoid too much and too little embedding of the cells. In Fig. 6.3 the basal part of a well embedded *E. gracilis* cell is shown. The material embedding the cell alters its surface roughness around 5 μm away from the cell. Such samples proved to be exellent for AFM imaging, especially in intermittent contact mode under ambient conditions and could well be used for for several days.

It was assumed that scanning under liquid, because of the absence of a water meniscus between tip and sample (see section 3.2.1, page 27, could enhance image resolution but was found to pose another range of difficulties. Algal cells do hardly attach to even functionalized (e.g. poly-l-lysine or gelatin coated) glass supports, and a stable positioning of the scanned surface was not reached. The imprint in Fig. 6.4 was left by a *E. gracilis* cell that detached from a poly-l-lysine coated glass slide in liquid. The negative forms of the algal pellicular strips in the substrate surface can be well seen. A comparison of cell length usually measuring more than 40 − 80 μm and imprint length around 6 μm indicates a relatively small area of contact. A stable imaging surface however is a prerequisite for reproducible high resolution AFM imaging.
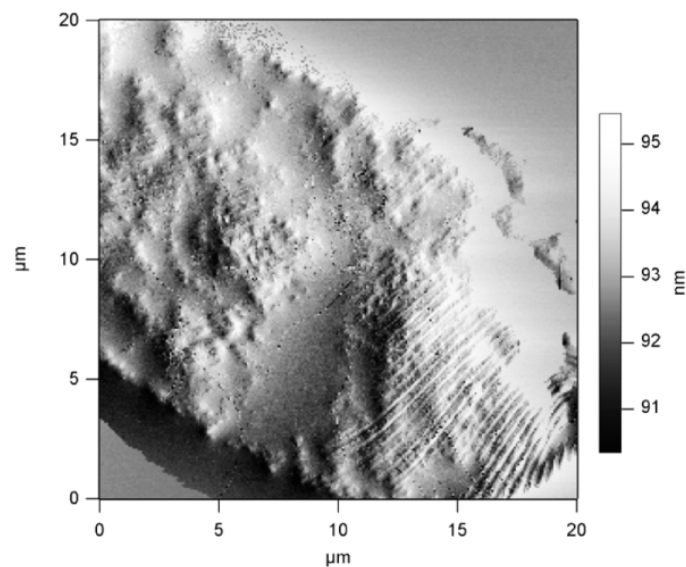
Figure 6.2: An embedded *E. gracilis* cell covered with remains of the nutrient solution after the drying process. The cell surface is not well suited for imaging with AFM. Intermittent contact mode AFM image, Amplitude trace.

Sample stability is an important challenge when scanning under liquid. In general, cells are high structures (several micrometers) and this greatly reduces stability for the AFM scan as the scanned pellicle surface is far from the pellicle part attached to the substrate. The algal cell seen in Fig. 6.5 could not be imaged with satisfactory results. Its surface did not maintain a stable position during the scan, such that the AFM imaging resulted in a slightly blurred image. Additionally the cantilever images itself as its pyramidal shaped sides touch the cell long before being exactly above it.
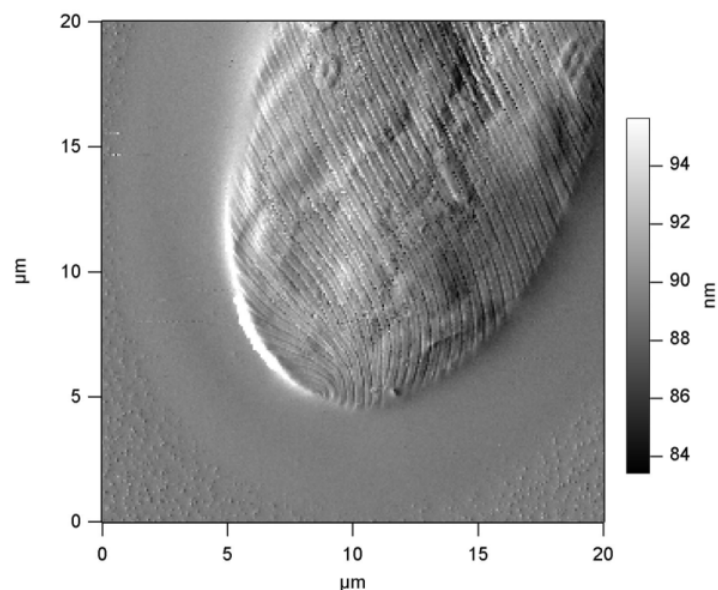
Figure 6.3: In contrast to Fig. 6.1, the cell seen here is correctly embedded by nutrient residue. This material is surrounding the cell and alters its surface roughness at around 5 μm away from the cell. Intermittent contact mode AFM image, Amplitude trace.
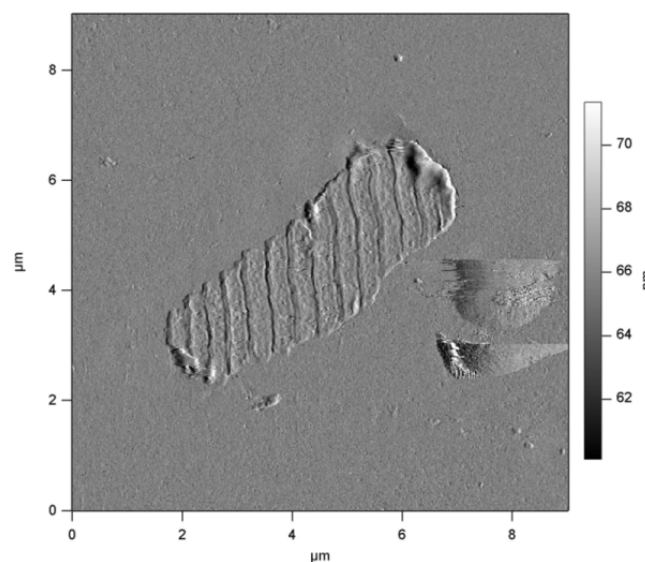
Figure 6.4: The imprint shown here was left by a *E. gracilis* cell that detached from the poly-l-lysine covered glass substrate. When scanning under liquid too little sample adhesion can pose a problem. Intermittent contact mode AFM image, Amplitude trace.
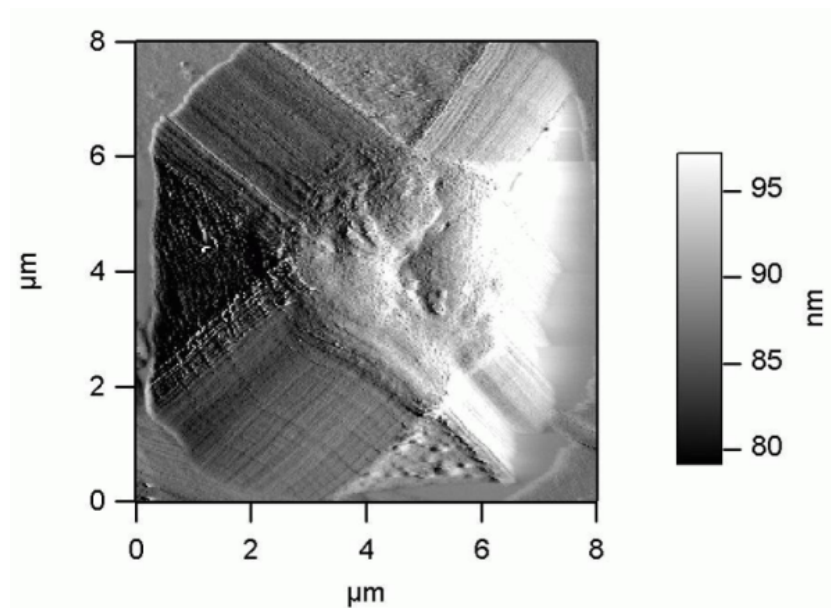
Figure 6.5: Scanning under liquid showed another considerable negative effect. This cell (no *Euglena* cell) is too high to provide a stable scanning surface for the AFM. Intermittent contact mode AFM image, Amplitude trace.

6.2 AFM data and cell features

Below some images in AFM xy-mode are presented. They clearly demonstrate the convenience of Atomic Force Microscopy as a tool for high resolution imaging of *E. gracilis* cells. AFM data could be acquired of various features of the *Euglena gracilis* cell, including cell walls, mucus excretion pellicle pores, crystalline cell parts and new surface features not previously reported or visible on SEM/TEM images available in the literature.

Fusing pellicle strips

In the left part of Fig. 6.6, the basal part of an *E. gracilis* cell shows the distinct fusing of its pellicle strips. To our knowledge this is the first time that the strip reduction patterns of *E. gracilis* have been imaged by AFM. Also in Fig. 6.6, to the right, a schematic drawing of a pellicular strip reduction pattern is given. Such patterns can provide information on algal evolutionary pathways and may also be derived from mathematical expressions ([118]). AFM easily resolves pellicular strip endings and can be used to compare how these differ from other strip parts.
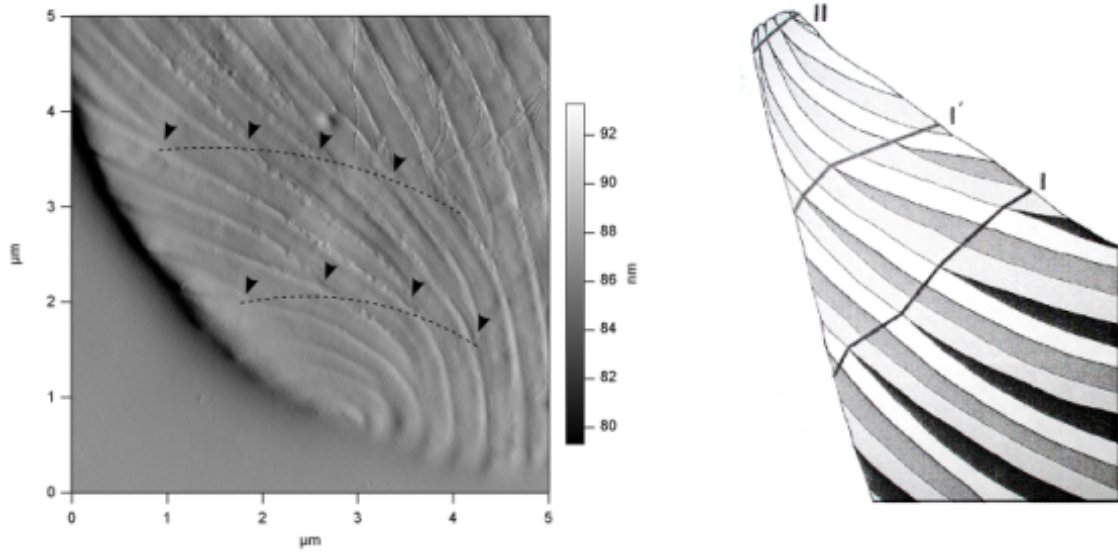

Figure 6.6: Left: Detail of the basal part of an *E. gracilis* cell. Arrowheads indicate end points of pellicular strips and broken lines hint at strip reduction patterns. Intermittent contact mode AFM image, Amplitude trace. Right: Diagram illustrating linear patterns of strip reduction at the posterior end of *Euglena mutabilis*. Three consecutive strips pass whorl **I**, two pass whorl **I'** and only one passes whorl **II**. Image adapted from [118].
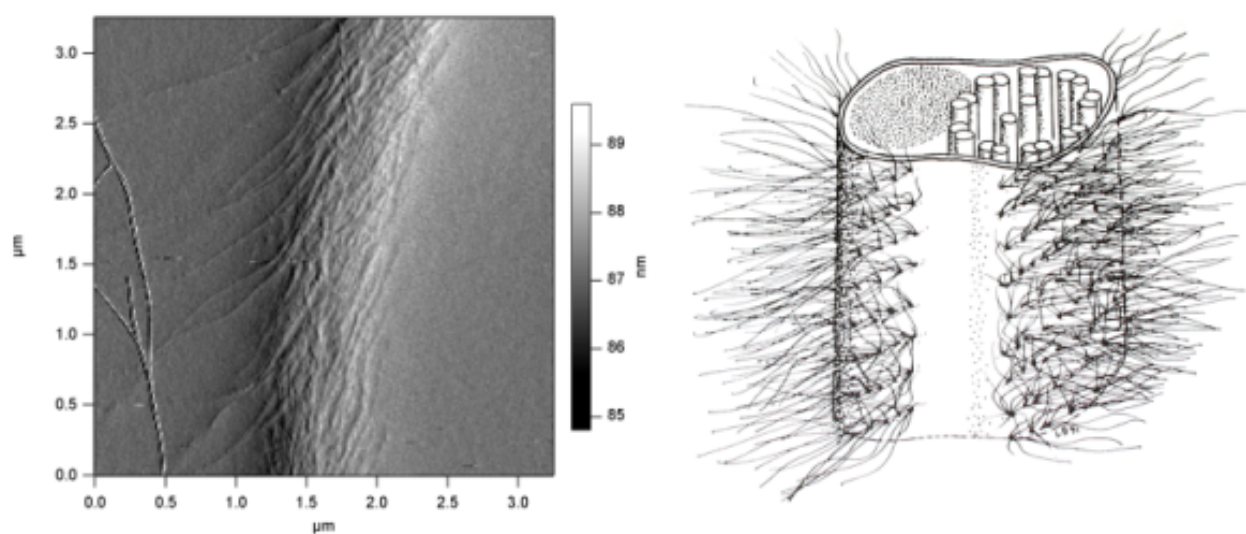
Flagellum

The flagellum of an *E. gracilis* cell can be seen emerging from the reservoir at the visible canal opening in Fig. 6.7. Toward the bottom region the pellicular strips bend inwards in order to form the reservoir inside the cell.

In the left part of the next figure, Fig. 6.8, a detail of the flagellum has been imaged. Confirming the SEM and TEM data from the literature, mastigonemes, hairlike structures of only around $10\,nm$ in diameter covering *Euglena's* flagellum could be resolved with AFM. However, the exact arrangement of mastigonemes along the flagellar surface is to date still unknown, and a diagram of a possible arrangement that was not contradicted by our AFM data is given in the right part of Fig. 6.8.

To our knowledge this is the first time that the flagellum as well as the canal opening from which it emerges has been imaged with AFM at this resolution.
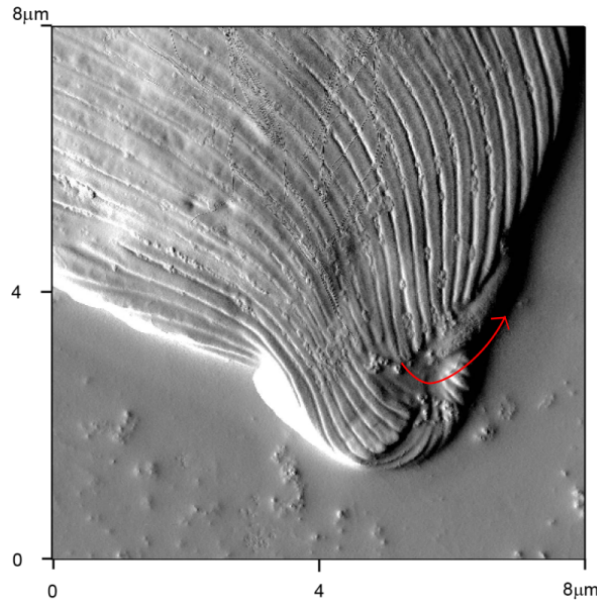
Figure 6.7: Apical part of an *E. gracilis* cell showing the location where the flagellum emerges from the canal (arrow). The flagellum in this image then turns under the cell body. Intermittent contact mode AFM image, Amplitude trace.

Figure 6.8: Left: Detail view of a part of an *E. gracilis* flagellum, completely covered by mastigonemes (fine hairlike structures). Intermittent contact mode AFM image, Amplitude trace. Right: Diagram illustrating a possible arrangement of mastigonemes along the flagellar surface. Image adapted from [82].

Pellicle

The pellicle of *E. gracilis* could be imaged with AFM with excellent resolution and detail. For example in Fig. 6.9 the apical part of such a cell is shown, revealing the flagellum, a deepened shape of the reservoir and an embossed shape of a crystalline storage grain (paramylum). The visibility of the reservoir and the paramylum grain results from the flattening of the cell due to the drying process where the algal pellicle sinks into the reservoir and relaxes over the hard paramylum grain.
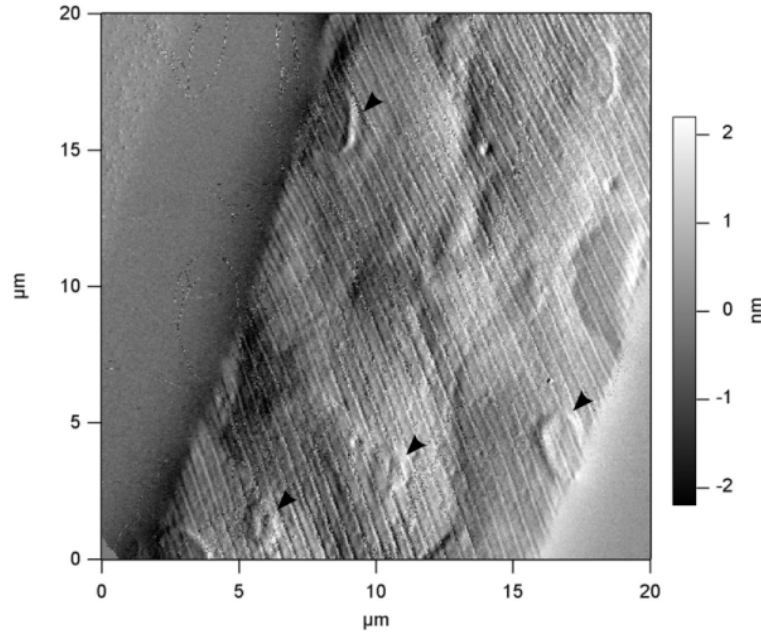
In Fig. 6.10, the middle part of an *E. gracilis*, the course of the pellicular strips is very distinct. They are arranged diagonally and are very uniform in thickness and direction. The pellicle usually grows as a left-handed spiral. Some paramylums show as cameo shapes in the pellicle.
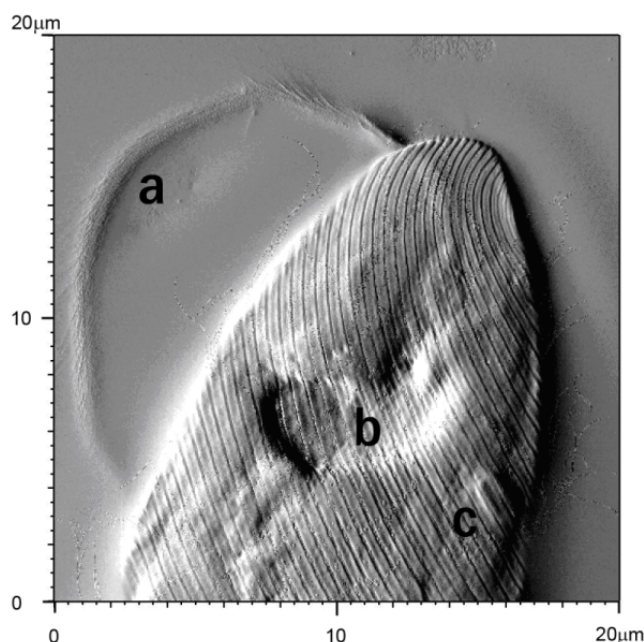
Figure 6.9: Apical part of an *E. gracilis* cell. **a** flagellum, **b** reservoir, **c** cameo shape of a paramylum grain. Image size $20 \times 20 \ \mu m^2$, Intermittent contact mode AFM image, Amplitude trace.

Zooming into the details of a typical pellicle of an *E. gracilis* cell, the articulations between the strips can be seen showing lubricant material features. In Fig. 6.11, a detail view of a group of pellicle strips is given. The small spots distributed mainly between the strips are mucilage, biological lubricant produced by the algae. The alga is able to actively slide its pellicle strips against each other in order to change its shape.

A high resolution detail of previous figure is given in Fig. 6.12 that shows again the mucilage between the strips as well as microtubuli that presumably stem from another disrupted cell. Euglenoid mucilage, a polysaccharide network specially

Figure 6.10: The middle part of an *E. gracilis* cell, the apical part would be found toward the top. Some crystalline storage grains, paramylums, show as cameo shapes (arrowheads) in the pellicle. They press against the pellicle after the drying process. Intermittent contact mode AFM image, Amplitude trace.

tuned to the alga's need of lubrication, could prove to be an excellent target for viscoelastic studies using AFM force curves.

As of our knowledge this is the first time that pellicular strips and mucilage of an *E. gracilis* cell were imaged at this resolution. The available data in the literature, mostly SEM and TEM data does not include reliable information about distribution and properties of *Euglena's* mucilage.

A feature that has not yet been observed by either SEM or TEM is presented in Fig. 6.13. The figure shows indentations as imaged by AFM that occur in the in the middle of pellicular strips. Such features are not to be seen in SEM and TEM images. Pellicle pores known from the literature differ in size and position from the features found. They are located to the side of a pellicular strip whereas the new indentations are found at the center of a strip. The fact that the new indentations can be imaged with the AFM might be due to our gentle preparation methods that differ from preparation methods for SEM/TEM.

For comparison, a SEM image is given in Fig. 6.14 that does not show any features in the middle of pellicular strips. The features seen are well known pellicle pores and they are not located centered on the strips as opposed to the indentations measured by AFM.
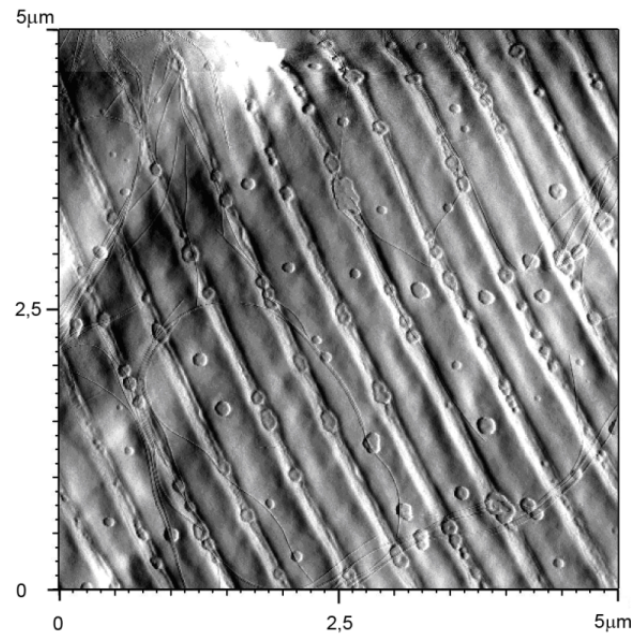
Figure 6.11: The pellicle of an *E. gracilis* cell showing details of the pellicle including mucilage in between and on the pellicular strips. Image size $5 \times 5\,\mu m^2$, Intermittent contact mode AFM image, Amplitude trace.
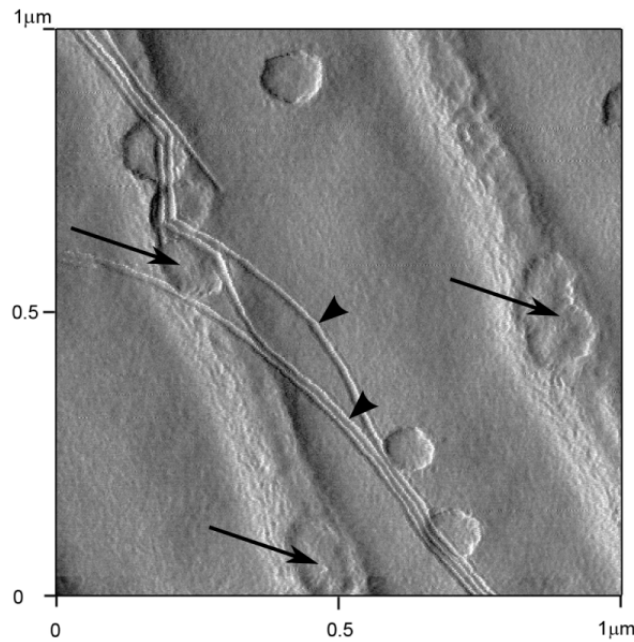
Figure 6.12: Pellicular strips of an *E. gracilis* cell showing ridges, mucilage (arrows) excreted at canal openings between the strips and a bundle of three microtubuli (arrowheads) presumably stemming from a disrupted cell. Image size $1\,\mu m^2$, Intermittent contact mode AFM image, Amplitude trace.
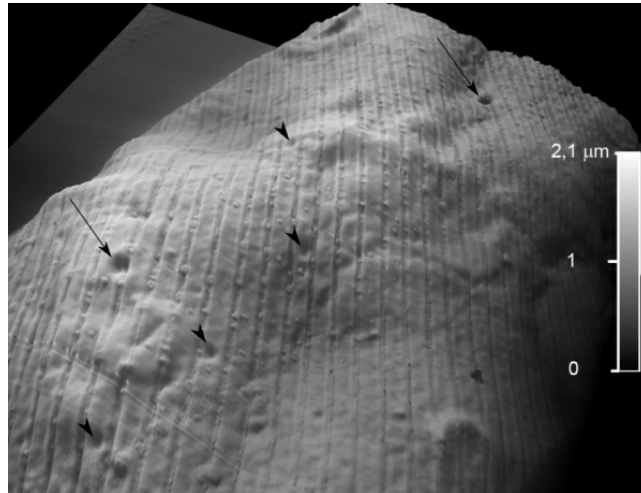
Figure 6.13: 3-D view of the middle part of a dried *E. gracilis* cell. The arrows point towards features clearly identified with pellicle pores, as they have been known from SEM investigations since the late 1960s ([116]). The arrowheads indicate new surface features that seems to have no correlation in other imaging data of *E. gracilis* such as acquired by SEM and TEM. Intermittent contact mode AFM data, 3D-view based on Height trace.
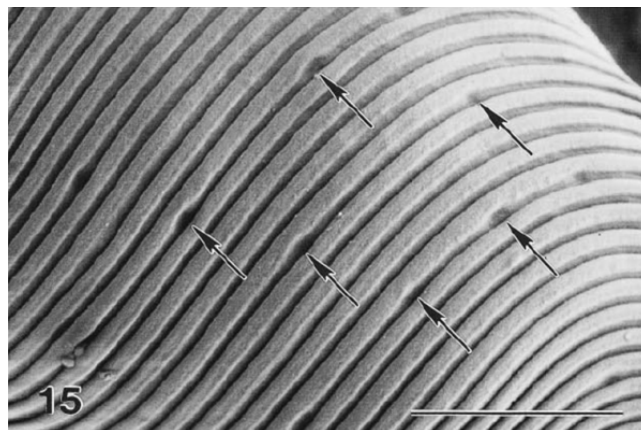
Figure 6.14: A SEM image of the pellicle of the alga *E. terricola*. The pellicle pores as indicated by the arrows are distributed along the ridges, creating small narrowings of the adjacent pellicular strips. Indentation features like these on the *Euglena* pellicle that appear centered on the strips are not to be found. Scale bar is $2\,\mu m$. Image adapted from [116].

Crystalline Cell Parts

Crystalline cell parts had to be imaged after a series of preparation and purification steps. Successful imaging included semicrystalline starch deposits (paramylum grains) and cell parts. AFM imaging of such a cell part solution has never been done before and in this sense the next images are unique. A view on a dried sample by optical microscopy is seen in Fig. 6.15. Small lumps of material aggregated and it often was difficult to locate intact cell parts within.

In comparison, in Fig. 6.16 a patch of dried crystalline cell part solution as imaged by AFM is shown. This patch is of good quality because it does not only contain the residue of dissolved biological material but also crystalline cell parts. E.g. a paramylum grain can be spotted to the lower left of the image.

In Fig. 6.17 a feature often found in such a dried crystalline cell parts preparation is seen. The size and shape of this feature correlate to those of a lipid body, one of *Euglena's* energy storage facilities.

The search for the photoreceptor of *E. gracilis* yielded the imaging of very interesting regular structures such as the one in Fig. 6.18. Despite the layered nature of the structure, further AFM investigation is needed for a more complete assessment. An *E. gracilis* cell contains only one photoreceptor at a mass of only about 1/20000th of that of the whole cell. Even in our purified solution a targeted approach using AFM is difficult.

The last figure, Fig. 6.19, gives a 3D-view of a paramylum grain based on AFM height information. It confirms the overall concentric pattern found in such a grain stemming from the crystalline assembly of microfibrils only $4\,nm$ in diameter. On page 60, Fig. 4.18 shows a SEM image of a freeze-fractured paramylum grain. The details of the microfibril assembly are not yet fully understood. ([108], [113])


Figure 6.15: The cantilever scanning over a dried solution of crystalline cell parts. Image taken by optical light microscopy (transmitted light).
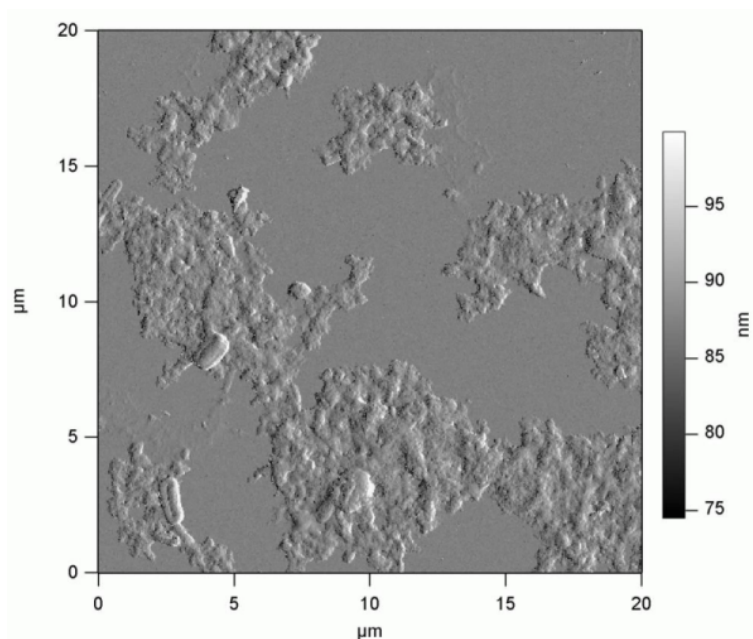
Figure 6.16: A patch of dried crystalline cell parts solution. Intermittent contact mode AFM image, Amplitude trace.
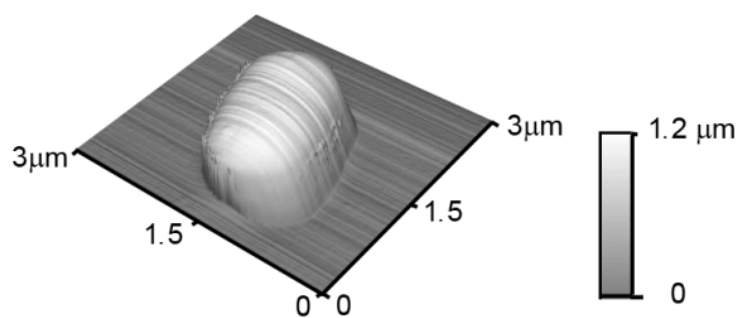
Figure 6.17: A feature repeatedly found in the crystalline cell parts preparation. The size and shape correlate to those of a lipid body. Intermittent contact mode AFM image, Amplitude trace.
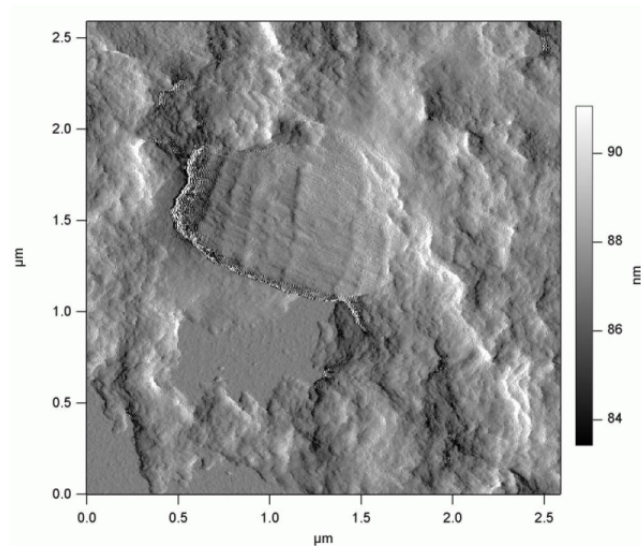
Figure 6.18: A layered structure that is a possible photoreceptor candidate. Intermittent contact mode AFM image, Amplitude trace.
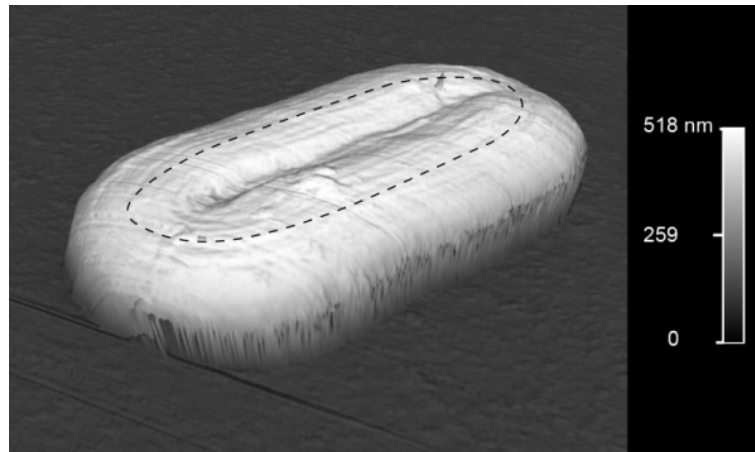
Figure 6.19: A paramylum grain of a *E. gracilis* cell showing its characteristic concentric pattern (indicated by the broken line). Image size $2.5 \times 2.5 \ \mu m^2$, Intermittent contact mode AFM data, 3D-view based on Height trace.

Chapter 7

Outlook

The Atomic Force Microscope (AFM) has proven to be a valuable tool for investigation of biomaterials at the small scale. In this work the single celled alga *Euglena gracilis* was investigated in the light of being a bionanotechnological system accommodating a wealth of functional units within only small volume. A method for AFM data acquisition of the alga *Euglena gracilis* was developed and further investigation can build upon this approach.

As this work is only a beginning of the AFM study of this alga, it focused on its morphology, on how to obtain first image data of *Euglena's* pellicle and some of its functional cell organelles with potential for technical applications. This undertaking can be seen as an ignition part in the investigation of algal materials exhibiting molecular precision achitecture and complexity inherent to living systems.

While the data obtained on whole cells as well as cell organelles provided essentially morphological data and proved the feasibility of such studies by means of AFM, other analytical characterization methods, e.g AFM force spectroscopy, are now possible on these and similar algae by making use of the preparation method developed herein. Since AFM yields information about the sample as well as it allows manipulation on the micro and nanoscale, future research attempts along these lines seem encouraging.

The exact nature of the novel features found, i.e. the indentations in the center of pellicular strips, should be further analyzed, especially with regards to the sample preparation techniques used. Equally interesting, AFM force spectroscopy shall characterize the mucus material ejected by mucus excretion pellicle pores.

Further, elucidation about the three-dimensional structure of the photoreceptor was attempted with this work, however, the fraction of crystalline parts contained too few photoreceptors to be found with the AFM tip, since crystalloid bodies, paramylon grains and not completely removed cell material amounted for a large portion of the fraction. Possible future approaches comprise the development of a preparation technique for a solution containing a plentitude of photoreceptors.

It might also be possible that combination with fluorescence microscopy simplifies observational search for the location of the photoreceptor.

As bottomline, a number of future research directions seem worthwhile. AFM can help relating structure to function in biomaterials, a precursor to develop bioinspired artifial systems. *Euglena gracilis* is an ideal object of study when general nanotechnological design principles of living systems are to be investigated. ([119])

Chapter 8

Acknowledgments

Appendix A

Acronyms

SPM Scanning Probe Microscope/Microscopy

STM Scanning Tunneling Microscope/Microscopy

TEM Transmission Electron Microscope/Microscopy

SEM Scanning Electron Microscope/Microscopy

AFM Atomic Force Microscope/Microscopy

3D three-dimensional

DC direct current

NASA National Aeronautics and Space Association

MFM Magnetic Force Microscope/Microscopy

UHV Ultra High Vacuum

Bibliography

[1] R. J. Szabo: *An Introduction to String Theory and D-Brane Dynamics*, Imperial College Press (2004)

[2] R. Feynman: *There's Plenty of Room at the Bottom*, Engineering and Science, CalTech, (1960)

[3] F. Aumayr, HP. Winter: *Inelastic interactions of slow ions and atoms with surfaces*, Nucl. Instrum. Meth. Phys. Res. B 233 (2005), pp. 111-124

[4] F. Aumayr, J. Stöckl, M. Fürsatz, W. Meissl, HP. Winter: *Interaction of slow multiply charged Ar ions with a LiF insulator surface*, e-Journal of Surface Science and Nanotechnology 4 (2006), pp. 388-393

[5] B. Edmonds, *What is Complexity? - The philosophy of complexity per se with application to some examples in evolution*, chap. from "The Evolution of Complexity", Kluwer, Dordrecht (1999)

[6] *MEMS structures*, from http://www.sensordynamics.cc/images/content/images

[7] C. Sanchez, H. Arribart, M. M. Giraud Guille: *Biomimetism and bioinspiration as tools for the design of innovative materials and systems*, Nature Materials 4 (2005), pp. 277-288

[8] B. Bushan (ed.): *Springer Handbook of Nanotechnology*, Springer-Verlag, Berlin, Heidelberg (2004), ISBN 3-540-01218-4

[9] *Leonardo da Vinci and Otto Lilienthal drawings*, from http://www.cicsworld.org/blogs/vramanan/2006/12/ leonardo_da_vinci_and_his_flyi.html

[10] http://www-scf.usc.edu/~tchklovs/Proposal.htm, alex.edfac.usyd.edu.au/.../Fatinah/page3.htm

[11] http://www.nasaexplores.com/show2_912a.php?id=02-025&gl=912

[12] *Definition of Nanotechnology*, National Science Foundation, http://www.nsf.gov/crssprgm/nano/reports/omb_nifty50.jsp

[13] A. Junk, F. Riess: *From an idea to a vision: There's plenty of room at the bottom*, Am. J. Phys., 74 Iss. 9 (2006), pp. 825-830

[14] L. Abicht, H. Freikamp, U. Schumann: *Identification of skill needs in nanotechnology*, Cedefop Panorama series 120, Luxembourg: Office for Official Publications of the European Communities (2006)

[15] E. Drexler: *Engines of Creation - The Coming Era of Nanotechnology*, Anchor Books, New York, (1986)

[16] R. Freitas, J. Gilbreath, W. Gilbreath (eds): *Advanced Automation for Space Missions*, Proceedings NASA/ASEE Summer Study, (1980)

[17] R. Merkle: *NASA and Self-Replicating Systems: Implications for Nanotechnology*, Foresight Update, Foresight Institute, 9 (1990), p. 4

[18] E. Drexler: *Nanosystems: Molecular Machinery, Manufacturing and Computation*, Wiley-Interscience (1992), chapt. 8

[19] *Classification of nanotechnology*, http://cnst.rice.edu/nano.cfm, The Richard E. Smalley Institute for Nanoscale Science and Technology, Rice University

[20] J. D. Chodera, W. C. Swope, J. W. Pitera, K. A. Dill: *Long-time protein folding dynamics from short-time molecular dynamics simulations*, Multiscale Modeling & Simulation 5 (4), (2006), pp. 1214-1226

[21] *IBM System Blue Gene solution*, http://www-03.ibm.com/servers/deepcomputing/bluegene.html

[22] *Distributed Computing - Protein Folding*, Folding@home, http://folding.stanford.edu/download.html

[23] http://www.kurzweilai.net/

[24] P. G. Piva, G. A. DiLabio, J. L. Pitters, J. Zikovsky, M.Rezeq, S. Dogel, W. A. Hofer, R. A. Wolkow: *Field regulation of single-molecule conductivity by a charged surface atom*, Nature 435, (2005), pp. 658-661

[25] E. G. Emberly, G. Kirczenow: *The Smallest Molecular Switch*, Phys. Rev. Lett. 91, (2003)

[26] *Nanomaterials*, http://materials.globalspec.com/

[27] *Nanoporous random glassy polymers*, United States Patent 20030229189

[28] G. Oberdorster, Z. Sharp, V. Atudorei, A. Elder, R. Gelein, A. Lunts, W. Kreyling, C. Cox: *Extrapulmonary translocation of ultrafine carbon particle following whole-body inhalation exposure of rats*, J. Toxicol. Environ. Health A 65, (2002), pp. 1531-1543.

[29] P. HM. Hoet, I. Brüske-Hohlfeld, O. V. Salata: *Nanoparticles – known and unknown health risks*, J. Bionanotechnology 2/12, (2004)

[30] *Risk Assessment of Nanoparticles*,
http://www.iom-world.org/research/nanoparticles.php

[31] G. Binnig, H. Rohrer, Ch. Gerber, E. Weibel: *Surface studies by scanning tunneling microscopy*, Phys. Rev. Lett., 49 (1982), pp. 57–61

[32] G. Binnig, C. F. Quate, Ch. Gerber: *Atomic force microscope*, Phys. Rev. Lett., 56 (1986), pp. 930–933

[33] I. Giaever: *Energy gap in superconductors measured by electron tunneling*, Phys. Rev. Lett., 5 (1960), pp. 147–148

[34] E. Meyer, H. J. Hug, R. Bennewitz: *Scanning probe microscopy: the lab on a tip*, Springer (2003)

[35] http://www.usbyte.com/common/AFM_storage.htm, US-Byte

[36] D. Sarid, V. Elings: *Review of scanning force microscopy*, J. Vac. Sci. Technol., B 9 (1991), pp. 431–437

[37] E. Meyer: *Atomic force microscopy*, Surf. Sci. 41 (1992), pp. 3–49

[38] G. Friedbacher, H. Fuchs: *Classification of scanning probe microscopies*, Pure Appl. Chem. 71 (7) (1999), pp. 1337 - 1357

[39] C. Rotsch, K. Jacobson, M. Radmacher: *Investigating live cells with the atomic force microscope*, Scanning Microsc. 11 (1997), pp. 1-8

[40] Y. Martin, C. C. Williams, and H. K. Wickramasinghe: *Atomic force microscope–force mapping and profiling on a sub 100-Å scale*, J. Appl. Phys. 61/10 (1987), pp. 4723-4729

[41] I. Gebeshuber, R. Smith, H. Winter, F. Aumayr: *Scanning probe microscopy across dimensions*, NATO Security through Science series -B: Physics and Biophysics - Vol. 3, pp. 139-165

[42] *Phase contrast images of hydrogel coatings*,
http://www.eaglabs.com/files/appnotes/BN1424.pdf

[43] O. Marti, B. Drake, P. K. Hansma: *Atomic force microscopy of liquid-covered surfaces: atomic resolution images*, Appl. Phys. Lett. 51 (1987), pp. 484–486

[44] T. R. Albrecht and C. F. Quate: *Atomic resolution imaging of a nonconductor by atomic force microscopy*, J. Appl. Phys. 62 (1987), pp. 2599–2602

[45] J. Ruan, B. Bhushan: *Atomic-scale and microscale friction of graphite and diamond using friction force microscopy*, J. Appl. Phys. 76 (1994), pp. 5022–5035

[46] F. Ohnesorge, G. Binnig: *True atomic resolution by atomic force microscopy through repulsive and attractive forces*, Science 260 (1993), pp. 1451–1456

[47] Y. Sugimoto, P. Pou, M. Abe, P. Jelinek, R. Pérez, S. Morita,Ó. Custance: *Chemical identification of individual surface atoms by atomic force microscopy*, Nature 446, (2007), pp. 64-67

[48] P. Hinterdorfer, W. Baumgartner, H. J. Gruber, K. Schilcher, H. Schindler: *Detection and Localization of Individual Antibody-Antigen Recognition Events by Atomic Force Microscopy*, Proc. Nat. Acad. Sci. USA 93 (1996), pp. 3477–3481

[49] R. Merkel, P. Nassoy, A. Leung, K. Ritchie, E. Evans: *Energy landscapes of receptor–ligand bonds explored with dynamic force spectroscopy*, Nature 397 (1999), pp. 50–53

[50] F. Kienberger, G. Kada, H. J. Gruber, V. Ph. Pastushenko, C. Riener, M. Trieb, H.-G. Knaus, H. Schindler, P. Hinterdorfer: *Recognition force spectroscopy studies of the NTA-His6 bond*, Single Mol. 1 (2000), pp. 59–65

[51] P. Hinterdorfer, K. Schilcher, W. Baumgartner, H. J. Gruber, H. Schindler: *A mechanistic study of the dissociation of individual antibody-antigen pairs by atomic force microscopy*, Nanobiology 4 (1998), pp. 39–50

[52] J. Fritz, A. G. Katopidis, F. Kolbinger, D. Anselmetti: *Force-mediated kinetics of single Pselectin/ligand complexes observed by atomic force microscopy*, Proc. Nat. Acad. Sci. USA 95 (1998), pp. 12283–12288

[53] W. Baumgartner, P. Hinterdorfer, W. Ness, A. Raab, D. Vestweber, H. Schindler, D. Drenckhahn: *Cadherin interaction probed by atomic force microscopy*, Proc. Nat. Acad. Sci. USA 97 (2000), pp. 4005–4010

[54] F. Schwesinger, R. Ros, T. Strunz, D. Anselmetti, H.-J. Güntherodt, A. Honegger, L. Jermutus, L. Tiefenauer, A. Plückthun: *Unbinding forces of single antibody-antigen complexes correlate with their thermal dissociation rates*, Proc. Nat. Acad. Sci. USA 29 (2000), pp. 9972–9977

[55] P. P. Lehenkari, M. A. Horton: *Single integrin molecule adhesion forces in intact cells measured by atomic force microscopy*, Biochem. Biophys. Res. Com. 259, (1999), pp. 645–650

[56] H. Wanga, R. Basha, D. Lohr: *Two-component atomic force microscopy recognition imaging of complex samples*, Anal. Biochem. 361/2, (2007), pp. 273-279

[57] M. Viani, L. Pietrasanta, J. Thompson, A. Chand, I. Gebeshuber, J. Kindt, M. Richter, H. Hansma, P. Hansma: *Probing Protein-Protein Interactions in Real Time*, Nature struct. biol. vol. 7 nbr 8 (2000), pp. 644-647

[58] B. Bhushan: *Handbook of Micro/Nanotribology*, 2nd edn. CRC, Boca Raton (1999)

[59] N. A. Burnham, D. D. Domiguez, R. L. Mowery, R. J. Colton: *Probing the surface forces of monolayer films with an atomic force microscope*, Phys. Rev. Lett. 64 (1990), pp. 1931–1934

[60] C. D. Frisbie, L. F. Rozsnyai, A. Noy, M. S. Wrighton, C. M. Lieber: *Functional group imaging by chemical force microscopy*, Science 265 (1994), pp. 2071–2074

[61] V. N. Koinkar, B. Bhushan: *Microtribological studies of unlubricated and lubricated surfaces using atomic force/friction force microscopy*, J. Vac. Sci. Technol. A 14 (1996), pp. 2378–2391

[62] B. Bhushan, S. Sundararajan: *Micro/Nanoscale friction and wear mechanisms of thin films using atomic force and friction force microscopy*, Acta Mater. 46 (1998), pp. 3793–3804

[63] *Magnetic Force Microscopy*, http://mechmat.caltech.edu/~kaushik/park/1-3-0.htm

[64] A. Hategan, R. Law, S. Kahn, D. E. Discher: *Adhesively-tensed cell membranes: Lysis kinetics and atomic force microscopy probing*, Biophysic Journal, 85 (2003), p. 2746

[65] N. A. Burnham, R. J. Colton: *Measuring the nanomechanical properties and surface forces of materials using an atomic force microscope*, J. Vac. Sci. Technol. A 7 (1989), pp. 2906–2913

[66] B. Bhushan, V. N. Koinkar: *Nanoindentation hardness measurements using atomic forcemicroscopy*, Appl. Phys. Lett. 75 (1994), pp. 5741–5746

[67] D. DeVecchio, B. Bhushan: *Localized surface elasticity measurements using an atomic force microscope*, Rev. Sci. Instrum. 68 (1997), pp. 4498–4505

[68] S. B. Schujman, R. Vajtai, Y. Shusterman, S. Biswas, B. Dewhirst, L. J. Schowalter, B. Q. Wei, P. M. Ajayan: *AFM-Based Surface Potential Measurements on Carbon Nanotubes*, Materials Research Society, Fall Meeting (2001), Symp. Z

[69] AsylumResearch, http://www.asylumresearch.co.uk

[70] M. Rief, M. Gautel, F. Oesterhelt, J. M. Fernandez, H. E. Gaub: *Reversible unfolding of individual titin immunoglobulin domains by AFM*, Science 276 (1997), pp. 1109–1112

[71] A. L. Weisenhorn, J. E. MacDougall, J. A. C. Gould, S. D. Cox, W. S. Wise, J. Massie, P. Maivald, V. B. Elings, G. D. Stucky, P. K. Hansma: *Imaging and manipulating of molecules on a zeolite surface with an atomic forcemicroscope*, Science 247 (1990), pp. 1330–1333

[72] O. M. Leung, M. C. Goh: *Orientation ordering of polymers by atomic force microscope tip-surface interactions*, Science 225 (1992), pp. 64–66

[73] D. W. Abraham, H. J. Mamin, E. Ganz, J. Clark: *Surface modification with the scanning tunneling microscope*, IBM J. Res. Dev. 30 (1986), pp. 492–499

[74] R. M. Silver, E. E. Ehrichs, A. L. de Lozanne: *Direct writing of submicron metallic features with a scanning tunnelling microscope*, Appl. Phys. Lett. 51 (1987), pp. 247–249

[75] A. Kobayashi, F. Grey, R. S. Williams, M. Ano: *Formation of nanometer-scale grooves in silicon with a scanning tunneling microscope*, Science 259 (1993), pp. 1724–1726

[76] B. Parkinson: *Layer-by-layer nanometer scale etching of two-dimensional substrates using the scanning tunneling microscopy*, J. Am. Chem. Soc. 112 (1990), pp. 7498–7502

[77] Yuan-Ron Ma, Yung Liou, Yeong-Der Yao: *Pushing nanoparticles of $La_{0.7}Sr_{0.3}Mn_{O3}$*, Journ. Magnetism and Magnetic Materials 282, (2004), pp. 342-345

[78] A. Majumdar, P. I. Oden, J. P. Carrejo, L. A. Nagahara, J. J. Graham, J. Alexander: *Nanometer-scale lithography using the atomic force microscope*, Appl. Phys. Lett. 61 (1992), pp. 2293–2295

[79] B. Bhushan: *Micro/Nanotribology and its applications to magnetic storage devices and MEMS*, Tribol. Int. 28 (1995), pp. 85–96

[80] L. Tsau, D. Wang, K. L. Wang: *Nanometer scale patterning of silicon(100) surface by an atomic force microscope operating in air*, Appl. Phys. Lett. 64 (1994), pp. 2133–2135

[81] E. Delawski, B. A. Parkinson: *Layer-by-layer etching of two-dimensional metal chalcogenides with the atomic force microscope*, J. Am. Chem. Soc. 114 (1992), pp. 1661–1667

[82] G. Rosati, F. Verni, L. Barsanti, V. Passarelli, P. Gualtieri: *Ultrastructure of the Apical Zone of Euglena Gracilis: Photoreceptros and Motor Apparatus*, Electron Microsc. Rev. 4 (1991), pp. 319-342

[83] http://www.bio.mtu.edu/the_wall/phycodisc/EUGLENOPHYTA/ gfx/EUGLENA_GAGGLE.jpg

[84] G. F. Leedale: *Euglenoid flagellates*, Englewood Cliffs, N.J., Prentice-Hall (1967)

[85] H. Zumstein: *Zur Morphologie und Physiologie der Euglena gracilis* Klebs. Jahrb. Wiss. Bot. 34 (1900), pp. 148-198

[86] V. Evangelista , V. Passarelli, L. Barsanti, P. Gualtieri: *Fluorescence behaviour of Euglena photoreceptor*, Photochemistry and Photobiology, 78 (2003), pp. 93-97

[87] G. Rosati, L. Barsanti, V. Passarelli, A. Giambelluca, P. Gualtieri: *Ultrastructure of a novel non-photosynthetic Euglena mutant*, Micron, 27 (1996), p. 367

[88] O. R. Anderson: *Comparative Protozoology*, Springer Verlag, NY (1988)

[89] B. Marin, A. Palm, M. Klingberg, M. Melkonian: *Phylogeny and taxonomic revision of plastid-containing euglenophytes based on SSU rDNA sequence comparisons and synapomorphic signatures in the SSU rRNA secondary structure*, Protist 154 (2003), pp. 99–145.

[90] *Phylogenetics*, http://en.wikipedia.org/wiki/Phylogenetics

[91] R. Dubreuil, G. Bouck: *The membrane skeleton of a unicellular organism consists of bridged, articulating strips.*, J Cell Biol., 101 (1985), pp. 1884-96

[92] H. Streble, D. Krauter: *Das Leben im Wassertropfen. Mikroflora und Mikrofauna des Süßwassers. Ein Bestimmungsbuch.* Franckh-Kosmos, 10. ed., Stuttgart (1988), pp. 148-49

[93] I. Mennerich: *Euglena - Augentierchen*, Schulbiologiezentrum Hannover, Arbeitshilfe 15.20, 2. ed., Hannover (2003)

[94] D. Trebbels: *Die Protozoen*, PDF-file (2002)

[95] *Das Augentierchen Euglena: ein einzelliger Geißelträger des Süßwassers*, from http://www.fortunecity.de/lindenpark/hundertwasser/517/Euglena.html

[96] R. W. Schoenlein, L. A. Peteanu, R. A. Mathies, C.V. Shank: *The first step in vision: femtosecond isomerization of rhodopsin*, Science 254 (1991), pp. 412-415

[97] P. Gualtieri, L. Barsanti: *Algae: Anatomy, Biochemistry, and Biotechnology*, Boca Raton, FL, Taylor & Francis (2006)

[98] E. Piccinni, M. Mammi: *Motor Apparatus of Euglena gracilis: ultrastructure of the basal portion of the flagellum and the paraflagellar body.* Boll. Zool. 45 (1978), pp. 405-414

[99] J. Wolken: *Photoprocess, Photoreceptors and Evolution*, Academic Press, N.Y., (1975)

[100] P. L. Walne, V. Passarelli, L. Barsanti, P. Gualtieri: *Rhodopsin: A photopigment for phototaxis in Euglena gracilis*, Critical Reviews in Plant Sciences, 17 (1998), p. 559

[101] T. K. Rosiere, J. A. Marts, G. B. Bouck: *A 39-kD Plasma Membrane Protein (IP39) Is an Anchor for the Unusual Membrane Skeleton of Euglena gracilis*, Dep. Biol. Sci., Univ. Illinois at Chicago, Chicago, Illinois (1990)

[102] B. Hinz: *Microtubules*, PhD Presentation, EPFL/SB/IPMC/LCB (2005)

[103] K. Svoboda, et al.: *Direct observation of kinesin stepping by optical trapping interferometry*, Nature 365, (1993), pp. 721–727

[104] A. Yildiz, M. Tomishige, R. D. Vale, and P. R. Selvin, *Kinesin walks hand-over-hand*, Science 303 (2004), pp. 676-678

[105] http://www.bgbm.org/kusber/GEO-Tag-2002-Algen.htm

[106] A. M. Smith, T. J. Quick, R. L. ST. Peter: *Differences in the Composition of Adhesive and Non-Adhesive Mucus From the Limpet Lottia Zimatula*, Dep. Biol. Sci., Butler University, Indianapolis, Indiana (1999)

[107] S. A. Wainwright, W. D. Biggs, J. D. Currey, J. M. Gosline: *Mechanical Design in Organisms*, Princeton University Press, Princeton (1976), pp. 423

[108] J. Z. Kiss, A. C. Vasconcelos, R. E. Triemer: *Structure of the Euglenoid storage carbohydrate, paramylon*, Amer. J. Bot. 74(6), (1987), pp. 877-882

[109] S. C. Holt, A. I. Stern: *The Effect of 3-(3,4-Dichlorophenyl)-1 ,1-dimnethylurea on Chloroplast Development and Maintenance in Euglena gracilis*, Plant Physiol. 45, (1970), pp. 475-483

[110] http://www.elmhurst.edu/∼chm/vchembook/548starchiodine.html

[111] Chu, Sang-Hyon et al.: *Patent application: Multilayer ferritin array for bionanobattery*, United States Patent Application 20070134552, (2007), http://appft1.uspto.gov

[112] T. Maddanimatha, G. Ramanath, K. Vijayamohanan: *Self-assembled molecular nanocathodes for rechargeable energy storage modules*, Chem, Phys. Let. 396/4-6, (2004), pp. 277-281

[113] D. Bäumer, A. Preisfeld, H. G. Ruppel: *Isolation and Characterization of Paramylon Synthase from Euglena gracilis (Euglenophyceae)*, Journ. Phycology 37/1, (2001), pp. 38-46

[114] M. Cramer, J. Myers: *Growth and photosynthetic characteristics of Euglena gracilis*, Arch. Microbiol. 17, pp. 384-402

[115] L. Barsanti, V. Passarelli, P. L. Walne, P. Gualtieri: *The photoreceptor protein of Euglena gracilis*, FEBS Letters, 482 (2000), p. 247

[116] H. J. Arnott, P. L. Walne: *Observations on the fine structure of the pellicle pores of Euglena granulata*, Protoplasma 64 (1967), p. 330

[117] C. Sanchez, H. Arribart, M. M. Giraud Guille: *Biomimetism and bioinspiration as tools for the designs of innovative materials and systems*, Nature materials, 4 (2005), p. 277

[118] B. S. Leander, M. A. Farmer: *Comparative morphology of the euglenid pellicle. I. Patterns of strips and pores*, J. Eukaryot. Microbiol. 47 (2000), p. 469

[119] C. Gruenberger, R. Ritter, F. Aumayr, H. Stachelberger, I. C. Gebeshuber: *Algal biophysics: Euglena gracilis investigated by atomic force microscopy*, Materials Science Forum Vol. 555 (2007), pp. 411-416

Annex 1

This Igor script was used in order to remove image artifacts from acquired image data as described in 5.2.3 under AFM Software and Fig. 5.5 (page 70 and 72 respectively).

```
#pragma rtGlobals = 1 // Use modern global access method.

menu "AFM_TUVIENNA" // add new entry into menu.
    "TraceRetrace Calculations... " ,    NewLayer()
end

function LateralTR (w) // function to add a new layer to an existing afm data wave
    Wave w
    Variable laynr

    laynr = DimSize(w, 2) //number of layers
    Redimension/N=(-1,-1,laynr+1) w // create a new layer
    w[][][laynr] = w[p][q][laynr -2] - w[p][q][laynr -1]
    // calculate the lateral T - R signal
    // change LayerLabel so that the MFP-3D extension displays the new layer
    SetDimLabel 2, laynr, UserIn0Trace, w
end

function min_htthtr (w) // function joining height trace and retrace
    Wave w
    Variable laynr

    laynr = DimSize(w, 2) // get the number of layers
    Redimension/N=(-1,-1,laynr+1) w // create a new layer

    w[][][laynr]=min(w[p][q][0],w[p][q][1])

    // change LayerLabel so that the MFP-3D extension displays the new layer
    SetDimLabel 2, laynr, UserIn1Trace, w
end
```

```
function join_amptampr (w) // joining amplitude trace and retrace
    Wave w
    Variable laynr
    Variable i
    Variable j
    Variable offset=0

    Variable used_offset

    Variable test
    Variable test1

    Variable separationline=0.00000005
    // used to distinguish from which area information comes
            Variable sep=0        // if 1: active
            Variable fuzz=0.2     // 0: offset to be used: mean-offset,
            // 1: dot-per-dot-offset, or use value in between

        print ("separation line height if present is:"), separationline
    print ("fuzz parameter is:"), fuzz

    laynr = DimSize(w, 2)     // number of layers
    Redimension/N=(-1,-1,laynr+1) w     // create a new layer

    for(i=0;i< DimSize(w, 0);i+=1)        // initialize variables;continue test
        for(j=0;j< DimSize(w, 1);j+=1)
            offset = offset+w[i][j][2]+w[i][j][3]
        endfor        // condition;update loop variables
    endfor
     //calculating mean offset for amplitude traces
    offset=offset/(2*DimSize(w, 0)*DimSize(w,1))

    print ("mean offset is:"), offset


    for(i=0;i< DimSize(w, 0);i+=1)        // initialize variables;continue test
        for(j=0;j< DimSize(w, 1);j+=1)

            used_offset = offset*(1-fuzz) +fuzz*(w[i][j][2]+w[i][j][3])/2

            if (w[i][j][0]==min(w[i][j][0],w[i][j][1]))
                w[i][j][laynr]=w[i][j][2]-used_offset
                //taken from amplTRACE if corresponding heightTRACE is min
                test=0
            else
```

106

```
                    w[i][j][laynr]=(w[i][j][3]-used_offset)*(-1)
                    // taken from amplRETRACE if corresponding heightRETRACE is min
                    test=1
                endif

                if (test1!=test && sep==1)
                    w[i][j][laynr]=separationline
                endif

                test1=test

        endfor          // condition;update loop variables
    endfor          // execute body code until continue test is FALSE

    // change LayerLabel so that the MFP-3D extension displays the new layer
    SetDimLabel 2, laynr, UserIn2Trace, w
end


function NewLayer()
    String workwave
    Variable op_number
    Variable i

    SetDataFolder root:images

    // generate list of afm data waves
    String wlist = SortList(WaveList("*0*", ";", ""))

    Prompt workwave, "Select Wave", popup wlist
    Prompt op_number, "Select New Layer Content", popup "Join Height;
    Lateral T - R;Join Amplitude;HeightnAmp for all;Delete Layer;"

    DoPrompt "Make Layer and calculate!", workwave, op_number
    if ( V_flag )
        return -1 // user canceled
    endif

    switch(op_number)   // numeric switch
        case 1: // execute if case matches expression
            min_htthtr($workwave)
            break       // exit from switch
        case 2:
            LateralTR($workwave)
            break
```

```
        case 3:
            join_amptampr($workwave)
            break
        case 4:
            for (i=0; i<ItemsInList(wlist); i+=1)
                workwave=stringfromlist(i,wlist)
                    min_htthtr($workwave)
                    join_amptampr($workwave)
                endfor
            break
    endswitch
    return 0
end
```